

COMPARATIVE EVALUATION OF CODES AND REGULATIONS
IN TURKEY FOR EARTHQUAKE PERFORMANCE ASSESSMENT OF
EXISTING BUILDINGS

by

Şahin Özdoğan Dede

B.S., Civil Engineering, Yıldız Technical University, 2016

Submitted to the Kandilli Observatory and Earthquake Research Institute
in partial fulfillment of the requirements for the degree of
Master of Science

Graduate Program in Earthquake Engineering

Boğaziçi University

2020

COMPARATIVE EVALUATION OF CODES AND REGULATIONS
IN TURKEY FOR EARTHQUAKE PERFORMANCE ASSESSMENT OF
EXISTING BUILDINGS

APPROVED BY:

Assoc. Prof. Dr. Ufuk Hancılar
(Thesis Supervisor)

.....

Prof. Dr. Eser Çaktı

.....

Prof. Dr. Kadir Güler

(Istanbul Technical University)

.....

DATE OF APPROVAL: 06.01.2020

ACKNOWLEDGEMENTS

I would like to express my deepest gratitude to my thesis supervisor Assoc. Prof. Dr. Ufuk Hancılar, who has broadened my horizons with his valuable thoughts and suggestions for his support, guidance, and contributions not only in my academic studies but also in other areas of my life.

I would like to express my gratitude to Prof. Dr. Bilge Doran, who has contributed significantly to me throughout my undergraduate education and has greatly influenced my character and values. I am also profoundly grateful to Dr. Murat Ergenekon Selçuk for his sincerity, trust, and contribution to me.

I thank my dearest friends Cem Yazar, Ramazan Akdağ, and Yasir İslam Kaplan for their priceless presence throughout the difficult times.

I also thank my colleagues Gülen Uncu, Nesrin Yenihayat and Tamer İzzet Beyazoğlu, for their recommendations and helpful attitude.

I would like to thank dear Nur Betül Çınar for her invaluable love, support, and joy she brought to my life.

And finally, I would like to express my deepest gratitude and admiration to my beloved parents Öznur Dede and Öner Dede, who have dedicated their life to me and my education.

ABSTRACT

COMPARATIVE EVALUATION OF CODES AND REGULATIONS IN TURKEY FOR EARTHQUAKE PERFORMANCE ASSESSMENT OF EXISTING BUILDINGS

New Turkish Building Seismic Code published in 2018 has been officially in force since January 1, 2019. The new code introduces significant changes not only in the countrywide seismic hazard maps but also in structural modeling and analysis issues for the design of new buildings as well as in the definition of performance objectives and assessment methodologies for existing buildings. In this study, a comparative earthquake performance assessment of a reinforced concrete building in Istanbul is presented. The building, which was constructed in 2006, has four stories rising above a basement floor. The lateral load-carrying system consists of moment-resisting frames with two shear walls around the staircase. Although it is assumed that the building was designed according to the provisions of the Turkish Building Seismic Code-1998, it was identified as a risky building last year based on the simplified guidelines by the Ministry of Environment and Urbanization (Riskli Yapıların Tespit Edilmesine İlişkin Esaslar-2013). Earthquake performance of the study building is evaluated for the requirements of the new Turkish Building Seismic Code (2018) and of its previous version (2007) as well. For this purpose, a three-dimensional finite element model of the building is elaborated on the basis of the blueprints. Geometrical and material characteristics are further verified by the reports on in situ measurements and field tests. Linear and nonlinear static and dynamic analyses procedures are implemented, and a detailed assessment of the building against the performance criteria by each code is performed. Additionally, the building is assessed on the basis of the updated guidelines by the Ministry of Environment and Urbanization (Riskli Yapıların Tespit Edilmesine İlişkin Esaslar-2019). Outcomes of the earthquake performance assessments are presented comparatively, and the differences/changes among the codes and guidelines are highlighted.

ÖZET

MEVCUT BİNALARIN DEPREM PERFORMANSININ BELİRLENMESİ KONUSUNDA TÜRKİYE'DEKİ YÖNETMELİKLERİN VE ESASLARIN KARŞILAŞTIRMALI DEĞERLENDİRMESİ

2018 senesinde yayımlanan yeni Türkiye Bina Deprem Yönetmeliği, 1 Ocak 2019 tarihinden itibaren resmen yürürlüktedir. Yeni yönetmelik ülke genelinde kullanılan sismik tehlike haritasında önemli değişiklikler getirmesinin yanında yeni yapılacak binaların yapısal modellemesi ve analizlerinde, deprem performans hedeflerinin tanımlarında ve mevcut binaların deprem performanslarının değerlendirilmesi konularında da önemli değişiklikler içermektedir. Bu çalışmada, İstanbul'da yer alan betonarme bir yapının karşılaştırmalı deprem performans değerlendirmesi sunulmaktadır. 2006 senesinde inşa edilen bu bina 1 bodrum kat üzerinde 4 normal kattan meydana gelmektedir. Yapının yatay yük taşıyıcı sistemi moment aktaran betonarme çerçeveler ile merdivenler etrafında yer alan iki adet perdeden oluşmaktadır. Binanın tasarımının Afet Bölgelerinde Yapılacak Yapılar Hakkında Yönetmelik 1998'deki hükümler usulünce olduğu kabul edilmesine rağmen, Çevre ve Şehircilik Bakanlığının Riskli Yapıların Tespit Edilmesine İlişkin Esasları kapsamında, geride bıraktığımız sene, "Riskli Bina" olarak tespit edilmiştir. Yapının deprem performans değerlendirmesi Deprem Bölgelerinde Yapılacak Binalar Hakkında Yönetmelik 2007'deki ve Türkiye Bina Deprem Yönetmeliği 2018'deki ilgili bölümlere uygun biçimde gerçekleştirilmiştir. Değerlendirme çalışmaları için, ayrıntılı planlarını esas alan üç boyutlu sonlu eleman modeli kurulmuştur. Bina geometrisi ve malzeme özellikleri saha çalışmaları ve testler sonucunda oluşturulan raporlar ile doğrulanmıştır. Yönetmeliklerin ilgili bölümleri takip edilerek doğrusal elastik statik hesap yöntemleri ve doğrusal elastik olmayan statik ve dinamik hesap yöntemleri ile yapının detaylı performans değerlendirmesi yapılmıştır. Ayrıca binanın, Çevre ve Şehircilik Bakanlığının güncellemesi ile yayımlanan Riskli Yapıların Tespit Edilmesine İlişkin Esaslar-2019 kapsamında da risk değerlendirmesi yapılmıştır. Deprem performans değerlendirmelerinin sonuçları karşılaştırmalı olarak sunulmuş ve kodlar ve esaslar arasındaki farklar/değişiklikler vurgulanmıştır.

TABLE OF CONTENT

ACKNOWLEDGEMENTS	iii
ABSTRACT.....	iv
ÖZET.....	v
TABLE OF CONTENT.....	vi
LIST OF FIGURES.....	viii
LIST OF TABLES	xii
LIST OF SYMBOLS AND ABBREVIATIONS	xviii
1. INTRODUCTION	1
1.1. Objectives and Outline of the Thesis.....	1
1.2. Literature Review	2
2. EARTHQUAKE PERFORMANCE ASSESSMENT OF EXISTING BUILDINGS ACCORDING TO TURKISH BUILDING SEISMIC CODES.....	4
2.1. Earthquake Ground Motion Levels and Performance Objectives Based on Turkish Building Seismic Codes	5
2.2. Special Rules for the Evaluation of Existing Building Systems Under Earthquake Effects Given in the Turkish Building Seismic Codes	11
2.2.1. Limited Knowledge Level in Reinforced Concrete Buildings	13
2.2.2. Comprehensive Knowledge Level in Reinforced Concrete Buildings	14
2.2.3. Damage Limits and Damage Regions of the Structural Members.....	17
2.2.4. General Principles and Rules Related to Earthquake Calculation	18
2.3. Determination of Earthquake Performance of Existing Buildings Based on the Turkish Seismic Codes	19
2.3.1. Limited Damage Performance Level in Existing Buildings.....	20
2.3.2. Level Of Controlled Damage Performance In Existing Buildings	20
2.3.3. Collapse Prevention Performance Level In Existing Buildings	21
2.3.4. Collapse	21
2.4. Evaluation and Strengthening of Existing Buildings by Turkish Building Seismic Code 2007	22
2.5. Principles for Identifying Risky Structures: RYTEIE 2019 and RYTEIE 2013...	23

3. A CASE STUDY: EARTHQUAKE PERFORMANCE ASSESSMENT OF AN EXISTING BUILDING USING LINEAR AND NONLINEAR ANALYSES	28
3.1. Building Description.....	29
3.2. Linear Analysis.....	35
3.2.1. Linear Assessment Based on the Turkish Building Seismic Code 2007 ..	35
3.2.2. Linear Assessment Based on Turkish Building Seismic Code 2018	56
3.3. Nonlinear Static Analysis.....	66
3.3.1. Nonlinear Static Analysis Based on Turkish Building Seismic Code 2007..	70
3.3.2. Nonlinear Static Analysis Based on Turkish Building Seismic Code 2018..	81
3.4. Nonlinear Dynamic Analysis	98
3.4.1. Verification of Models	103
3.4.2. Analysis Procedure.....	105
3.4.3. Analysis Results	108
3.5. Principles for Identifying Risky Structures (RYTEIE).....	109
3.5.1. Assessment Based on RYTEIE 2013	109
3.5.2. Assessment Based on RYTEIE 2019	118
4. RESULTS	121
REFERENCES.....	124

LIST OF FIGURES

Figure 2.1. Damage limits and regions in TBSC 2018	17
Figure 2.2. Damage limits and regions in TBSC 2007	22
Figure 2.3 Assumed performance level of the risky buildings	23
Figure 3.1. Floor plan of the normal stories	30
Figure 3.2. Floor plan of the basement story	31
Figure 3.3. Analytical model of the building.....	41
Figure 3.4. The 5%-damped elastic acceleration response spectrum of TBSC 2007	43
Figure 3.5. Deformed shape of the building under equivalent earthquake load in the positive X direction (top view)	45
Figure 3.6. Deformed shape of the building under equivalent earthquake load in the positive Y direction (top view)	45
Figure 3.7. Deformed shape of the building under earthquake loading in the positive X direction.....	46
Figure 3.8. Deformed shape of the building under earthquake loading in the positive Y direction.....	46
Figure 3.9. Visual demand/capacity inspection for C01 under EXN loading	49
Figure 3.10. Visual demand/capacity inspection for C13 under EXN loading	49
Figure 3.11. Visual demand/capacity inspection for P101 under EXN loading.....	54

Figure 3.12. Visual demand/capacity inspection for P102 under EXN loading.....	54
Figure 3.13. Location of the building (taken from https://tdth.afad.gov.tr/)	58
Figure 3.14. Elastic acceleration spectrum	59
Figure 3.15. Concrete material defined in XTRACT for TBSC 2007 and TBSC 2018, respectively	68
Figure 3.16. Steel material defined in XTRACT for TBSC 2007 and TBSC 2018, respectively	69
Figure 3.17. The first mode of the analytical model of TBSC 2007.....	71
Figure 3.18. The second mode of the analytical model of TBSC 2007	71
Figure 3.19. The third mode of the analytical model of TBSC 2007.....	72
Figure 3.20. Moment-curvature analysis of a beam section in XTRACT.....	73
Figure 3.21. P-M interaction diagram for S101	74
Figure 3.22 P-M interaction diagram for P101	75
Figure 3.23. Moment-curvature analysis of column C01	75
Figure 3.24. Pushover curve for positive X direction	77
Figure 3.25. Pushover curve for positive Y direction	77
Figure 3.26. Modal capacity curve and modal displacement demand for positive X direction	78
Figure 3.27. Modal capacity curve and modal displacement demand for the positive Y direction.....	79

Figure 3.28. Deformed shape of the structure and plastic hinges at $uxN1(p) = 0.121$	80
Figure 3.29. Deformed shape of the structure and plastic hinges at $uyN1(p) = 0.146$ m	80
Figure 3.30 The first mode of the analytical model of TBSC 2018.....	83
Figure 3.31. The second mode of the analytical model of TBSC 2018	84
Figure 3.32. The third mode of the analytical model of TBSC 2018.....	84
Figure 3.33. Comparison of S33 hinge properties for TBSC 2018 and TBSC 2007, respectively	86
Figure 3.34. Comparison of P-M interaction curves for C101 (40x60).....	87
Figure 3.35. Comparison of P-M interaction curves for W101 (245x25).....	87
Figure 3.36. Load case definition in SAP2000 for concurrent pushover loading.....	89
Figure 3.37. Pushover curves on the X loading direction	89
Figure 3.38. Pushover curves on the Y loading direction	90
Figure 3.39. Modal capacity diagram and modal displacement demand for positive X direction.....	91
Figure 3.40. Modal capacity diagram and modal displacement demand for positive Y direction.....	92
Figure 3.41. Deformed shape of the structure and plastic hinges at $uxN1(p) = 0.182$ m	93
Figure 3.42. Deformed shape of the structure and plastic hinges at $uyN1(p) = 0.239$ m	93
Figure 3.43. C02 axial force-curvature diagram.....	95

Figure 3.44. Visual damage inspection for column C02	96
Figure 3.45. The hysteretic stress-strain relationship of the concrete04 material	102
Figure 3.46. Hysteretic stress-strain relationship of the steel02 material without isotropic hardening	102
Figure 3.47. Comparison of torsional mode	104
Figure 3.48. Comparison of translational modes	104
Figure 3.49. Matched spectrum for TBSC 2007 (North-South components).....	106
Figure 3.50. Matched spectrum for TBSC 2018 (East-West components)	106
Figure 3.51. Matched spectrum for TBSC 2018.....	107
Figure 3.52. Moment-curvature history obtained from left end of B283 under Tadoka-1 time history record	107
Figure 3.53. Axial stress-strain time history of the corner reinforcement at the bottom section of the wall P101 under Delta-352 time history record.....	108
Figure 3.54. Elastic acceleration spectrum.....	111

LIST OF TABLES

Table 2.1. Minimum performance objectives for different earthquake levels defined in TBSC 2007	7
Table 2.2. Building usage classes and building importance factors	8
Table 2.3. Earthquake Design Classes (DTS).....	9
Table 2.4. Building Height Intervals Based On The Building Height Classes And Earthquake Design Classes	10
Table 2.5. Performance Objectives for Existing Cast-in-Place Reinforced Concrete, Precast Reinforced Concrete and Steel Structures (Except High-Rise Buildings $BYS \geq 2$)	11
Table 2.6. Information level coefficients for buildings.....	16
Table 2.7 Information level coefficient defined in RYTEIE 2013 and RYTEIE 2019	24
Table 2.8 Column classification table	25
Table 2.9 Shear wall classification table	25
Table 2.10 m_{limit} and $(\delta/h)_{limit}$ values for columns in group A.....	25
Table 2.11 m_{limit} and $(\delta/h)_{limit}$ values for columns in group B	26
Table 2.12 m_{limit} and $(\delta/h)_{limit}$ values for columns in group C	26
Table 2.13 m_{limit} and $(\delta/h)_{limit}$ values for shear walls in group A.....	26
Table 2.14 m_{limit} and $(\delta/h)_{limit}$ values for shear walls in group B.....	26

Table 2.15 Story shear force limit values based on the average axial compressive stress shear walls and columns	27
Table 3.1. Geometrical properties and reinforcement details of the beam sections	32
Table 3.2. Geometrical properties and reinforcement details of columns and shear walls .	33
Table 3.3. Sample cross-sections	34
Table 3.4. Concrete compressive strength test results as reported.....	34
Table 3.5. Effective section stiffness values for first story columns.....	37
Table 3.6. Effective section stiffness values for second story columns	38
Table 3.7. Effective section stiffness values for third story columns	39
Table 3.8. Effective section stiffness values for fourth story columns	40
Table 3.9. Calculation of the fundamental natural vibration periods.....	42
Table 3.10. Effective ground acceleration coefficient	42
Table 3.11 Spectrum characteristic periods.....	42
Table 3.12. Equivalent earthquake forces acting on each story.....	43
Table 3.13. Torsional irregularity control for the negative X direction	44
Table 3.14. Torsional irregularity control for the positive X direction.....	44
Table 3.15. Torsional irregularity control for the negative Y direction	44
Table 3.16. Torsional irregularity control for the positive Y direction.....	44

Table 3.17. Beam damage states under X direction earthquakes.....	47
Table 3.18. Beam damage states under Y direction earthquakes.....	47
Table 3.19. Column damage states under EXN loading	50
Table 3.20. Column damage states under EXP loading	51
Table 3.21. Column damage states under EYP loading	52
Table 3.22. Column damage states under EYN loading	53
Table 3.23. Damage levels of the wall section	55
Table 3.24. Existing material strength for TBSC 2018	56
Table 3.25. Effective section stiffness modifiers for elastic analysis	57
Table 3.26. Buildings for which equivalent earthquake load method is applicable	59
Table 3.27. Earthquake Design Classes	60
Table 3.28. Comparison of periods including and excluding basement floor.....	60
Table 3.29. Building height intervals based on the building height classes and earthquake design classes.....	61
Table 3.30. Performance Objectives for Existing Cast-in-Place Reinforced Concrete, Precast Reinforced Concrete and Steel Structures (Except High-Rise Buildings $BYS \geq 2$)	61
Table 3.31. Dominant natural vibration periods	63
Table 3.32. Rayleigh period calculations	63

Table 3.33. Torsional irregularity control for the negative X direction	64
Table 3.34. Torsional irregularity control for the positive X direction.....	64
Table 3.35. Torsional irregularity control for the negative Y direction	64
Table 3.36. Torsional irregularity control for the positive Y direction.....	64
Table 3.37. Material properties used to model hinges and interaction curves	67
Table 3.38. Mass participation ratios	70
Table 3.39. Parameters used to model hinge S02	73
Table 3.40. Conversion to the modal capacity diagram for positive X direction	78
Table 3.41. Conversion to the modal capacity diagram for positive Y direction	79
Table 3.42. Damage states of structural members at first story under top story displacement demands.....	81
Table 3.43. Calculation table to find effective stiffness about 2-2 local axis.....	81
Table 3.44. Calculation table to find effective stiffness about 3-3 local axis.....	82
Table 3.45. Effective stiffness comparison for columns	82
Table 3.46. Comparison of periods and mass participations	83
Table 3.47. Torsional irregularity control for negative X direction.....	85
Table 3.48. Torsional irregularity control for positive X direction.....	85
Table 3.49. Torsional irregularity control for negative Y direction.....	85

Table 3.50. Torsional irregularity control for positive Y direction.....	85
Table 3.51. Mass participation ratios	86
Table 3.52. Conversion to the modal capacity diagram for positive X direction	91
Table 3.53. Conversion to the modal capacity diagram for positive Y direction	92
Table 3.54. Comparison of strain limits given for concrete	94
Table 3.55. Comparison of strain limits given for steel	94
Table 3.56. Damage states of structural members at first story under displacement demands	97
Table 3.57. Material properties used in nonlinear dynamic analyses	103
Table 3.58. Comparison of analytical models in OpenSees and SAP2000 software.....	103
Table 3.59. Selected Records for TBSC 2007	105
Table 3.60. Selected Records for TBSC 2018	105
Table 3.61. Beam evaluation table	109
Table 3.62. Existing material strength for RYTEIE 2013	110
Table 3.63. Calculation of the first natural vibration periods.....	110
Table 3.64. Parameters to construct elastic acceleration spectrum.....	111
Table 3.65. Equivalent earthquake loads acting on the each story	111
Table 3.66. Torsional irregularity control for the negative X direction	112

Table 3.67. Table 54 Torsional irregularity control for the positive X direction	112
Table 3.68. Table 54 Torsional irregularity control for the negative Y direction.....	112
Table 3.69. Table 54 Torsional irregularity control for the positive Y direction	112
Table 3.70. Calculation table used to find column classes and m values (negative X earthquake loading).....	113
Table 3.71. Results for negative X direction	114
Table 3.72. Results for positive X direction	115
Table 3.73. Results for negative Y direction	116
Table 3.74. Results for positive Y direction	117
Table 3.75. Comparison of risky members' total shear forces with limits.....	118
Table 3.76. Existing material strength for RYTEIE 2019	118
Table 3.77. Mass participation ratios of the modes	119
Table 3.78. Comparison of m values obtained for walls	120

LIST OF SYMBOLS/ABBREVIATIONS

A_c	Cross section area (m ²)
BKS	Building Usage Class
BYS	Building Height Class
DTS	Earthquake Design Classes
EXN	Earthquake loading in negative X direction
EXP	Earthquake loading in positive X direction
EYN	Earthquake loading in negative Y direction
EYP	Earthquake loading in positive Y direction
$E_d^{(H)}$	Horizontal earthquake component
$E_d^{(z)}$	Vertical earthquake component
f_{cm}	Existing concrete compressive strength
G	Dead loads
GÖ	Collapse Prevention
H	Height of floor
h	Section height (m)
H_N	Building height
I	Building Importance Factors
KH	Controlled Damage
KK	Continuous Usage
L_p	Length of plastic hinge (m)
L_s	Shear span (m)
m	Mass
SH	Limited Damage

Q	Live load
S	Snow load
S_1	1.0 second period map spectral acceleration coefficient
S_{d1}	1.0 second period design spectral acceleration coefficient
S_{ds}	Short period design spectral acceleration coefficient
S_s	Short period map spectral acceleration coefficient
T	Natural period (s)
TBSC	Turkish Building Seismic Code
TDTH	National Seismic Hazard Map of Turkey
V_t	Base shear force
Δ	Interstory drift
Φ	Reinforcement diameter
Φ_U	Ultimate curvature (m^{-1})
Φ_Y	Yield curvature (m^{-1})
θ_P	Plastic rotation

1. INTRODUCTION

1.1. Objectives and Outline of the Thesis

Seismic analysis is a tool used to evaluate the earthquake performance of existing structures. Different methods for seismic analysis are developed as a result of research studies to be used in practical applications, and practical versions are provided through seismic codes. Therefore, advances in computer technology and advances in research studies play a pioneering role in practical applications by promoting innovations in seismic codes. In countries like Turkey, where the building stock, and hence the population in the country is concentrated over seismically active regions, keeping up with these developments, conducting new research studies, and updating existing provisions is seen as a necessity.

Performance evaluation of existing structures was firstly taken its place in the TBSC 2007 officially. With the publication of TBSC 2018, significant changes were made both in the parameters related to the earthquake hazard and in the evaluation methods and approaches of existing structures. The primary purpose of this study is to investigate these changes through the earthquake performance assessment study of an existing reinforced concrete residential building. In this context, differences in earthquake demand, changes in the analysis methods, and changes in the limit values, which are the basis of evaluation, are studied. Within the scope of this study, three main methods used in performance evaluation are examined, which are linear static analysis, nonlinear static analysis, and nonlinear dynamic analysis. SAP2000 program was utilized for static analyses, and the OpenSees program was utilized for dynamic analyses.

Another objective of this study is to address the differences in the newer version of guidelines of the Ministry of Environment and Urbanization (Riskli Yapıların Tespit Edilmesine İlişkin Esaslar-RYTEIE) to be used for reducing the earthquake risk in Turkey. This simplified guideline published in 2013 and revised in 2019 in terms of earthquake hazard, analysis methods, and buildings that can be evaluated.

1.2. Literature Review

The earthquake performance of the existing structures has been an important study area since the publication of TBSC 2007 in our country, and many studies have been carried out. It is seen that some of these studies focused on the comparison of the seismic analysis methods. After TBSC 2018 came into force, a few studies have been conducted comparing seismic analysis methods and various parameters in the scope of the earthquake performance of the existing structures.

Çavdar and Bayraktar (2014) conducted a study to investigate the nonlinear behavior of a reinforced concrete building designed according to TBSC 1975 employing nonlinear static analysis and nonlinear dynamic analysis. The building was a collapsed residential building in the Van earthquake on October 23, 2011. TBSC 2007 is adopted to evaluate the performance of the building, and the building presented collapse performance level under the earthquake loads. They indicated that nonlinear static analysis and nonlinear dynamic analysis showed different performance levels at the member sections. The results from the nonlinear dynamic analyses showed higher damage ratios for the first-story beams and columns than the results from the linear static and nonlinear static analyses.

Arslan et al. (2018) investigated the effect of torsional irregularity on eight dissimilar five-story and seven-story reinforced concrete designed according to TBSC 2007. Buildings had torsional irregularities with and without beam discontinuity in the plan. To realize this, they have performed linear elastic analysis, nonlinear static analysis, and nonlinear dynamic analysis following the regulations in the TBSC 2007. It is stated that nonlinear static analysis yielded closer results to the results of nonlinear dynamic analysis than linear elastic analysis does if considered building exhibits in-plan irregularity. They emphasized that using linear elastic analysis on a building with in-plan irregularity can result in unreliable and conservative results.

Demir et al. (2013) evaluated ten different buildings designed according to TBSC 1997 from different regions utilizing linear elastic analysis and nonlinear static analysis following the regulations in TBSC 2007. Results showed that the linear elastic analysis method and nonlinear static analysis method yielded in different performance levels due to the discrepancies among performances of the columns. The linear elastic analysis resulted in more critical results compared to the nonlinear static analysis method. Evaluated buildings did not meet the life safety performance objective, and they emphasized that it is a controversial issue to select the method to be used.

Elci and Goker (2018) compared the seismic performance of the reinforced concrete columns based on the TBSC 2018 and TBSC 2007. They had carried out a theoretical and experimental study on four different column members. Columns had experimentally investigated under hysteretic loading and constant axial load. It is concluded that TBSC 2018 provides safer and more ductile limits compared to TBSC 2007.

Yön and Onat (2019) compared the unit deformation demands for TBSC 2018 and TBSC 2007 on a generic two-dimensional reinforced concrete frame building by performing incremental dynamic analysis. For the nonlinearity of the model, the distributed plasticity approach through fiber elements is adopted. They concluded that damages for almost all earthquakes procured according to TBEC-2018 more than TSC-2007 and stated that the new code stays on the safe side according to the previous code.

2. EARTHQUAKE PERFORMANCE ASSESSMENT OF EXISTING BUILDINGS ACCORDING TO TURKISH BUILDING SEISMIC CODES

Although TBSC 2018 has brought significant innovations compared to TBSC 2007 and RYTEIE 2019 compared to RYTEIE 2013, the main steps and outlines of the performance evaluation study of the existing structures are the same. In this section, steps to be followed according to codes are presented. Priority is given to current codes, and a summary is provided with the differences in the previous codes.

In the first four sections of this chapter, the steps to be followed for the performance evaluation process, according to TBSC 2018 and TBSC 2007 is given. Afterward, regulations of RYTEIE 2019 and RYTEIE 2013 is presented in the same manner. The details of the analysis methods used for the evaluation purposes are presented with their applications in Chapter 3.

2.1. Earthquake Ground Motion Levels and Performance Objectives Based on Turkish Building Seismic Codes

The main factor in the performance evaluation of a structure, regardless of the method, is the determination of the earthquake hazard to which the performance objective will be determined. Earthquake ground motion, as opposed to TBSC 2007 and previous regulations, is discussed in detail in an independent section in TBSC 2018. For the determination of the seismic forces in TBSC 2007, Turkey Earthquake Zone Map published in 1996 had been used. This map was replaced by the revised National Seismic Hazard Map of Turkey (TDTH) with the release of TBSC 2018. In this context, with TDTH, which was published together with TBSC 2018, a significant change was made in the definition of earthquake hazard. Above all, the earthquake zone approach based on the assumption of the constant effective ground acceleration through the earthquake zones was abolished. The map is no longer a zone map consisting of four different earthquake zone. By means of TDTH, earthquake hazard can be defined individually at each location, not as a constant measure on a regional basis. This definition is made on the short period spectral accelerations and 1.0 second period spectral acceleration instead of the effective ground acceleration used in TBSC 2007. These data are then used to determine the acceleration spectrum parameters and to establish the acceleration spectrum (TBSC 2018 Training Manual).

The performance objectives of the buildings shall be defined under earthquake ground motions at various levels. For this reason, four different earthquake ground motion levels have been defined in TBSC 2018. The new map allows these parameters to be obtained for four different earthquake ground motion levels as well. There were three different levels of earthquake ground motion defined for the evaluation of existing structures in TBSC 2007, and these earthquake ground motion levels were achieved by increasing or decreasing 50% of the effective ground acceleration obtained through the design earthquake definition.

Within the scope of TBSC 2018, four different earthquake ground motion levels are given in the following.

- (a) Earthquake ground motion level-1, DD-1, characterizes the very rare earthquake ground motion where the spectral parameters having 2% probability of exceedance in 50 years, and the corresponding recurrence period is 2475 years. This earthquake ground motion is also called the largest earthquake ground motion considered.
- (b) Earthquake ground motion level-2, DD-2, characterizes the rare earthquake ground motion where the spectral parameters having 10% probability of exceedance in 50 years, and the corresponding recurrence period is 475 years. This earthquake ground motion is also called the standard design earthquake ground motion.
- (c) Earthquake ground motion level-3, DD-3, characterizes the frequent earthquake ground motion, where the spectral parameters having 50% probability of exceedance in 50 years, and the corresponding recurrence period is 72 years.
- (d) Earthquake ground motion level-4, DD-4, characterizes very frequent earthquake ground motion where the spectral magnitudes having 68% (50% probability of exceedance in 30 years) probability of exceedance in 50 years and the corresponding recurrence period is 43 years. This earthquake ground motion is also called service earthquake ground motion.

In TBSC 2018, significant changes in earthquake hazard and effect of the local soil conditions, which form the standard acceleration spectrum, are included, and the analytical expression of the spectrum has changed. The vertical ground motion spectrum was also defined for the first time in TBSC 2018 (TBSC 2018 Training Manual).

The minimum performance objectives foreseen under different earthquake levels for the existing buildings in TBSC 2007 are given in Table 2.1. The earthquake level with 10% probability of exceedance in 50 years corresponds to the design earthquake defined in TBSC 2007. Earthquakes with 50% and 2% probability of exceedance in 50 years had been achieved by decreasing and increasing the design effective ground accelerations by 50%.

Table 2.1. Minimum performance objectives for different earthquake levels defined in TBSC 2007.

Building Usage Purpose and Building Type	Probability of Exceedance of the Earthquake		
	50% in 50 years	10% in 50 years	2% in 50 years
Buildings required to be used after an earthquake: Hospitals, dispensaries, health centers, fire brigade buildings and facilities, PTT and other communication facilities, transportation stations and terminals, power generation and distribution facilities, governorship, district governorship, and municipal administration buildings, first aid and disaster planning stations	-	HK	CG
Buildings where people are occupied for a long time and extensively: Schools, miscellaneous training buildings and facilities, dormitories and hostels, military barracks, prisons, museums, etc.	-	HK	CG
Buildings where people occupied for a short-term and densely: Cinema, theater, concert halls, places of worship, sports facilities, etc.	HK	CG	-
Buildings containing hazardous materials: Buildings where toxic, explosive, flammable substances are located or stored	-	HK	GÖ
Other buildings: Buildings not included in the definitions above (Houses, workplaces, hotels, touristic facilities, building type of industrial structures, etc.)	-	CG	-

The process to define the minimum performance objectives for the existing structures in TBSC 2018 is also more detailed than the previous code. Earthquake Design Class (DTS) and Building Height Class (BYS) should be determined in order to define the performance objective of the building, according to TBSC 2018. DTS can be considered as the equivalent of the concept of earthquake zones abolished with the publication of TBSC 2018. They are used in defining the performance objectives and in the selection of calculation and design methods. In order to define DTS, design short period spectral acceleration and Building Usage Class (BKS) shall be determined. The BKS table is given below. The table provided is similar to the table in TBSC 2007.

In order to be the basis for the determination of Earthquake Design Classes (DTS), Building Usage Classes (BKS), depending on the purpose of the usage of buildings, are defined in Table 2.2.

Table 2.2. Building usage classes and building importance factors.

Building Usage Class	Building Usage Purpose	Building Importance Factor (<i>I</i>)
BKS = 1	<p>Buildings that need to be used after the earthquake, buildings where people are occupied for a long time and extensively, buildings where valuable goods are stored and buildings containing dangerous goods</p> <p>a) Buildings required to be used immediately after an earthquake (Hospitals, dispensaries, health centers, fire brigade buildings and facilities, PTT and other communication facilities, transportation stations and terminals, power generation and distribution facilities, governorship, district governorship, and municipal administration buildings, first aid and disaster planning stations)</p> <p>b) Schools, miscellaneous training buildings and facilities, dormitories and hostels, military barracks, prisons, etc.</p> <p>c) Museums</p> <p>d) Buildings where toxic, explosive, flammable substances are located or stored</p>	1.5
BKS=2	<p>Buildings where people occupied for a short-term and densely</p> <p>Shopping centers, sports facilities, cinema, theater, concert halls, places of worship, etc.</p>	1.2
BKS=3	<p>Other buildings</p> <p>Buildings not included in the definitions given for BKS = 1 and BKS = 2 (Houses, workplaces, hotels, building type of industrial structures, etc.)</p>	1

Depending on Building Usage Classes, Building Importance Factors are defined in Table 2.2.

Depending on the Building Usage Classes defined and the short period design spectral acceleration coefficient for the DD-2 earthquake ground motion level, the Earthquake Design Classes (DTS), which shall be the basis for design under earthquake effect in this regulation, shall be determined according to Table 2.3. Earthquake Design Classes (DTS).

Table 2.3. Earthquake Design Classes (DTS).

Short Period Map Spectral Acceleration Under DD-2 Level Earthquake Ground Motion (S_{DS})	Building Usage Class	
	BKS = 1	BKS = 2, 3
$S_{DS} < 0.33$	DTS = 4a	DTS = 4
$0.33 \leq S_{DS} < 0.50$	DTS = 3a	DTS = 3
$0.50 \leq S_{DS} < 0.75$	DTS = 2a	DTS = 2
$0.75 \leq S_{DS}$	DTS = 1a	DTS = 1

Following the definition of DTS, BYS can be determined. Building height classes are defined so to vary with the DTS.

In buildings with basement floors satisfying both of the conditions given in (a) and (b), the base of the building shall be defined at the floor level above the basement floors.

- (a) Rigid basement walls surround the building from all sides or at least from three sides
- (b) In the dominant vibration modes for each orthogonal direction, the ratio between *the natural vibration period* which is calculated for the whole building including basement floors, and *the natural vibration period* calculated excluding basement masses and ground floor is less than 1.1 ($T_{p,all} \leq T_{p,upper}$)

In buildings with basement floors and buildings without basement floors, those are not satisfying any of the conditions above, the base of the building shall be defined at the upper elevation of the foundation.

Table 2.4. Building Height Intervals Based On The Building Height Classes and Earthquake Design Classes.

Building Height Class	Building Height Intervals Based on the Building Height Classes and Earthquake Design Classes		
	DTS = 1, 1a, 2, 2a	DTS = 3, 3a	DTS = 4, 4a
BYS = 1	$H_N > 70$	$H_N > 91$	$H_N > 105$
BYS = 2	$56 < H_N \leq 70$	$70 < H_N \leq 91$	$91 < H_N \leq 105$
BYS = 3	$42 < H_N \leq 56$	$56 < H_N \leq 70$	$56 < H_N \leq 91$
BYS = 4	$28 < H_N \leq 42$	$42 < H_N \leq 56$	
BYS = 5	$17.5 < H_N \leq 28$	$28 < H_N \leq 42$	
BYS = 6	$10.5 < H_N \leq 17.5$	$17.5 < H_N \leq 28$	
BYS = 7	$7 < H_N \leq 10.5$	$10.5 < H_N \leq 17.5$	
BYS = 8	$H_N \leq 7$	$H_N \leq 10.5$	

By determining DTS and BYS, the performance objective of the existing building can be identified.

In order to be the basis for the definition of Building Performance Targets for building structural systems under earthquake effects, Building Performance Levels are defined in the following.

- (a) *Continuous Usage (KK) Performance Level* corresponds to the situation where structural damage does not occur on the structural system of the building, or where the damage is negligible.
- (b) *Limited Damage (SH) Performance Level* corresponds to the level of damage where limited damage occurs in structural members of the building; in other words, the damage level where non-linear behavior is limited.
- (c) *Controlled Damage (KH) Performance Level* corresponds to the level of damage where damage is not too heavy and is often repairable in the structural members of the building to ensure life safety.
- (d) *Collapse Prevention (GÖ) Performance Level* corresponds to the pre-collapse situation where significant damage occurs in the structural members of the building. A partial or complete collapse of the building has been prevented.

Building performance objectives under earthquake effect refer to the performance levels targeted under earthquake ground motion levels. For the defined four ground motion levels, to be applied to buildings within the scope of TBSC 2018, defined for Normal Performance Objectives for the Earthquake Design Classes DTS = 1, 2, 3, 3a, 4, 4a and defined for Advanced Performance Objectives for the Earthquake Design Classes DTS = 1a, 2a is given in Table 2.5. Depending on the requests of the owner, more advanced performance objectives corresponding to the ground motion levels in Table 2.5 can be selected.

Table 2.5. Performance Objectives for Existing Cast-in-Place Reinforced Concrete, Precast Reinforced Concrete and Steel Structures (Except High-Rise Buildings $BYS \geq 2$).

Ground Motion Level	DTS = 1, 2, 3, 3a, 4, 4a		DTS = 1a, 2a	
	Ordinary Performance Objective	Evaluation/Design Approach	Advanced Performance Objective	Evaluation/Design Approach
DD-3	-	-	SH	ŞGDT
DD-2	KH	ŞGDT	-	-
DD-1	-	-	KH	ŞGDT

In the scope of this thesis, attention is only given to the performance objectives of the existing buildings.

2.2. Special Rules for the Evaluation of Existing Building Systems Under Earthquake Effects Given in the Turkish Building Seismic Codes

The reliability of the information about the structure in performance evaluation studies is one of the most critical parts of the process. Acceptances at this part have a strong impact on the outcome of the assessment. For this reason, earthquake codes and regulations set sharp rules about the data to be collected from the building to be evaluated.

The details and dimensions of the elements to be used in the determination of the capacities of the structural system elements of the existing buildings, the evaluation of the earthquake resistance, the geometry of the structural system, and the material properties shall be obtained from the projects and reports of the buildings, the observations and measurements to be made in the building, and the experiments to be applied to the material samples taken from the building.

Procedures for the collection of information from buildings are the definition of structural system, determination of building geometry, foundation system and ground characteristics, determination of existing damage and previous interventions and/or repairs if any, measurement of element dimensions, determination of material properties, and compliance of the collected information to the project.

Inspection, data collection, evaluation, material sampling, and testing procedures defined within the scope of collecting information from buildings shall be carried out under the responsibility of civil engineers.

Based on the scope of the collected data, information level, and information level coefficient shall be defined for each structure. There are two information levels; limited and comprehensive. Obtained information levels shall be used to calculate the capacities of the members.

In the limited knowledge level, properties of the structural system are determined by building surveys. Limited knowledge level shall only be applied to Other Structures (BKS=3) defined in Table 2.2.

In the comprehensive knowledge level, there are more measurements compared to the limited knowledge level.

The strength of the materials to be used in the calculation of the capacities of the structural members is defined as *existing material strength* through this chapter of the code.

2.2.1. Limited Knowledge Level in Reinforced Concrete Buildings

Building Geometry: Structural system plan relief shall be obtained through building survey. The acquired information shall include the location and material of all reinforced concrete elements and partition walls on each floor, axis clearances, heights and dimensions, and shall be sufficient to construct the calculation model of the building. Architectural projects can be used as an aid to survey. The foundation system shall be investigated by a sufficient number of inspection holes to be opened inside or outside of the building. Short columns and similar unfavorable situations shall be recorded on the plan relief and sections. The relation of the building with neighboring buildings (contiguous, discontinuous, presence of seismic joints) shall be determined.

Member Details: It is assumed that the amount and details of the reinforcement in the reinforced concrete members meet the minimum reinforcement conditions at the construction time of the building. In order to verify this assumption or to determine the rate at which it is realized, reinforcement shall be determined by scratching the concrete cover of at least 5% of the shear walls and columns on each floor. In order to determine reinforcements, the concrete cover of one beam at each floor shall be scratched. Scratching shall be done in a third of the clear length of the columns and beams at the span. Scratched surfaces shall be covered with high strength repairing mortar. Besides, the number and location of transverse and longitudinal reinforcement in 20% of the shear walls and columns, whose concrete cover is not scratched, shall be determined by reinforcement detection devices. *Reinforcement realization coefficient*, expressing the ratio of the existing reinforcement to the minimum reinforcement, shall be calculated based on the reinforced concrete shear walls and columns whose reinforcement is determined. This coefficient shall not be greater than 1 and shall be applied to all other walls and columns, where reinforcement is not determined, to determine the probable amount of reinforcement. For the beams, required reinforcement under the effect of vertical design loads shall be used only.

Material Characteristics: At least three concrete samples shall be taken from each column or shear walls in accordance with the conditions specified in TS EN 12504-1. The strength values obtained by testing the cores with a length and nominal diameter equal to 100 mm can be used to determine the existing concrete strength without applying a coefficient. The conversion of test results obtained from cores of different length/diameter ratios should be based on the appropriate conversion coefficients. If the total number of samples is three, the lowest compressive strength obtained from the samples shall be taken as the existing concrete strength without statistical assessment. If the number of samples is more than three, the greater of the value obtained from the samples (mean minus standard deviation) and the value (0.85 times average) shall be taken as the *existing concrete strength*. By evaluating the difference between the minimum value and the average of the remaining results among the test results of a group of concrete samples, it will be checked whether the smallest value is a statistically deviating result. For this purpose, if the lowest single value is less than 75% of the average of the remaining results, this sample shall not be taken into consideration in the evaluation of the sample results in the group. The reinforcement steel grade shall be determined by visual inspection on the scratched surfaces as defined in the member details section, and *existing steel strength* shall be determined based on the yield strength of the steel grade. If corrosion observed on any members, they shall be marked in the plan, and corrosion shall be taken into consideration in the calculation of member capacities.

2.2.2. Comprehensive Knowledge Level in Reinforced Concrete Buildings

Building Geometry: If projects of the building are present, the measurements of the building shall check the conformity of the existing geometry to the projects. If there are show significant differences with the measurements, the project shall be ignored. If the project is not present, the building system shall be investigated by building survey. The acquired information shall include the location and material of all reinforced concrete elements and partition walls on each floor, axis clearances, heights and dimensions, and shall be sufficient to construct the calculation model of the building. The foundation system shall be investigated by a sufficient number of inspection holes to be opened inside or outside of the building. Short columns and similar unfavorable situations shall be recorded on the plan relief and sections. The relation of the building with neighboring buildings (contiguous,

discontiguous, presence of seismic joints) shall be determined. Building geometry information should contain the details necessary to define the mass of the building accurately.

Element Details: If there are reinforced concrete detail projects of the building, the procedures specified in 15.2.4.2 shall be applied in the same amount of reinforced concrete elements to check the reliability of the reinforcement with the project. In addition, the number and location of transverse and longitudinal reinforcement in 20% of the shear walls and columns, and 10% of the frame beams, with not scratched clear cover shall be determined, by reinforcement detection devices. If there is a mismatch between the project and the application in place, the reinforcement realization coefficient, which represents the ratio of the existing reinforcement in the reinforced concrete elements to the reinforcement given in the project, shall be determined individually for the shear walls, columns, and beams. This coefficient, which is used in the calculation of element capacities, shall not be greater than 1 and, shall be applied to all other walls and columns, where reinforcement is not determined, to determine the probable amount of reinforcement. If there are no reinforced concrete projects or as-built drawings, reinforcement shall be determined by scratching the concrete cover of 10% of the columns and shear walls, at least two on each floor. Scratched surfaces will then be covered with high strength repairing mortar. In addition, the number and location of transverse and longitudinal reinforcement in 30% of the columns and shear walls without scratched concrete cover and 15% of beams shall be determined by reinforcement detection devices.

Material Properties: From columns or shear walls, in accordance with the conditions specified in TS EN 12504-1, one concrete sample on each 400 m² shall be taken so to satisfy that number of samples shall not be less than three in the ground floor and not less than two in the other floors and not less than nine in the building to conduct the tests. The strength values obtained by testing the cores with a length and nominal diameter equal to 100 mm can be used to determine the existing concrete strength without applying a coefficient. The conversion of test results obtained from cores of different length/diameter ratios should be based on the appropriate conversion coefficients. In order to calculate the capacities of the members, the greater of the value obtained from the samples (mean minus standard deviation) and the value (0.85 times average) shall be taken as the *existing concrete strength*.

By evaluating the difference between the minimum value and the average of the remaining results among the test results of a group of concrete samples, it will be checked whether the smallest value is a statistically deviating result. For this purpose, if the lowest single value is less than 75% of the average of the remaining results, this sample shall not be taken into consideration in the evaluation of the sample results in the group. The reinforcement steel grade shall be determined by visual inspection on the scratched surfaces as defined in the member details section, one sample shall be taken for each grade of steel (S220, S420, etc.) and the yield stress, tensile strength and deformation characteristics of the steel shall be determined by evaluating the suitability for the project. If it is suitable for the project, the characteristic yield stress of the steel used in the project shall be taken as the current steel yield stress for the capacity calculations of the members. If it is not suitable, at least three more samples shall be taken, and the most unfavorable yield stress obtained from the tests shall be taken as the current steel yield stress for the capacity calculations of the members. If corrosion observed on any members, they shall be marked in the plan, and corrosion shall be taken into consideration in the calculation of member capacities.

The information level coefficients that shall be applied to the member capacities according to the information levels acquired from the examination buildings are given in Table 2.6.

Table 2.6. Information level coefficients for buildings.

Information Level	Information Level Coefficient
Limited	0.75
Comprehensive	1.00

2.2.3. Damage Limits and Damage Regions of the Structural Members

For ductile members, three damage states and damage limits are defined at the cross-sectional level. These are Limited Damage (SH), Controlled Damage (KH) ve Collapse Prevention (GÖ) states, and their limit values. Limited damage refers to a limited amount of inelastic behavior in the section, controlled damage refers to the inelastic behavior in which cross-sectional strength can be achieved safely, and collapse prevention damage refers to advanced inelastic behavior in the section. This classification does not apply to brittle members.

Members with critical sections having damage below SH falls into the *Limited Damage Region*, between SH and KH falls into the *Visible Damage Region*, between KH and GÖ falls into the *Significant Damage Region*, and members with critical sections exceeding GÖ falls into the *Collapse Region*. Section damage regions can be seen in Figure 2.1.

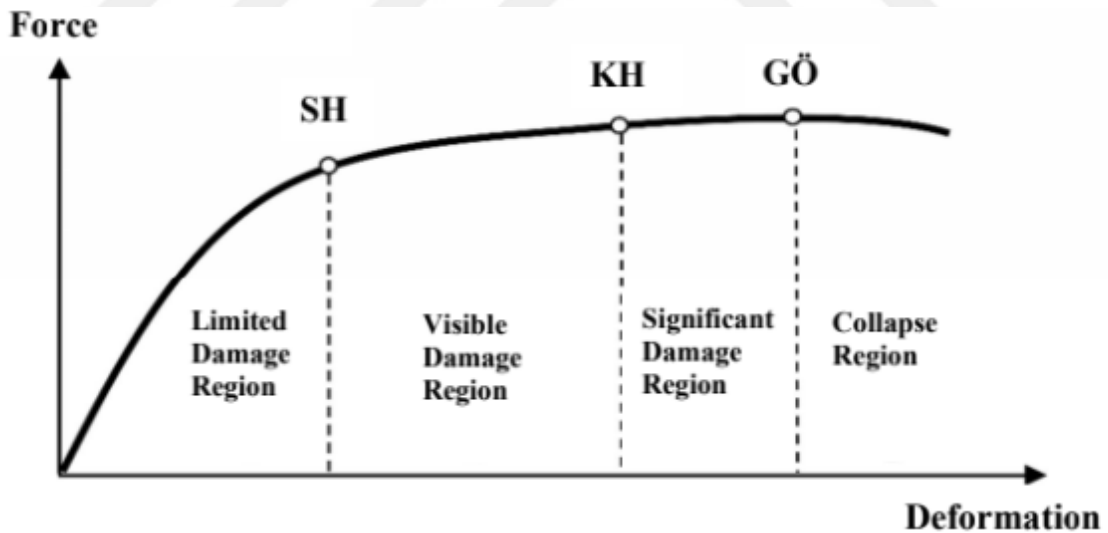


Figure 2.1. Damage limits and regions in TBSC 2018.

By comparing the internal forces and/or deformations, calculated by the elastic or inelastic assessment methods, with the deformation values corresponding to the cross-sectional damage limits, it shall be decided which damage regions the cross-sections are fallen into. Member damage shall be determined according to the section having the highest damage.

2.2.4. General Principles and Rules Related to Earthquake Calculation

The purpose of the earthquake calculation, according to this section of the TBSC 2018, is to determine the earthquake performance of existing or strengthened buildings. For this purpose, linear methods and nonlinear methods defined in the relevant parts of the code can be used. However, performance evaluations conducted employing these methods, which are theoretically based on different approaches, can yield different results. The general principles and rules described below apply to both types of methods.

- In the definition of earthquake effect, the horizontal elastic design spectrum shall be used for earthquake ground motion levels. Building importance factor shall not be applied in the earthquake calculations ($I=I$)
- Earthquake performance of buildings shall be evaluated under the combined effects of vertical loads and earthquake effects on the building. The masses shall be defined according to the equations below.

$$w_j^{(S)} = w_{Gj}^{(S)} + nw_{Qj}^{(S)} \quad ; \quad m_j^{(S)} = \frac{w_j^{(S)}}{g} \quad (2.1)$$

- Earthquake forces shall be acted on the building in both directions for both positive and negative ways
- The structural system of the building shall be prepared with sufficient accuracy to calculate the internal force, displacement, and deformation of the structural elements under the combined effects of earthquake loads and vertical loads.
- In buildings where the slabs behave as a rigid diaphragm in the horizontal plane, the degrees of freedom of rotation about the vertical axis and translations on two horizontal axes shall be considered. Story degrees of freedom shall be defined at the center of mass of each floor, and no additional eccentricity shall be applied.
- Uncertainties in the structural systems of the existing buildings shall be considered in the calculation methods by means of the information level coefficients defined according to the scope of the data collected from the building.

- Columns defined as short columns shall be defined by their actual free lengths in the model of the structural system.
- Conditions for defining the interaction diagrams of reinforced concrete sections under uniaxial or biaxial bending and axial force are given below:
 - (a) The existing material strengths of the concrete and reinforcing steel shall be based on the existing material strength determined according to information level
 - (b) The ultimate compressive strain of the concrete can be taken as 0.0035, and the ultimate strain of the reinforcing steel may be taken as 0.01.
 - (c) Interaction diagrams can be modeled as multi-linear or multi-plane diagrams by appropriately linearizing them.
- In the definition of member dimensions of reinforced concrete systems, the joints can be considered as rigid ends
- Effective section stiffnesses of cracked shall be used in reinforced concrete elements under the bending effect. Effective section stiffness shall be calculated according to 4.5.8.
- In the calculation of the positive and negative plastic moments of the reinforced concrete beams, flange concrete and reinforcement in it can be considered
- In case of insufficient overlapping lengths of reinforced concrete elements, the yield stress of the corresponding reinforcing steel shall be reduced in proportion to the lack of overlapping length in the calculation of the cross-sectional capacity moment.
- Soil properties shall be reflected in the analysis model, where deformations on the ground may affect the behavior of the building.

2.3. Determination of Earthquake Performance of Existing Buildings Based on the Turkish Seismic Codes

To determine the earthquake performance of existing buildings or buildings to be strengthened, the earthquake ground motion levels and the minimum performance objectives for buildings at these earthquake ground motion levels are given in Table 2.5.

The earthquake performance of the existing buildings is related to the condition of the damage expected to occur in the building under the effect of the earthquake excitation and is defined based on four different damage states. With the application of the calculation methods, the earthquake performance level of the building is determined. The rules to be applied to determine the earthquake performance of the buildings are given in the following. The rules given here are valid for reinforced concrete, precast concrete, and steel buildings.

2.3.1. Limited Damage Performance Level in Existing Buildings

At any floor of reinforced concrete buildings, as a result of the calculation made for each earthquake direction applied, up to 20% of the beams may pass to the Significant Damage Zone, but all of the other load-bearing elements are in the Limited Damage Zone. Buildings in this situation are considered to have a Limited Damage Performance, provided that the damaged brittle elements, if any, shall be strengthened. These exceptions are not valid for steel and prefabricated reinforced concrete buildings.

2.3.2. Level Of Controlled Damage Performance In Existing Buildings

Provided that the damaged brittle elements, if any, shall be strengthened, the buildings those meet the following conditions are considered to be in the Controlled Damage Performance Level:

- (a) At any floor of the reinforced concrete buildings, as a result of the calculation for each earthquake direction applied, excluding each secondary beams (not the part of horizontal load-bearing system), up to 35% of beams and vertical elements (columns, walls, and reinforced partition walls) as defined in paragraph (b) below can pass into the Advanced Damage Zone. These exceptions are not valid for steel and prefabricated reinforced concrete buildings.
- (b) The total contribution of the vertical elements in the Advanced Damage Zone to the shear force resisted by the vertical elements on each floor shall be less than 20%. The ratio of the total shear forces of the vertical elements in the Advanced Damage Zone on the top floor to the sum of the shear forces of all vertical elements on that floor can be up to 40%.

- (c) All other structural members are in the Limited Damage Zone or the Significant Damage Zone. However, in any floor, the ratio of shear forces resisted by vertical elements whose Significant Damage Limit has been exceeded in both the lower and upper sections should not exceed 30% (In the linear calculation, the columns provided columns stronger than beams condition at both the lower and upper joints are not included in this account).

2.3.3. Collapse Prevention Performance Level In Existing Buildings

Considering that all brittle damaged elements are in the Collapse Zone, the buildings that meet the following conditions are considered as in the Collapse Prevention Performance Level:

- (a) On any floor of reinforced concrete buildings, as a result of the calculation for each applied earthquake direction, excluding each secondary beams (not the part of the horizontal load-bearing system), up to 35% of beams may pass into the Collapse Zone. These exceptions are not valid for steel and prefabricated reinforced concrete buildings.
- (b) All other structural elements are in the Limited Damage Zone, in the Significant Damage Zone or the Advanced Damage Zone. However, in any floor, the ratio of shear forces resisted by vertical elements whose Significant Damage Limit has been exceeded in both the lower and upper sections should not exceed 30% (In the linear calculation, the columns provided from Equation (7.3) to both the lower and upper node points are not included in this account).
- (c) The use of the building in its current condition is inconvenient in terms of life safety.

2.3.4. Collapse

If the building cannot meet the Collapse Prevention Performance Level, it is in the state of Collapse. The use of the building is inconvenient in terms of life safety.

2.4. Evaluation and Strengthening of Existing Buildings by Turkish Building Seismic Code 2007

In TBSC 2007, Chapter 7 was devoted to the evaluation of existing buildings. In terms of data collection, procedures were very similar to the TBSC 2018 except few changes. The most important ones of these changes are the omission of the medium knowledge level in TBSC 2007 and the change in the definition of the existing material strength determined according to the limited knowledge level. In TBSC 2007, the existing material strength of concrete was taken as the minimum strength obtained from the tests, whereas in TBSC 2018, there is a statistical approach that yields higher results than the minimum if there are three or more samples.

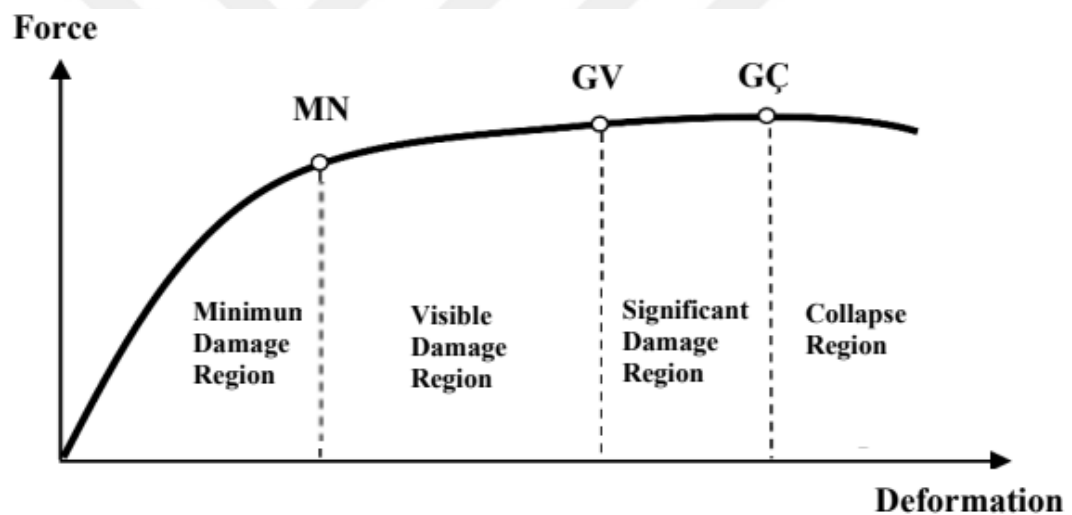


Figure 2.2. Damage limits and regions in TBSC 2007.

2.5. Principles for Identifying Risky Structures: RYTEIE 2019 and RYTEIE 2013

Principles for Identifying Risky Structures (RYTEIE) first came into force in 2013 within the Law on Transformation of Areas Under Disaster Risk (law number 6306). In RYTEIE 2013, the aim was to identify risky buildings through fast and realistic methods familiar to the engineering community. Here, the risky building was defined as the building that was located in or out of the risky area, completed its economic life, or had the risk of collapse or severe damage determined based on the scientific and technical data. The risky building's performance level was foreseen to be between Life Safety and Collapse Prevention, and generally closer to the collapse prevention. The rules of RYTEIE 2013 were based on the relatively simple and easy implementation of the elastic methods in the TBSC 2007. The scope of RYTEIE 2013 was limited to masonry buildings and reinforced concrete buildings not higher than 25 meters and whose number of stories is less than 8. In this way, simple principles were provided for common low-rise buildings, whereas other buildings were directed to the TBSC 2007. Evaluation for the identification of the risk was made based on the critical story. The critical story was defined as the bottom story that is having less stiffness compared to floors below it, having no reinforced concrete walls surrounding from the perimeter, or whose lateral translation was not held by the ground. In this way, fewer samples were taken compared to TBSC 2007; hence a relatively faster evaluation process was made possible.

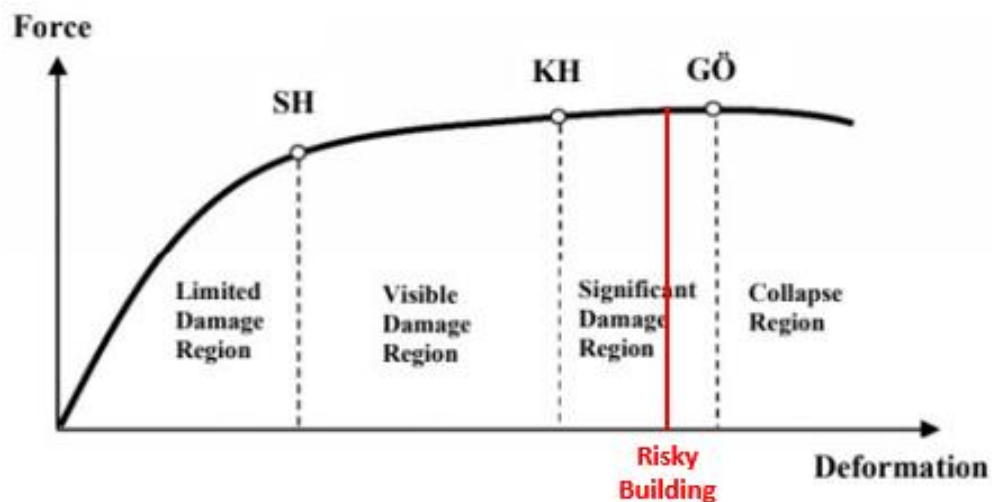


Figure 2.3 Assumed performance level of the risky buildings.

After the publication of TDTH, the necessity for updating RYTEIE 2013 has arisen as a result of the changes in the concepts to define the earthquake hazard in addition to the abolishment of TBSC 2007. As a result, an updated version of RYTEIE was released in 2019. Earthquake hazard in RYTEIE 2019 is determined based on TDTH as in TBSC 2018. In addition, the critical floor approach was abandoned, and the investigation floor approach was adopted. As a result, more detailed information collection has become a need. Stricter and more detailed rules have been introduced in numerical modeling.

Information levels were kept the same for both of the principles. The information level of the structural system may be minimum or comprehensive. In the case of Minimum Information Level, the structural system projects of the building are not present. For the Comprehensive Information Level, the building's structural system project is present, and the in-situ controlled structural properties, section dimensions, and reinforcement details are the same as the project. In case of any discrepancy in these characteristics, the Minimum Information Level shall be accepted. Information level coefficients are given in Table 2.7.

Table 2.7 Information level coefficient defined in RYTEIE 2013 and RYTEIE 2019.

Information Level	Information Level Coefficient
Limited	0.90
Comprehensive	1.00

The capacities of the structural elements shall be calculated by using the Existing Material Strength and multiplied by the Information Level Coefficients.

Unlike RYTEIE 2013, RYTEIE 2019 includes principles not only for low-rise buildings but also for medium-rise and high-rise buildings. The definition of low-rise buildings almost corresponds to buildings covered in RYTEIE 2013. Unlike in 2013, low-rise buildings are not higher than 30 meters, and the number of stories is less than 10. Only the mode superposition method is allowed for the low-rise buildings.

All columns are classified into three groups according to V_e/V_r ratio and the reinforcement detail in the confinement zone. In Table 2.8, it shall be assumed that, in the final state, columns in the group A are subjected to flexure failure, columns in group B are subjected to flexure-shear failure and columns in group C are subjected to shear failure.

Table 2.8 Column classification table.

V_e/V_r	Columns having stirrups spacing $s \leq 100$ mm, hooked 135° at both ends, and total transverse reinforcement area is verifying the equation of $A_{sh} \geq 0.06 s b_k (f_{cm}/f_{yw})$	Other Situations
$V_e/V_r \leq 0.7$	A	B
$0.7 < V_e/V_r \leq 1.1$	B	B
$1.1 < V_e/V_r$	B	C

All shear walls are classified into two groups as brittle or ductile according to the (V_e/V_r) ratio and (H_w/l_w) ratio. In Table 2.9, it shall be assumed that, in the final state, walls in group A are subjected to flexure failure, walls in group B are subjected to flexure-shear or shear failure.

Table 2.9 Shear wall classification table.

H_w/l_w	$V_e/V_r < 1.0$	$1.0 \leq V_e/V_r$
$2.0 \leq H_w/l_w$	A	B
$H_w/l_w < 2.0$	B	B

The moment capacities of reinforced concrete elements shall be calculated based on the rules given in TS 500, taking into account the existing material strengths and knowledge level coefficient. The Demand/Capacity Ratio (m) shall be calculated by dividing the section moment, resulted under the combined effect of gravity loads and earthquake loads, to the section capacity of the reinforced concrete column or shear wall. Section capacities shall be obtained for the $(G + nQ \pm E/6)$ load combination.

Table 2.10 m_{limit} and $(\delta/h)_{limit}$ values for columns in group A.

$N_k/(f_{cm}A_c)$	m_{limit}	$(\delta/h)_{limit}$
≤ 0.1	5.0	0.035
≥ 0.6	2.5	0.0125

Table 2.11 m_{limit} and $(\delta/h)_{limit}$ values for columns in group B.

$N_k/(f_{cm}A_c)$	$A_{sh} / (sb_k)$	m_{limit}	$(\delta/h)_{limit}$
≤ 0.1	≤ 0.0005	2.0	0.01
	≥ 0.0006	5.0	0.03
≥ 0.6	≤ 0.0005	1.0	0.005
	≥ 0.0006	2.5	0.0075

Table 2.12 m_{limit} and $(\delta/h)_{limit}$ values for columns in group C.

m_{limit}	$(\delta/h)_{limit}$
5.0	0.035

If the δ/h and m values calculated for the members exceed $(\delta/h)_{smir}$ and m_{smir} values, it shall be accepted that the member has exceeded the risk limit. The risk assessment shall be made for all stories. If risk limits were exceeded in any story, the building shall be considered as Risky Building.

Table 2.13 m_{limit} and $(\delta/h)_{limit}$ values for shear walls in group A.

$N_K/(f_{cm}A_c)$	$V_e/(b_wdf_{ctm})$	Boundary Zone	m_{limit}	$(\delta/h)_{limit}$
< 0.1	≤ 0.9	Present	6.0	0.0300
		Absent	4.0	0.0150
	≥ 1.3	Present	3.5	0.0150
		Absent	2.0	0.0075
> 0.25	≤ 0.9	Present	3.5	0.0200
		Absent	2.0	0.0100
	≥ 1.3	Present	2.0	0.0100
		Absent	1.5	0.0050

Table 2.14 m_{limit} and $(\delta/h)_{limit}$ values for shear walls in group B.

$V_e/(b_wdf_{ctm})$	m_{limit}	$(\delta/h)_{limit}$
≤ 0.9	4.0	0.0200
≥ 1.3	2.0	0.0100

The story shear force ratio shall be calculated by dividing the sum of the shear forces of the columns and shear walls, which are exceeded the risk limits by the story shear force. Depending on the calculated column and shear wall axial stress values, building exceeding the values given in Table 2.15 shall be considered as risky building. Linear interpolation shall be applied for the intermediate values in the table.

Table 2.15 Story shear force limit values based on the average axial compressive stress shear walls and columns.

The average axial compressive stress of shear walls and columns	Story shear force ratio limit values
$\geq 0.65f_{cm}$	0
$0.1f_{cm} \geq$	0.35

3. A CASE STUDY: EARTHQUAKE PERFORMANCE ASSESSMENT OF AN EXISTING BUILDING USING LINEAR AND NONLINEAR ANALYSES

In this chapter, step by step earthquake performance assessment of an existing residential building based on the regulations of TBSC 2007 and TBSC 2018 is presented. The building was selected for the study because it was tagged as a risky building last year based on the simplified guidelines of the Ministry of Environment and Urbanisation, although it was constructed in 2006. Considering the fact that the building was constructed after TBSC 1997, whose design regulations are the same with TBSC 2007, being a risky building is unexpected. The purpose of this section is to determine the expected performance level of the building by conducting detailed analyses following the regulations in the TBSC 2018 and TBSC 2007. Moreover, step by step analyses and results are given at the end of the chapter for the latest and former simplified guidelines of the Ministry of Environment and Urbanisation, namely, RYTEIE 2019 and RYTEIE 2013. For analytical modeling, cross-sectional characteristics and material properties are taken from the official risk identification report of the real structure, and then different finite element models are elaborated for different types of structural analyses as required by different codes.

Firstly, the assessment of the building through elastic methods was performed utilizing SAP2000 software (CSI, 2019). Secondly, the nonlinear static analysis was performed by enabling the building to exhibit nonlinear behavior with the modifications made in SAP2000 software. Thirdly, the numerical model was established in the OpenSees (Open System for Earthquake Simulation, UC Berkeley, 2019) environment, and performance evaluation was performed with nonlinear dynamic analyses. The last covers the assessment of the structure based on the methods presented in RYTEIE 2019 and RYTEIE 2013.

3.1. Building Description

The building is located in Üsküdar, İstanbul and approximately 18 km away from the closest segment of the North Anatolian Fault. The building has four regular stories in addition to one basement story. The ground floor of the building is 2.9 m in height, and the upper stories are 3 m in height resulting in a total height of 11.9 meters above the basement floor. Floor plans and the sections of the members are given in the following figures and tables.



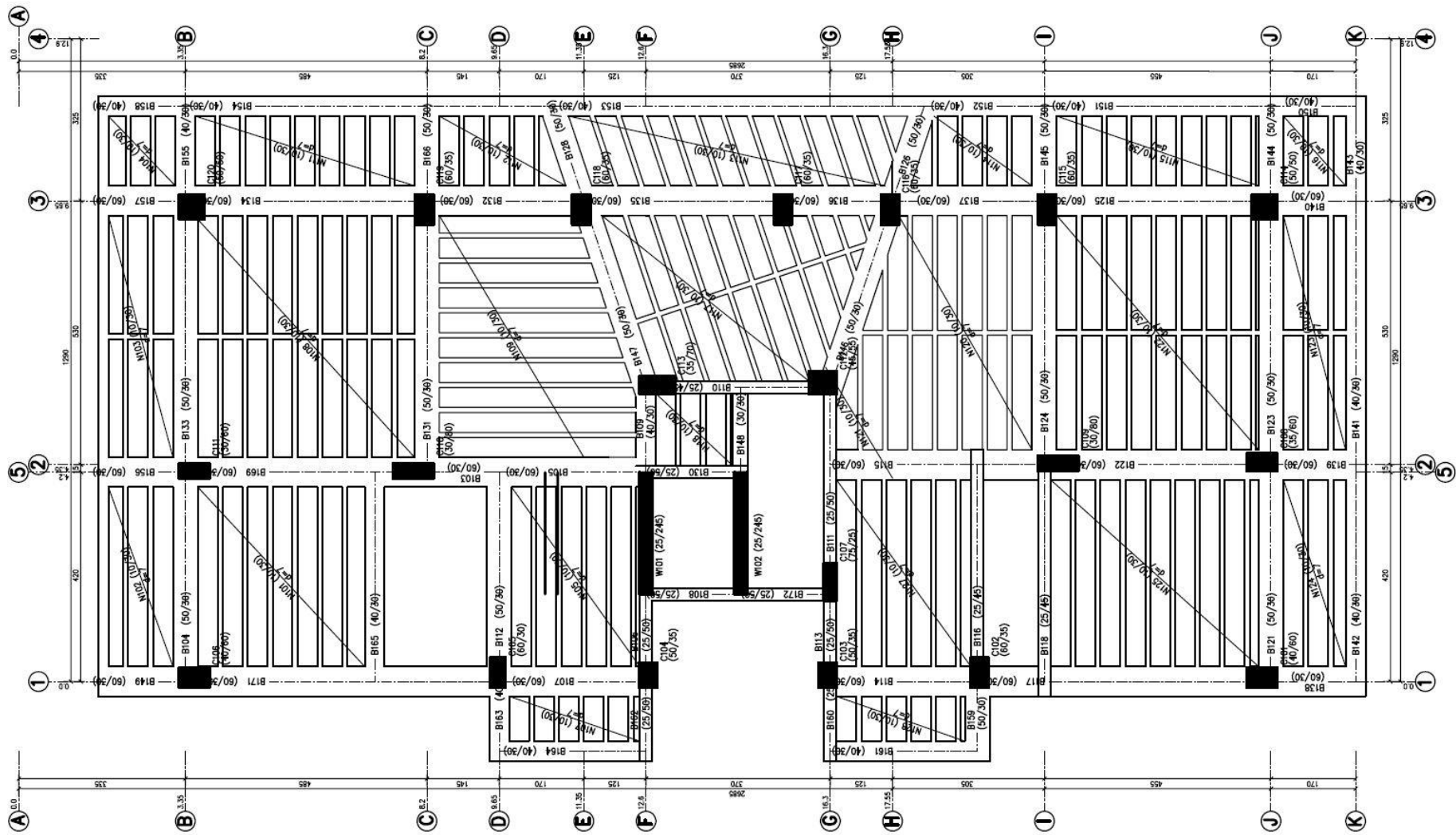


Figure 3.1. Floor plan of the normal stories.

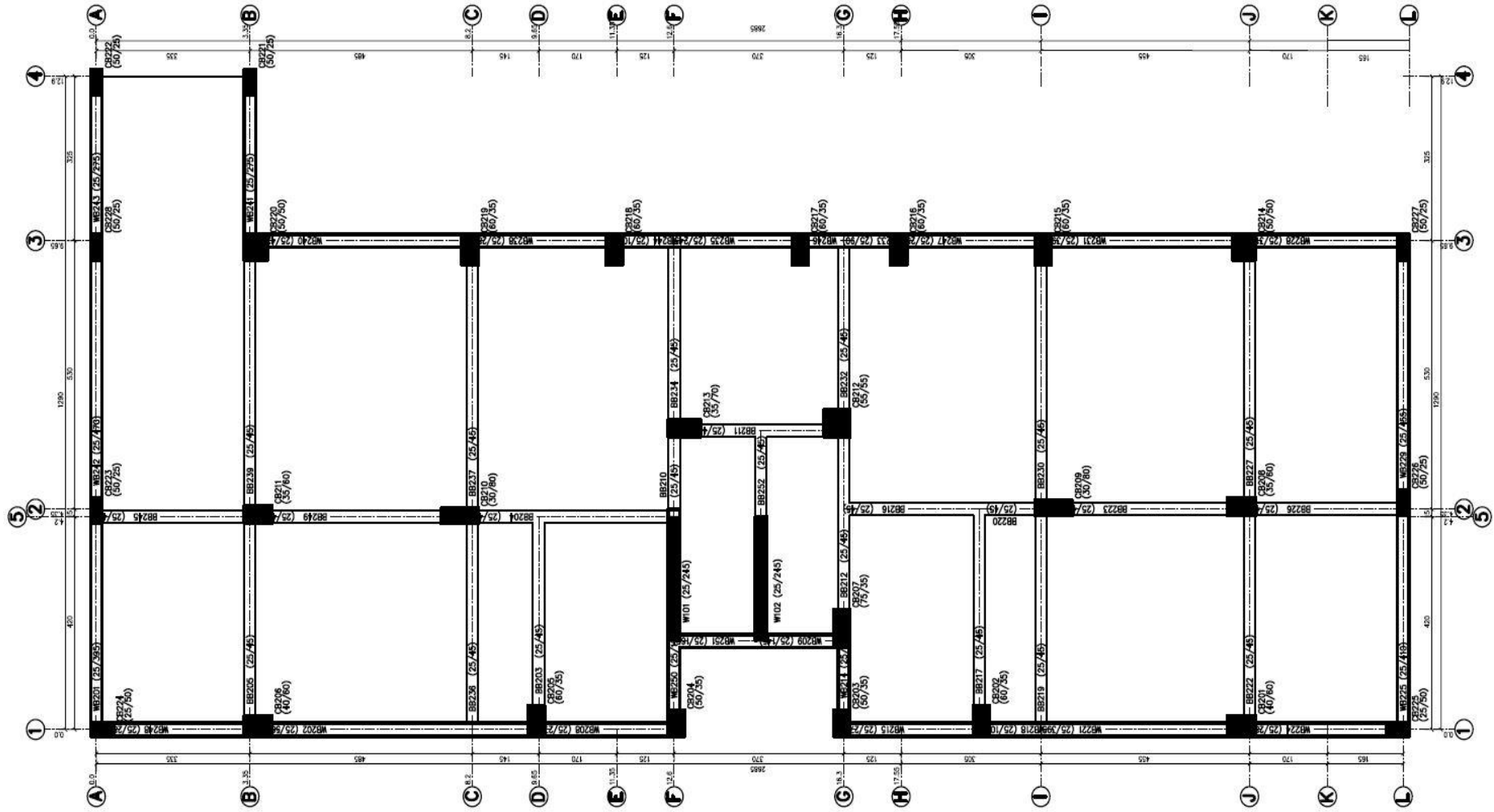


Figure 3.2. Floor plan of the basement story.

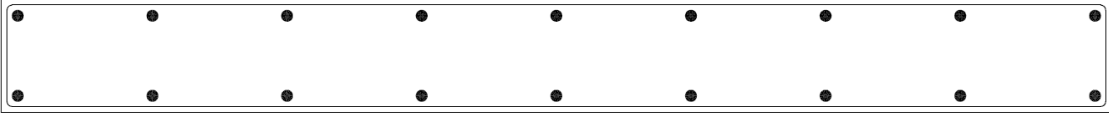
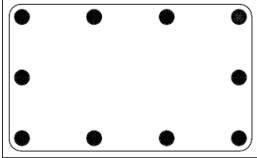
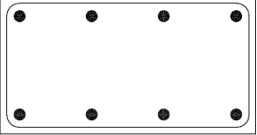
Table 3.1. Geometrical properties and reinforcement details of the beam sections.

Beam Section	Top Reinforcement	Bottom Reinforcement	bw(m)	h(m)
S01	4Ø12	4Ø12	0.6	0.3
S02	5Ø12	4Ø12	0.6	0.3
S03	6Ø12	4Ø12	0.6	0.3
S04	7Ø12	4Ø16	0.6	0.3
S05	4Ø12+1Ø14	4Ø12	0.6	0.3
S06	4Ø12+4Ø16	4Ø12	0.6	0.3
S07	5Ø12+1Ø16	4Ø12	0.6	0.3
S08	6Ø12+3Ø16	4Ø12	0.6	0.3
S09	4Ø12+3Ø16	4Ø12	0.6	0.3
S10	5Ø12+1Ø14	4Ø12	0.6	0.3
S11	6Ø12+1Ø14	4Ø12	0.6	0.3
S12	4Ø12+1Ø14	4Ø12	0.6	0.3
S13	5Ø12+1Ø14	4Ø12	0.6	0.3
S14	4Ø12+1Ø16	4Ø12	0.6	0.3
S15	4Ø12+2Ø16	4Ø12	0.6	0.3
S16	5Ø12	4Ø12	0.5	0.3
S17	5Ø12+1Ø14	4Ø12	0.5	0.3
S18	6Ø12	4Ø12	0.5	0.3
S19	7Ø12	4Ø12	0.5	0.3
S20	10Ø12	4Ø12	0.5	0.3
S21	4Ø12+1Ø14	4Ø12	0.5	0.3
S22	4Ø12	4Ø12	0.5	0.3
S23	3Ø12	4Ø12	0.5	0.3
S24	4Ø12	3Ø12	0.4	0.3
S25	3Ø12	3Ø12	0.4	0.3
S26	6Ø12	4Ø12	0.4	0.3
S27	4Ø12	4Ø12	0.4	0.3
S28	5Ø12	4Ø12	0.4	0.3
S29	3Ø12+1Ø14	3Ø12	0.4	0.3
S30	3Ø12	2Ø12	0.3	0.3
S31	3Ø12	2Ø12	0.25	0.45
S32	2Ø12	2Ø12	0.25	0.45
S33	3Ø12	3Ø12	0.25	0.5
S34	2Ø12+1Ø14	3Ø12	0.25	0.5
S35	3Ø12	2Ø12	0.25	0.5
S36	2Ø12	3Ø12	0.25	0.5
S37	2Ø12	2Ø12	0.25	0.5

Table 3.2. Geometrical properties and reinforcement details of columns and shear walls.

Column Section	Reinforcement	b (m)	h (m)
C101	10Ø16	0.40	0.60
C102	10Ø16	0.60	0.35
C103	8Ø16	0.50	0.35
C104	8Ø16	0.50	0.35
C105	10Ø16	0.60	0.30
C106	10Ø16	0.40	0.60
C107	12Ø16	0.75	0.35
C108	10Ø16	0.35	0.60
C109	10Ø16	0.30	0.80
C110	10Ø16	0.30	0.80
C111	10Ø16	0.35	0.60
C112	12Ø16	0.45	0.55
C113	10Ø16	0.35	0.70
C114	12Ø16	0.50	0.50
C115	10Ø16	0.60	0.35
C116	8Ø16	0.60	0.35
C117	8Ø16	0.60	0.35
C118	10Ø16	0.60	0.35
C119	8Ø16	0.60	0.35
C120	10Ø16	0.50	0.50
W101	18Ø12	2.45	0.25
W102	18Ø12	2.45	0.25

Table 3.3. Sample cross-sections.

Member	Section	b (m)	h (m)	Longitudinal Reinforcement	Transverse Reinforcement
					
Wall	W101-W102	2.45	0.25	18Ø12	Ø8/25 ^{cm} /25 ^{cm}
					
Column	C15-C18	0.60	0.35	10Ø16	Ø8/12 ^{cm} /12 ^{cm}
					
Beam	S01	0.60	0.30	8Ø12	Ø8/8 ^{cm} /15 ^{cm}

The results of the compressive strength tests conducted on core samples taken from the building are given in Table 3.4.

Table 3.4. Concrete compressive strength test results as reported.

Core Sample	Corrected Compressive Strength (Mpa)
C1	20.27
C2	22.13
C3	16.28
C4	22.32
C5	20.27

According to the report, no corrosion was observed in the structural members, and it is emphasized that 135-degree hooking, a requirement for special earthquake transverse reinforcements, was not observed through building surveys.

Based on the soil investigation report, the foundation of the structure located over C type of soil having local site class Z_3 . According to the summary of seismic refraction tests, average shear wave velocity at the upper 30 meters of the soil 360 m/s. Since the identification report was done through RYTEIE 2013, earthquake parameters are based on the seismic zone definitions, which is 2nd degree seismic zone for the case study building.

3.2. Linear Analysis

3.2.1. Linear Assessment Based on the Turkish Building Seismic Code 2007

The building knowledge level is accepted as the limited knowledge level since there are insufficient core samples according to the knowledge level criteria of TBSC 2007. As it is shown in Table 3.4, existing concrete compressive strength is taken as the minimum of the sample results according to TBSC 2007.

In order to conduct the linear analysis, the SAP2000 analysis program has been utilized. Analytical model is constructed so to reflect the behavior of the building correctly under the combined effect of equivalent earthquake loads and gravity loads. In the model, frame elements and shear walls are defined as line elements connected to nodes representing the beam-column joints.

In order to model the shear walls around the staircase, the equivalent beam-column element model is adopted. Equivalent beam-column element model is one of the most common approaches used to model planar shear walls (e.g., FEMA 356, *Prestandard and Commentary for the Seismic Rehabilitation*, PEER/ATC 72-1, *Modeling and Acceptance Criteria for Seismic Design and Analysis of Tall Buildings*). In this approach, an equivalent column is modeled so to represent the flexural behavior of the wall at the center of gravity of the wall, and rigid beams are framed into that column at each story level. In this mode, the rocking motion of the wall may not be captured (Orakcal et al., 2006). Furthermore, interaction with any other framing element is affected by the properties of the beam, and this interaction may not be appropriately presented.

Ribbed floor slabs are not included in the model, but it is investigated that the floor slabs were sufficient stiffness to provide the rigid diaphragm effect. Therefore, joints at each story level are constrained so to reflect rigid diaphragm behavior. Earthquake loads are applied to the diaphragm center of masses as it is depicted in the TBSC 2007. Walls surrounding the basement level are modeled as shell elements.

All columns and walls are fixed for all degrees of freedom at the very base of the building. Rigid basement walls are modeled by using shell elements.

Cracked section stiffnesses values are calculated by following formula given in the TBSC 2007:

- For beams $(EI)_e = 0.40(EI)_o$
- For columns and walls,
 - If $N_d/(A_c f_{cm}) \leq 0.10$, $(EI)_e = 0.40(EI)_o$
 - If $N_d/(A_c f_{cm}) \geq 0.40$, $(EI)_e = 0.80(EI)_o$

Cracked section stiffness values for columns and walls are presented from Table 3.5 to Table 3.8.

Table 3.5. Effective section stiffness values for first story columns.

Column	Loading	N_d (kN)	b (m)	h (m)	$N_d/(A_c f_{ck})$	$(EI)_e$
C101	G+0.3Q	477.52	0.40	0.60	0.122	0.430
C102	G+0.3Q	681.07	0.60	0.35	0.199	0.532
C103	G+0.3Q	231.60	0.50	0.35	0.081	0.400
C104	G+0.3Q	202.89	0.50	0.35	0.071	0.400
C105	G+0.3Q	646.98	0.60	0.35	0.189	0.519
C106	G+0.3Q	496.88	0.40	0.60	0.127	0.436
C107	G+0.3Q	272.16	0.75	0.35	0.064	0.400
C108	G+0.3Q	671.42	0.35	0.60	0.196	0.529
C109	G+0.3Q	901.91	0.30	0.80	0.231	0.574
C110	G+0.3Q	756.74	0.30	0.80	0.194	0.525
C111	G+0.3Q	714.44	0.35	0.60	0.209	0.545
C112	G+0.3Q	479.78	0.45	0.55	0.119	0.425
C113	G+0.3Q	292.75	0.35	0.70	0.073	0.400
C114	G+0.3Q	799.48	0.50	0.50	0.196	0.529
C115	G+0.3Q	675.93	0.60	0.35	0.198	0.530
C116	G+0.3Q	520.82	0.60	0.35	0.152	0.470
C117	G+0.3Q	431.84	0.60	0.35	0.126	0.435
C118	G+0.3Q	551.14	0.60	0.35	0.161	0.482
C119	G+0.3Q	607.95	0.60	0.35	0.178	0.510
C120	G+0.3Q	751.98	0.50	0.50	0.185	0.520
W101	G+0.3Q	383.93	2.45	0.25	0.039	0.400
W102	G+0.3Q	568.90	2.45	0.25	0.057	0.400

Table 3.6. Effective section stiffness values for second story columns.

Column	Loading	N_d (kN)	b (m)	h (m)	$N_d/(A_c f_{ck})$	$(EI)_e$
C201	G+0.3Q	357.62	0.40	0.60	0.092	0.400
C202	G+0.3Q	507.42	0.60	0.35	0.148	0.470
C203	G+0.3Q	172.06	0.50	0.35	0.060	0.400
C204	G+0.3Q	145.71	0.50	0.35	0.051	0.400
C205	G+0.3Q	479.51	0.60	0.30	0.164	0.490
C206	G+0.3Q	372.85	0.40	0.60	0.095	0.400
C207	G+0.3Q	198.97	0.75	0.25	0.065	0.400
C208	G+0.3Q	503.34	0.35	0.60	0.147	0.470
C209	G+0.3Q	675.87	0.30	0.80	0.173	0.510
C210	G+0.3Q	573.76	0.30	0.80	0.147	0.470
C211	G+0.3Q	533.06	0.30	0.60	0.182	0.510
C212	G+0.3Q	357.73	0.45	0.55	0.089	0.400
C213	G+0.3Q	226.63	0.35	0.70	0.057	0.400
C214	G+0.3Q	599.62	0.50	0.50	0.147	0.470
C215	G+0.3Q	506.33	0.60	0.35	0.148	0.470
C216	G+0.3Q	389.06	0.60	0.35	0.114	0.418
C217	G+0.3Q	324.80	0.60	0.35	0.095	0.400
C218	G+0.3Q	416.18	0.60	0.35	0.122	0.440
C219	G+0.3Q	461.35	0.60	0.35	0.135	0.450
C220	G+0.3Q	563.82	0.50	0.50	0.139	0.460
W201	G+0.3Q	296.88	2.45	0.25	0.030	0.400
W202	G+0.3Q	432.32	2.45	0.25	0.043	0.400

Table 3.7. Effective section stiffness values for third story columns.

Column	Loading	N_d (kN)	b (m)	h (m)	$N_d/(A_c f_{ck})$	$(EI)_e$
C301	G+0.3Q	237.39	0.40	0.60	0.061	0.400
C302	G+0.3Q	337.91	0.60	0.35	0.099	0.400
C303	G+0.3Q	113.74	0.50	0.35	0.040	0.400
C304	G+0.3Q	95.53	0.50	0.35	0.034	0.400
C305	G+0.3Q	318.12	0.60	0.30	0.109	0.411
C306	G+0.3Q	247.48	0.40	0.60	0.063	0.400
C307	G+0.3Q	131.13	0.75	0.25	0.043	0.400
C308	G+0.3Q	334.53	0.35	0.60	0.098	0.400
C309	G+0.3Q	449.70	0.30	0.80	0.115	0.420
C310	G+0.3Q	389.98	0.30	0.80	0.100	0.400
C311	G+0.3Q	354.75	0.30	0.60	0.121	0.430
C312	G+0.3Q	235.43	0.45	0.55	0.058	0.400
C313	G+0.3Q	156.60	0.35	0.70	0.039	0.400
C314	G+0.3Q	399.26	0.50	0.50	0.098	0.400
C315	G+0.3Q	337.02	0.60	0.35	0.099	0.400
C316	G+0.3Q	255.91	0.60	0.35	0.075	0.400
C317	G+0.3Q	217.44	0.60	0.35	0.064	0.400
C318	G+0.3Q	281.38	0.60	0.35	0.082	0.400
C319	G+0.3Q	314.10	0.60	0.35	0.092	0.400
C320	G+0.3Q	375.39	0.50	0.50	0.092	0.400
W301	G+0.3Q	201.92	2.45	0.25	0.020	0.400
W302	G+0.3Q	289.92	2.45	0.25	0.029	0.400

Table 3.8. Effective section stiffness values for fourth story columns.

Column	Loading	N_d (kN)	b (m)	h (m)	$N_d/(A_c f_{ck})$	$(EI)_e$
C401	G+0.3Q	116.97	0.35	0.60	0.034	0.400
C402	G+0.3Q	170.99	0.60	0.35	0.050	0.400
C403	G+0.3Q	55.44	0.50	0.35	0.019	0.400
C404	G+0.3Q	48.23	0.50	0.35	0.017	0.400
C405	G+0.3Q	160.13	0.50	0.35	0.056	0.400
C406	G+0.3Q	121.75	0.35	0.60	0.036	0.400
C407	G+0.3Q	66.39	0.70	0.30	0.019	0.400
C408	G+0.3Q	166.04	0.30	0.60	0.057	0.400
C409	G+0.3Q	224.07	0.30	0.80	0.057	0.400
C410	G+0.3Q	206.85	0.30	0.80	0.053	0.400
C411	G+0.3Q	177.32	0.30	0.60	0.061	0.400
C412	G+0.3Q	113.75	0.45	0.40	0.039	0.400
C413	G+0.3Q	86.14	0.30	0.65	0.027	0.400
C414	G+0.3Q	198.57	0.45	0.45	0.060	0.400
C415	G+0.3Q	167.92	0.60	0.30	0.057	0.400
C416	G+0.3Q	123.32	0.60	0.30	0.042	0.400
C417	G+0.3Q	109.36	0.60	0.30	0.037	0.400
C418	G+0.3Q	147.10	0.60	0.30	0.050	0.400
C419	G+0.3Q	167.14	0.60	0.30	0.057	0.400
C420	G+0.3Q	186.58	0.45	0.45	0.057	0.400
W401	G+0.3Q	98.28	2.45	0.25	0.010	0.400
W402	G+0.3Q	143.89	2.45	0.25	0.014	0.400

Analytical model of the building is given in Figure 3.3.

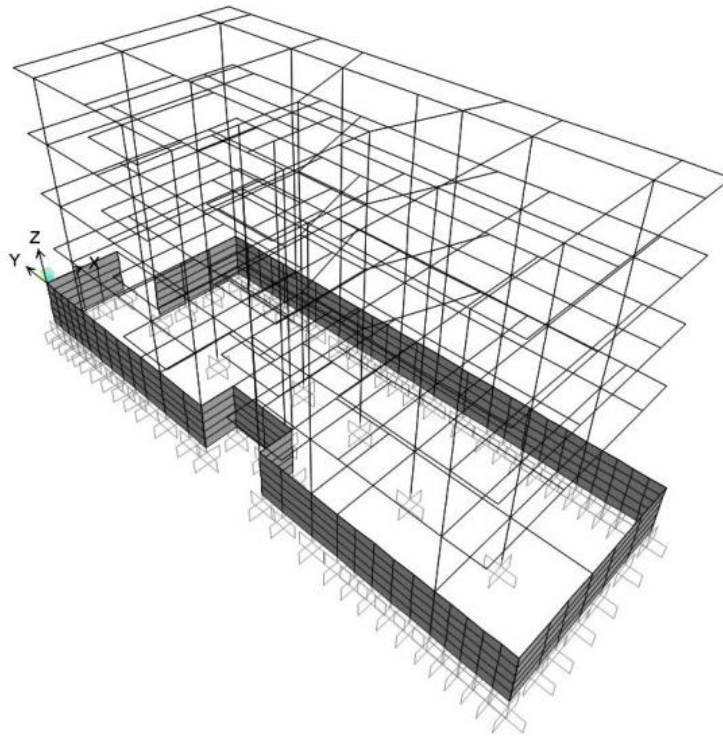


Figure 3.3. Analytical model of the building.

In order to decide whether the Equivalent Earthquake Load Method is applicable or not, several criteria shall be investigated. The torsional irregularity factor at each story shall be less than 1.4. Besides, building height above the basement shall be less than 25 m, and the story number shall be less than 8. Torsional irregularity factors for each story were calculated for both orthogonal directions in each positive and negative ways. Calculation of the torsional irregularity factor was done using Equivalent Earthquake Load Method. Therefore, equivalent earthquake loads are calculated as if the building ensures the restrictions and controlled accordingly. At the end of the calculations, it is verified that the Equivalent Earthquake Load Method is applicable for the case study building by verifying the provisions.

The first natural vibration periods of the structural system was determined based on the Rayleigh Quotient as it is given in Table 3.9.

$$T_1 = 2\pi \left(\frac{\sum_{j=1}^N m_i d_{fi}^2}{\sum_{j=1}^N F_{fi} d_{fi}} \right)^{1/2} \quad (3.1)$$

Table 3.9. Calculation of the fundamental natural vibration periods.

Story	h_i	H_i	m_i	w_i (kN)	F_{fi}	$dF_{i,x}$	$dF_{i,y}$
4	3.0	11.9	294	2883	392	0.02044	0.04039
3	3.0	8.9	306	3005	305	0.01509	0.03237
2	3.0	5.9	308	3021	203	0.00905	0.02097
1	2.9	2.9	308	3019	100	0.00335	0.00829
						$T_{1,x} =$	0.769
						$T_{1,y} =$	1.108

Seismic zone and soil class, which are the two fundamental parameters to calculate the elastic spectrum, are given in Chapter 3.1. Effective ground acceleration coefficient and spectrum characteristic periods are determined based on the seismic zone and soil class information, respectively.

Table 3.10. Effective ground acceleration coefficient.

Seismic Zone	A_0
1	0.40
<u>2</u>	<u>0.30</u>
3	0.20
4	0.10

Table 3.11 Spectrum characteristic periods.

Local Site Class	T_A (second)	T_B (second)
Z1	0.10	0.30
Z2	0.15	0.40
<u>Z3</u>	<u>0.15</u>	<u>0.60</u>
Z4	0.20	0.90

The elastic spectrum was constructed based on the aforementioned parameters and given in Figure 3.4.

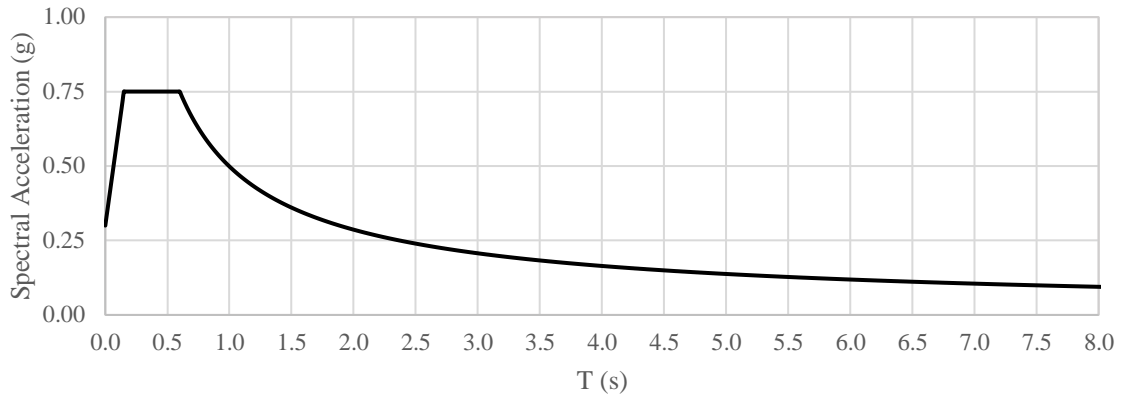


Figure 3.4. The 5%-damped elastic acceleration response spectrum of TBSC 2007.

In the assessment procedure, the building importance factor and the earthquake load reduction factor shall be taken as unity, unlike design procedure. Also, the right-hand side of the equations below is multiplied with a factor of $\lambda=0.85$ since the number of stories above the basement is greater than 2.

$$V_{tx} = \frac{WA(T_{1X})}{R_a(T_{1X})} \lambda = 6237.15 \text{ kN}$$

$$V_{ty} = \frac{WA(T_{1Y})}{R_a(T_{1Y})} \lambda = 4655.83 \text{ kN}$$

Total equivalent earthquake load is distributed among the floors based on the following equation, and calculated story forces are given in Table 3.12.

$$F_i = (V_t - \Delta F_N) \frac{w_i H_i}{\sum_{j=1}^N w_j H_j} \quad (3.2)$$

$$\Delta F_N = 0.0075 N V_t \quad (3.3)$$

Table 3.12. Equivalent earthquake forces acting on each story.

Story	w_i (kN)	H_i (m)	$F_{i,X}$ (kN)	$F_{i,Y}$ (kN)
4	2883.16	11.9	2555.81	1907.83
3	3004.80	8.9	1846.29	1378.19
2	3020.99	5.9	1230.54	918.55
1	3019.42	2.9	604.53	451.26
		Σ	6237.15	4655.83
Basement	2896.11	0	868.83	868.83
		Σ	7105.99	5524.66

In order to verify that the building is appropriate to be assessed by the Equivalent Earthquake Load method, the torsional irregularity check is a provision to be satisfied. The deformed shape of the building in plan, under equivalent earthquake loads, is presented in Figure 3.5. Torsional irregularity check was conducted for corner joints, and results can be seen from Table 3.13 to Table 3.16.

Table 3.13. Torsional irregularity control for the negative X direction.

Loading	Joint	U_x	U_y	U_z	Δ	Joint	U_x	U_y	U_z	Δ	η_{bi}
EXN	TRC1	-0.154	-0.010	0.018	0.038	TLC1	-0.097	-0.010	0.016	0.029	1.128
EXN	TRC2	-0.116	-0.009	0.023	0.045	TLC2	-0.068	-0.009	0.019	0.030	1.202
EXN	TRC3	-0.072	-0.007	0.025	0.044	TLC3	-0.039	-0.007	0.019	0.025	1.272
EXN	TRC4	-0.028	-0.003	0.021	0.028	TLC4	-0.013	-0.003	0.015	0.013	1.352

Table 3.14. Torsional irregularity control for the positive X direction.

Loading	Joint	U_x	U_y	U_z	Δ	Joint	U_x	U_y	U_z	Δ	η_{bi}
EXP	TRC1	0.154	0.010	-0.018	0.038	TLC1	0.097	0.010	-0.016	0.029	1.128
EXP	TRC2	0.116	0.009	-0.023	0.045	TLC2	0.068	0.009	-0.019	0.030	1.202
EXP	TRC3	0.072	0.007	-0.025	0.044	TLC3	0.039	0.007	-0.019	0.025	1.272
EXP	TRC4	0.028	0.003	-0.021	0.028	TLC4	0.013	0.003	-0.015	0.013	1.352

Table 3.15. Torsional irregularity control for the negative Y direction.

Loading	Joint	U_x	U_y	U_z	Δ	Joint	U_x	U_y	U_z	Δ	η_{bi}
EYN	TRC1	-0.011	-0.193	-0.014	0.039	BRC1	-0.011	-0.179	-0.016	0.036	1.048
EYN	TRC2	-0.009	-0.154	-0.023	0.054	BRC2	-0.009	-0.144	-0.024	0.051	1.032
EYN	TRC3	-0.006	-0.099	-0.029	0.060	BRC3	-0.006	-0.093	-0.031	0.056	1.032
EYN	TRC4	-0.003	-0.039	-0.028	0.039	BRC4	-0.003	-0.036	-0.029	0.036	1.039

Table 3.16. Torsional irregularity control for the positive Y direction.

Loading	Joint	U_x	U_y	U_z	Δ	Joint	U_x	U_y	U_z	Δ	η_{bi}
EYP	TRC1	0.011	0.193	0.014	0.039	BRC1	0.011	0.179	0.016	0.036	1.048
EYP	TRC2	0.009	0.154	0.023	0.054	BRC2	0.009	0.144	0.024	0.051	1.032
EYP	TRC3	0.006	0.099	0.029	0.060	BRC3	0.006	0.093	0.031	0.056	1.032
EYP	TRC4	0.003	0.039	0.028	0.039	BRC4	0.003	0.036	0.029	0.036	1.039

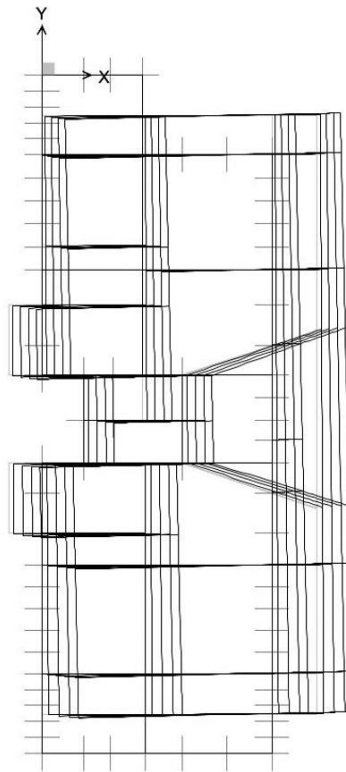


Figure 3.5. Deformed shape of the building under equivalent earthquake load in the positive X direction (top view).

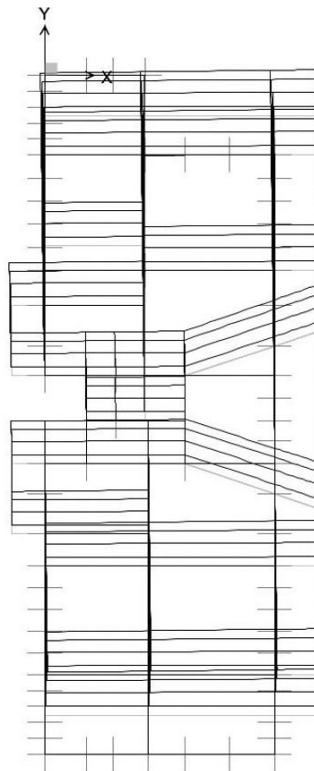


Figure 3.6. Deformed shape of the building under equivalent earthquake load in the positive Y direction (top view).

Under the earthquake loads calculated in the previous chapter, analysis has been done. Statically equivalent earthquake loads are applied as joint loads to the mass centers of each diaphragm, which all the joints at the floor levels are connected to. Resulted deformed shape of the building is presented in Figure 3.7 and Figure 3.8.

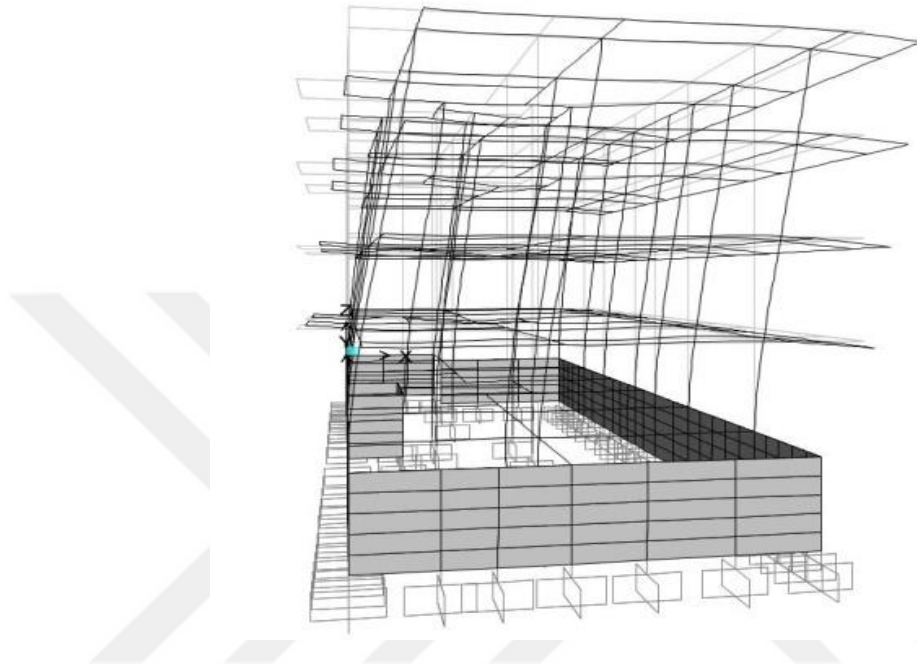


Figure 3.7. Deformed shape of the building under earthquake loading in the positive X direction.

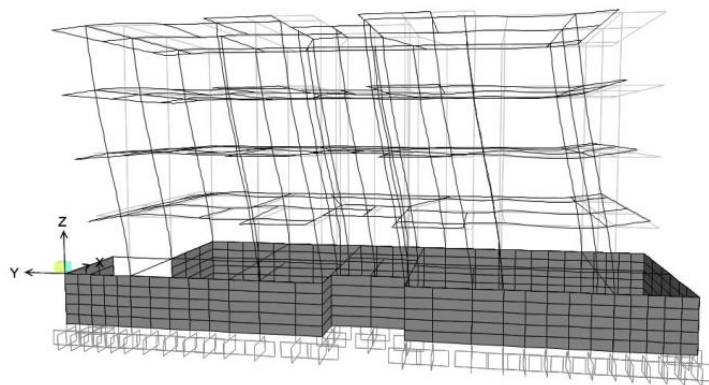


Figure 3.8. Deformed shape of the building under earthquake loading in the positive Y direction.

In this chapter, the performance evaluation of beams at the section level is presented. In order to evaluate the performance at the section level, the failure type of the section shall be identified, whether it is a brittle type of failure or a ductile type of failure. Failure type

classification shall be made based on the shear strength of the section calculated according to regulations in the TS-500.

After the checks are carried out separately for orthogonal directions considering positive and negative ways, demand/capacity ratios (r) are investigated.

Obtained demand/capacity ratios are compared with the demand/capacity ratio limits related to damage levels which are dependent on the fundamental properties affecting the ductility of the section, namely, reinforcement ratio at the section, presence of the transverse reinforcement at the confinement zones and ratio of the shear force to the concrete material's axial tension force over the section.

Table 3.17. Beam damage states under X direction earthquakes.

<i>Beam Damage States</i>	X DIRECTION EARTHQUAKE							
	Positive Direction				Negative Direction			
Story	Minimum Damage	Visible Damage	Significant Damage	Collapse	Minimum Damage	Visible Damage	Significant Damage	Collapse
4	74%	13%	6%	7%	87%	4%	3%	6%
3	69%	16%	7%	9%	73%	16%	4%	7%
2	67%	14%	10%	9%	71%	17%	3%	9%
1	74%	14%	3%	9%	83%	6%	4%	7%

Table 3.18. Beam damage states under Y direction earthquakes.

<i>Beam Damage States</i>	Y DIRECTION EARTHQUAKE							
	Positive Direction				Negative Direction			
Story	Minimum Damage	Visible Damage	Significant Damage	Collapse	Minimum Damage	Visible Damage	Significant Damage	Collapse
4	84%	13%	3%	0%	84%	13%	3%	0%
3	71%	6%	19%	4%	70%	7%	21%	1%
2	66%	6%	10%	19%	67%	6%	10%	17%
1	67%	7%	10%	16%	67%	7%	14%	11%

This chapter is devoted to the evaluation of columns. As it is the case for the beams, identifying the failure type of the column sections is critical to determine their damage states. For this reason, at the critical column sections, shear forces generated from the capacity moments shall be calculated.

Since the lower end of the columns located on the top of the basement capacity of the columns at that joint was calculated as in the columns connected to the foundation.

After the controls for orthogonal directions for positive and negative ways, the next step is to obtain demand/capacity ratios for the column sections. In order to determine the capacity moment to be considered in the demand/capacity ratio, interaction diagrams were obtained utilizing XTRACT software (Chadwell and Imbsen, 2004) based on the existing material strengths and the deformation values for $\epsilon_{cu}=0.003$ and $\epsilon_{su}=0.01$, as given in the TBSC 2007.

The axial force value to which the capacity moment is determined is the axial force that occurs under the combined effect of vertical loads and earthquake loads. However, this axial force has an upper limit, as specified in the annex of TBSC 2007. This upper limit is the axial force resulting from the cumulative effect of the shear forces transferred from the beams which are framed into that specific column. If the axial force under the combined effects of vertical loads and earthquake loads exceeds this upper limit, the moment capacity is obtained for the limiting axial force value.

Demand/capacity ratios are acquired through P-M interaction curves. Figure 3.9 and Figure 3.10 are given to illustrate the methodology summarized below;

- Axial force, N_d , and moment, M_d , of the section under gravity loads are calculated
- Axial force, N_E , and moment, M_E , of the section under the combined effect of gravity loads and earthquake loads are calculated
- P-M interaction curves are defined based on the existing material strengths and for deformation values of $\epsilon_{cu}=0.003$ and $\epsilon_{su}=0.01$
- A line from (M_d, N_d) to (M_E, N_E) cuts through the P-M interaction curve. The intersection point is the moment capacity of the section, M_p
- The residual moment is calculated considering whether the N_d exceeds the axial force upper limit

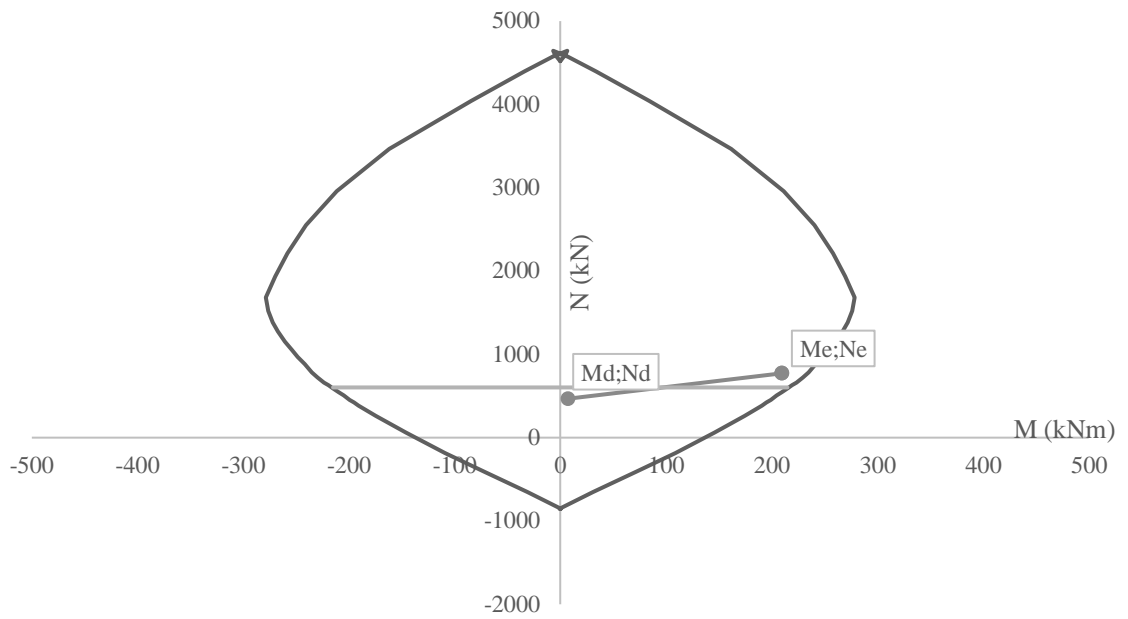


Figure 3.9. Visual demand/capacity inspection for C01 under EXN loading.

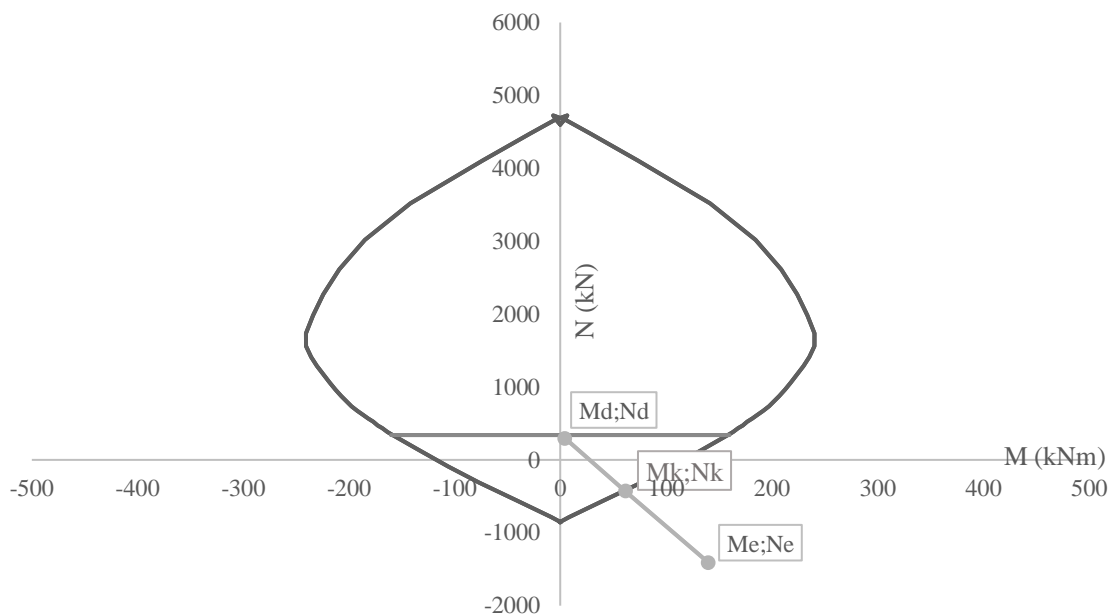


Figure 3.10. Visual demand/capacity inspection for C13 under EXN loading.

Table 3.19. Column damage states under EXN loading.

Columns	r	$N_k/A_c F_{cm}$	$V_e/b_w d f_{ctm}$	r_{MN}	r_{GV}	r_{GC}	r_{state}	(δ/h)	$(\delta/h)_{state}$	Damage State
S01	1.00	0.000	0.257	2.00	3.50	5.00	MN	0.009	MN	MN
S02	1.00	0.226	0.436	1.79	2.87	4.16	MN	0.008	MN	MN
S03	1.00	0.144	0.393	1.93	3.28	4.70	MN	0.007	MN	MN
S04	1.73	0.124	0.363	1.96	3.38	4.84	MN	0.006	MN	MN
S05	1.00	0.256	0.264	1.74	2.72	3.96	MN	0.006	MN	MN
S06	1.00	0.160	0.103	1.90	3.20	4.60	MN	0.005	MN	MN
S07	2.31	0.019	0.467	2.00	3.50	5.00	BH	0.007	MN	BH
S08	1.00	0.226	0.279	1.79	2.87	4.16	MN	0.009	MN	MN
S09	1.52	0.164	0.238	1.89	3.18	4.57	MN	0.008	MN	MN
S10	1.00	0.198	0.105	1.84	3.01	4.35	MN	0.006	MN	MN
S11	1.00	0.226	0.189	1.79	2.87	4.16	MN	0.005	MN	MN
S12	1.83	0.025	0.327	2.00	3.50	5.00	MN	0.007	MN	MN
S13	1.72	0.000	0.196	2.00	3.50	5.00	GC	0.006	MN	MN
S14	1.00	0.138	0.330	1.94	3.31	4.75	MN	0.009	MN	MN
S15	1.00	0.161	0.344	1.90	3.19	4.59	MN	0.008	MN	MN
S16	3.43	0.083	0.293	2.00	3.50	5.00	BH	0.007	MN	BH
S17	1.00	0.106	0.198	1.99	3.47	4.96	MN	0.007	MN	MN
S18	1.00	0.104	0.222	1.99	3.48	4.97	MN	0.006	MN	MN
S19	1.00	0.139	0.184	1.93	3.30	4.74	MN	0.006	MN	MN
S20	1.00	0.146	0.140	1.92	3.27	4.69	MN	0.005	MN	MN

Table 3.20. Column damage states under EXP loading.

Columns	r	$N_k/A_c F_{cm}$	$V_e/b_w d f_{ctm}$	r_{MN}	r_{GV}	r_{GC}	r_{state}	(δ/h)	$(\delta/h)_{state}$	Damage State
S01	3.07	0.04	0.23	2.00	3.50	5.00	BH	0.007	MN	BH
S02	1.64	0.11	0.44	1.99	3.46	4.95	MN	0.006	MN	MN
S03	2.30	0.12	0.29	1.96	3.39	4.85	BH	0.006	MN	BH
S04	3.04	0.16	0.25	1.90	3.21	4.61	BH	0.005	MN	BH
S05	1.00	0.09	0.26	2.00	3.50	5.00	MN	0.007	MN	MN
S06	1.00	0.07	0.10	2.00	3.50	5.00	MN	0.006	MN	MN
S07	1.76	0.13	0.49	1.96	3.37	4.83	MN	0.007	MN	MN
S08	1.00	0.22	0.28	1.80	2.91	4.22	MN	0.009	MN	MN
S09	1.00	0.29	0.23	1.69	2.57	3.77	MN	0.008	MN	MN
S10	1.00	0.21	0.10	1.82	2.97	4.29	MN	0.006	MN	MN
S11	1.00	0.22	0.19	1.79	2.88	4.17	MN	0.005	MN	MN
S12	1.00	0.24	0.34	1.77	2.80	4.07	MN	0.007	MN	MN
S13	1.00	0.11	0.20	1.98	3.43	4.91	MN	0.006	MN	MN
S14	1.00	0.23	0.33	1.78	2.84	4.11	MN	0.009	MN	MN
S15	1.00	0.23	0.34	1.78	2.83	4.11	MN	0.008	MN	MN
S16	1.00	0.20	0.29	1.83	2.99	4.32	MN	0.007	MN	MN
S17	1.00	0.13	0.20	1.96	3.37	4.83	MN	0.007	MN	MN
S18	1.00	0.20	0.22	1.84	3.01	4.34	MN	0.006	MN	MN
S19	1.00	0.21	0.18	1.81	2.93	4.24	MN	0.006	MN	MN
S20	1.00	0.22	0.14	1.80	2.91	4.22	MN	0.005	MN	MN

Table 3.21. Column damage states under EYP loading.

Columns	r	$N_k/A_c F_{cm}$	$V_e/b_w d f_{ctm}$	r_{MN}	r_{GV}	r_{GC}	r_{state}	(δ/h)	$(\delta/h)_{state}$	Damage State
S01	2.86	0.09	0.03	2.00	3.50	5.00	BH	0.013	BH	BH
S02	2.43	0.15	0.02	1.92	3.27	4.69	BH	0.013	BH	BH
S03	2.27	0.09	0.06	2.00	3.50	5.00	BH	0.013	BH	BH
S04	3.01	0.03	0.07	2.00	3.50	5.00	BH	0.013	BH	BH
S05	2.32	0.22	0.00	1.80	2.90	4.21	BH	0.013	BH	BH
S06	2.46	0.16	0.04	1.90	3.19	4.58	BH	0.013	BH	BH
S07	3.27	0.00	0.03	2.00	3.50	5.00	BH	0.013	BH	BH
S08	2.24	0.13	0.03	1.95	3.34	4.79	BH	0.013	BH	BH
S09	2.76	0.23	0.00	1.78	2.83	4.11	BH	0.013	BH	BH
S10	2.71	0.20	0.01	1.84	3.01	4.35	BH	0.013	BH	BH
S11	2.08	0.25	0.06	1.75	2.76	4.01	BH	0.013	BH	BH
S12	2.31	0.07	0.01	2.00	3.50	5.00	BH	0.013	BH	BH
S13	2.71	0.06	0.01	2.00	3.50	5.00	BH	0.013	BH	BH
S14	2.61	0.16	0.07	1.90	3.20	4.60	BH	0.013	BH	BH
S15	2.35	0.19	0.04	1.85	3.05	4.40	BH	0.013	BH	BH
S16	3.25	0.10	0.03	2.00	3.49	4.98	BH	0.013	BH	BH
S17	3.05	0.10	0.00	2.00	3.49	4.99	BH	0.013	BH	BH
S18	2.55	0.13	0.03	1.95	3.34	4.79	BH	0.013	BH	BH
S19	2.80	0.16	0.04	1.90	3.19	4.58	BH	0.013	BH	BH
S20	2.63	0.22	0.08	1.79	2.88	4.17	BH	0.013	BH	BH

Table 3.22. Column damage states under EYN loading.

Columns	r	$N_k/A_c F_{cm}$	$V_e/b_w d f_{ctm}$	r_{MN}	r_{GV}	r_{GC}	r_{state}	(δ/h)	$(\delta/h)_{state}$	Damage State
S01	2.56	0.15	0.03	1.92	3.26	4.68	BH	0.013	BH	BH
S02	2.19	0.22	0.02	1.80	2.90	4.20	BH	0.013	BH	BH
S03	3.16	0.00	0.06	2.00	3.50	5.00	BH	0.013	BH	BH
S04	2.55	0.08	0.07	2.00	3.50	5.00	BH	0.013	BH	BH
S05	2.48	0.14	0.00	1.93	3.30	4.73	BH	0.013	BH	BH
S06	2.91	0.09	0.04	2.00	3.50	5.00	BH	0.013	BH	BH
S07	3.22	0.02	0.03	2.00	3.50	5.00	BH	0.013	BH	BH
S08	1.93	0.24	0.03	1.77	2.82	4.09	BH	0.013	BH	BH
S09	2.90	0.19	0.00	1.85	3.05	4.40	BH	0.013	BH	BH
S10	2.75	0.17	0.01	1.88	3.15	4.53	BH	0.013	BH	BH
S11	2.54	0.16	0.06	1.90	3.19	4.58	BH	0.013	BH	BH
S12	2.07	0.12	0.01	1.97	3.40	4.86	BH	0.013	BH	BH
S13	3.47	0.00	0.01	2.00	3.50	5.00	BH	0.013	BH	BH
S14	2.33	0.24	0.07	1.77	2.81	4.08	BH	0.013	BH	BH
S15	2.31	0.20	0.04	1.83	2.98	4.31	BH	0.013	BH	BH
S16	2.70	0.18	0.03	1.87	3.10	4.47	BH	0.013	BH	BH
S17	3.21	0.06	0.00	2.00	3.50	5.00	BH	0.013	BH	BH
S18	2.57	0.13	0.03	1.95	3.36	4.81	BH	0.013	BH	BH
S19	2.67	0.15	0.04	1.92	3.27	4.69	BH	0.013	BH	BH
S20	2.97	0.15	0.08	1.92	3.26	4.68	BH	0.013	BH	BH

In order to determine the type of the failure in the walls, the shear force, V_e , in accordance with the bending capacity of the wall's cross-sections shall be compared with the shear strength V_r of the section.

If the calculated value of V_e is greater than the shear force obtained from the V_R , V_R will be used to determine the failure type.

After determining the type of failure, the demand/capacity ratio was determined by means of interaction diagrams for the walls as for the columns. The following figures show the case for the negative X earthquake loading.

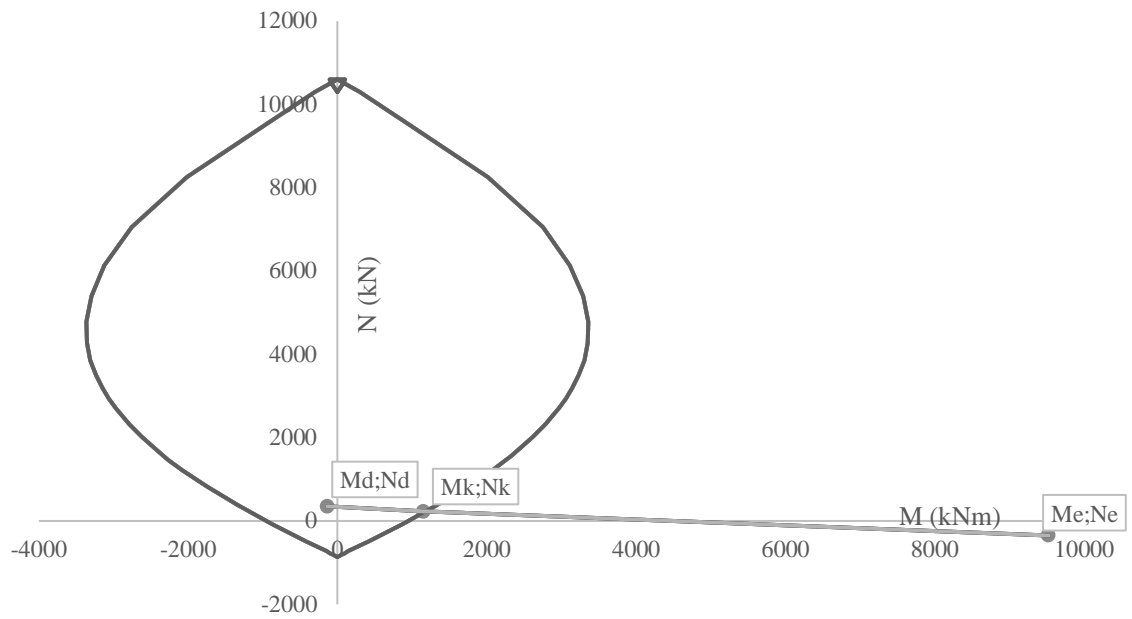


Figure 3.11. Visual demand/capacity inspection for P101 under EXN loading.

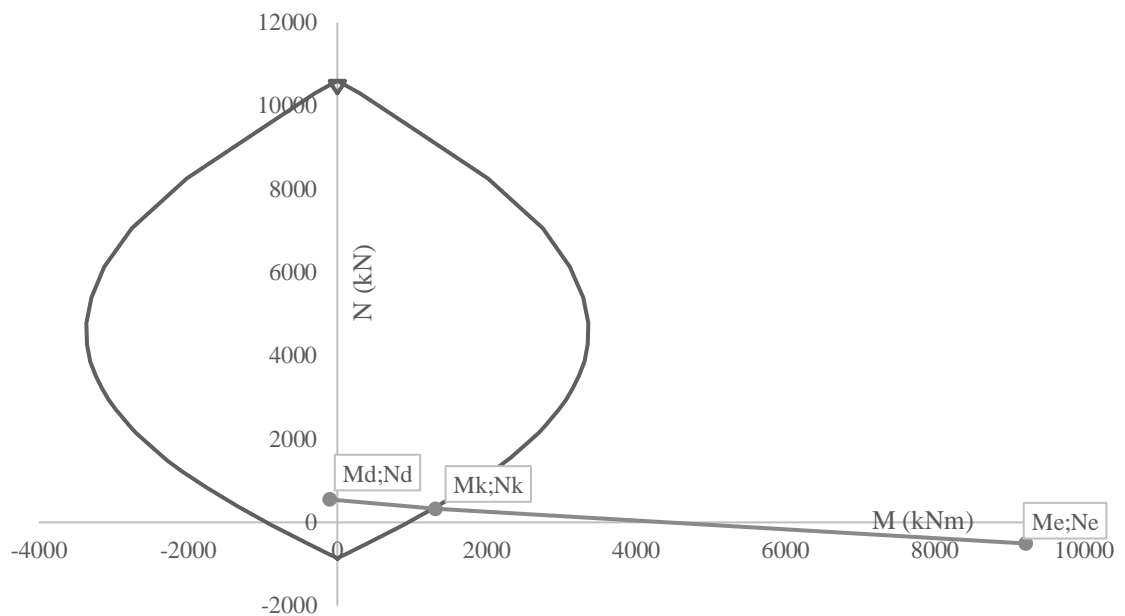


Figure 3.12. Visual demand/capacity inspection for P102 under EXN loading.

If damage levels resulted from the drift ratios are more unfavorable than from the ones obtained by means of demand/capacity ratios, the ones determined from the drift ratios shall be taken into account. The relative displacement ratios and the demand/capacity ratios of the walls are presented in Table 3.23.

Table 3.23. Damage levels of the wall section.

Loading	Story	Columns	r	r _{MN}	r _{GV}	r _{GC}	r _{state}	(δ/h)	(δ/h) _{state}	Damage State
EXN	First	P101	7.44	2	4	6	GC	0.0076	MN	GC
	Second	P201	4.88	2	4	6	İH	0.0117	BH	İH
	Third	P301	2.79	2	4	6	BH	0.0124	BH	BH
	Fourth	P401	1.19	2	4	6	MN	0.0111	BH	BH
	First	P102	6.99	2	4	6	GC	0.0073	MN	GC
	Second	P202	5.40	2	4	6	İH	0.0112	BH	İH
	Third	P302	3.36	2	4	6	BH	0.0120	BH	BH
	Fourth	P402	2.77	2	4	6	BH	0.0109	BH	BH
EXP	First	P101	11.49	2	4	6	GC	0.0076	MN	GC
	Second	P201	5.25	2	4	6	İH	0.0117	BH	İH
	Third	P301	2.29	2	4	6	BH	0.0124	BH	BH
	Fourth	P401	1.00	2	4	6	MN	0.0111	BH	BH
	First	P102	9.17	2	4	6	GC	0.0073	MN	GC
	Second	P202	5.46	2	4	6	İH	0.0112	BH	İH
	Third	P302	2.93	2	4	6	BH	0.0120	BH	BH
	Fourth	P402	2.58	2	4	6	BH	0.0109	BH	BH
EYN	First	P101	4.19	2	4	6	İH	0.0128	BH	İH
	Second	P201	6.26	2	4	6	GC	0.0191	BH	GC
	Third	P301	5.94	2	4	6	İH	0.0172	BH	İH
	Fourth	P401	5.05	2	4	6	İH	0.0121	BH	İH
	First	P102	4.18	2	4	6	İH	0.0128	BH	İH
	Second	P202	6.69	2	4	6	GC	0.0191	BH	GC
	Third	P302	4.49	2	4	6	İH	0.0172	BH	İH
	Fourth	P402	3.65	2	4	6	BH	0.0121	BH	BH
EYP	First	P101	5.22	2	4	6	İH	0.0128	BH	İH
	Second	P201	7.71	2	4	6	GC	0.0191	BH	GC
	Third	P301	6.41	2	4	6	GC	0.0172	BH	GC
	Fourth	P401	5.05	2	4	6	İH	0.0121	BH	İH
	First	P102	3.73	2	4	6	BH	0.0128	BH	BH
	Second	P202	4.87	2	4	6	İH	0.0191	BH	İH
	Third	P302	4.35	2	4	6	İH	0.0172	BH	İH
	Fourth	P402	3.39	2	4	6	BH	0.0121	BH	BH

3.2.2. Linear Assessment Based on Turkish Building Seismic Code 2018

The building knowledge level is accepted as the limited knowledge level since there are insufficient core samples according to the knowledge level criteria of TBSC 2018. As it is shown in Table 3.24, existing concrete compressive strength is taken as 18.08 MPa due to the provision defined for limited knowledge level. TBSC 2018 is dictating that if the number of samples is more than three, the greater of the value obtained from the samples (mean minus standard deviation) and the value (0.85 times average) shall be taken as the *existing concrete strength*.

Table 3.24. Existing material strength for TBSC 2018.

Core Sample	Corrected Compressive Strength (Mpa)
C1	20.27
C2	22.13
C3	16.28
C4	22.32
C5	20.27
	$f_{cm}=18.08$

In order to conduct the linear analysis, the SAP2000 analysis program has been used. Analytical model is constructed so to reflect the behavior of the building correctly under the combined effect of equivalent earthquake loads and gravity loads. In the model, frame elements and shear walls are defined as line elements connected to nodes representing the beam-column joints.

Unlike TBSC 2007, TBSC 2018 dictates strict rules for modeling of structural systems. According to rules defined for the models to be used for elastic analysis in TBSC 2018, to model the shear walls as equivalent line elements, the ratio of the largest shear wall arm length to the total shear wall height shall not exceed 1/2. For elastic analyses, if the shear walls that meet this condition are modeled as line elements:

- At floor levels, the dependent degrees of freedom of the joints where the shear wall connected with the beam and/or floor finite elements in the plan shall be constrained kinematically to the six independent degrees of freedom of the joints of equivalent line element which is defined at the shear wall's center of mass. Constrain shall ensure that connected joints exhibit three-dimensional rigid body motion.
- The effective section stiffnesses under bending and shear for shear walls modeled as equivalent line elements shall be determined according to 4.5.8.

Considering these limitations, the equivalent beam-column element approach adopted in TBSC 2007 model was not used for TBSC 2018. The joints of the equivalent line elements are connected to the surrounding joints employing body constraints so that the joints show three-dimensional rigid body motion.

The effective section stiffnesses for elastic behavior are given in 4.5.4.7. In contrast to the regulations in TBSC 2007, effective section stiffnesses for elastic behavior in columns and walls are constant values independent of axial force.

Table 3.25. Effective section stiffness modifiers for elastic analysis.

Effective Section Stiffness Modifiers		
Line Elements	Bending	Shear
Coupling Beam	0.15	1.00
Beam	0.35	1.00
Column	0.70	1.00
Shear Wall (Equivalent Line Element)	0.50	0.50

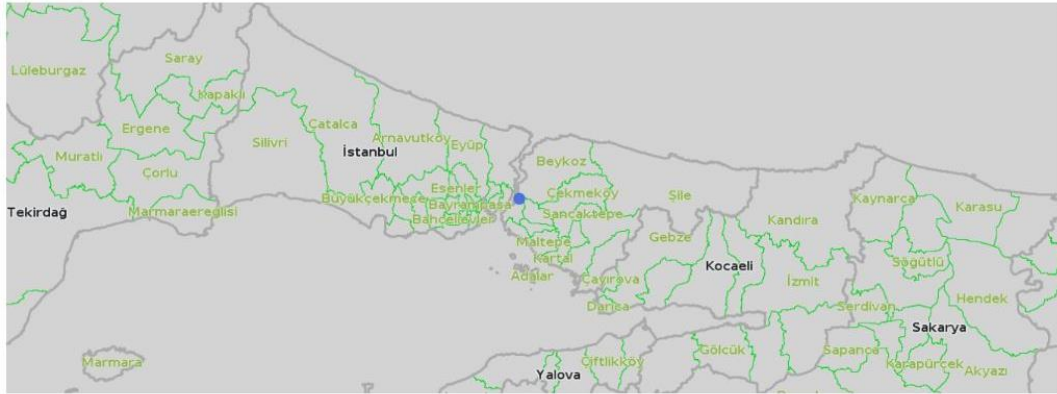


Figure 3.13. Location of the building (taken from <https://tdth.afad.gov.tr/>).

In order to construct the 5%-damped elastic acceleration response spectrum, *the sort-period map spectral acceleration coefficient* and *the map spectral acceleration coefficient of 1.0 second period* are obtained from <https://tdth.afad.gov.tr/> website. Obtained parameters are given as follows;

$$S_s = 0.773$$

$$S_1 = 0.219$$

Based on the S_s and S_1 , for ZD class of sites;

$$F_s = 1.191$$

$$F_1 = 2.162$$

Consequently, design spectral acceleration coefficients are;

$$S_{DS} = S_s F_s = 0.920$$

$$S_{D1} = S_1 F_1 = 0.423$$

The site-specific elastic spectrum of TBSC 2018 is constructed and given in Figure 3.14, with the one calculated in the previous chapter based on the regulations of TBSC 2007.

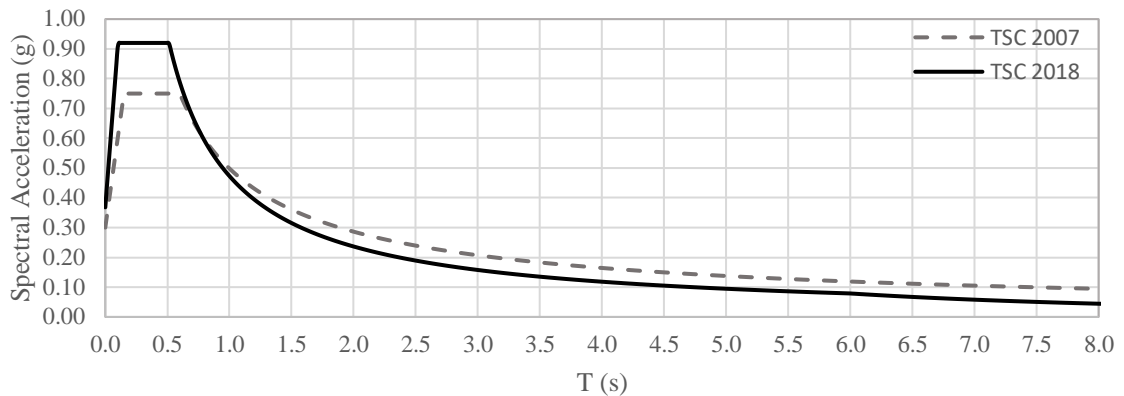


Figure 3.14. Elastic acceleration spectrum.

The linear assessment methods shall be used to determine the earthquake performance of buildings are the Equivalent Earthquake Load Method and the Mode Superposition Method.

The buildings where the equivalent earthquake load method can be applied are given in Table 3.26.

Table 3.26. Buildings for which equivalent earthquake load method is applicable.

Building Type	Permitted Building Height Class	
	DTS=1, 1a, 2, 2a	DTS=3, 3a, 4, 4a
Buildings with torsional irregularity coefficient satisfying the condition $\eta_{bi} \leq 2.0$ at every story and at the same time without type B2 irregularity	BYS ≥ 4	BYS ≥ 5
All buildings	BYS ≥ 5	BYS ≥ 6

Earthquake design class definition is based on two parameters; building usage class and short period map spectral acceleration under DD-2 level earthquake ground motion. Earthquake design class definitions are given in Table 3.27

Table 3.27. Earthquake Design Classes

Short Period Map Spectral Acceleration Under DD-2 Level Earthquake Ground Motion (S_{DS})	Building Usage Class	
	BKS = 1	BKS = 2, 3
$S_{DS} < 0.33$	DTS = 4a	DTS = 4
$0.33 \leq S_{DS} < 0.50$	DTS = 3a	DTS = 3
$0.50 \leq S_{DS} < 0.75$	DTS = 2a	DTS = 2
$0.75 \leq S_{DS}$	DTS = 1a	<u>DTS = 1</u>

- Case study structure is a residential building, therefore BKS = 3
- $S_{DS} = 0.920$ for the location of the building

As it can be deduced from the table, DTS = 1 for the case study building. Considering Table 3.26, BYS shall be greater than 4 to adopt equivalent seismic load methodology.

In order to determine BYS, the building height and the base of the building should be identified. According to TBSC 2018 3.3.1.1, in buildings with basement floors satisfying both of the conditions given in (a) and (b), the base of the building shall be defined at the floor level above the basement floors.

- (c) Rigid basement walls surround the building from all sides or at least from three sides
- (d) In the dominant vibration modes for each orthogonal direction, the ratio between *the natural vibration period* which is calculated for the whole building including basement floors, and *the natural vibration period* calculated excluding basement mass and the ground floor is less than 1.1 ($T_{p,all} \leq T_{p,upper}$)

The case study building satisfies the condition defined in (a). To investigate (b), the mass of the basement floor and walls and loads acting right above the basement are neglected. Results are presented in Table 3.28

Table 3.28. Comparison of periods including and excluding basement floor.

Natural Vibration Period of The Building Including Basement Floor				Natural Vibration Period of The Building Excluding Basement Floor			
Mode	Period (s)	Ux(%)	Uy(%)	Mode	Period (s)	Ux(%)	Uy(%)
2	0.946	0.003	0.603	2	0.939	0.004	0.760
3	0.705	0.602	0.002	3	0.698	0.754	0.002

According to results, the base of the building shall be defined right above the basement. Consequently, the building height is 11.9 m , and the building height class is 6, as given in Table 3.29.

Table 3.29. Building height intervals based on the building height classes and earthquake design classes.

Building Height Class	Building Height Intervals Based on the Building Height Classes and Earthquake Design Classes		
	DTS = 1, 1a, 2, 2a	DTS = 3, 3a	DTS = 4, 4a
BYS = 1	$H_N > 70$	$H_N > 91$	$H_N > 105$
BYS = 2	$56 < H_N \leq 70$	$70 < H_N \leq 91$	$91 < H_N \leq 105$
BYS = 3	$42 < H_N \leq 56$	$56 < H_N \leq 70$	$56 < H_N \leq 91$
BYS = 4	$28 < H_N \leq 42$	$42 < H_N \leq 56$	
BYS = 5	$17.5 < H_N \leq 28$	$28 < H_N \leq 42$	
<u>BYS = 6</u>	<u>$10.5 < H_N \leq 17.5$</u>	$17.5 < H_N \leq 28$	
BYS = 7	$7 < H_N \leq 10.5$	$10.5 < H_N \leq 17.5$	
BYS = 8	$H_N \leq 7$	$H_N \leq 10.5$	

At this point, it is also possible to identify the performance objective of the building. The building performance objective refers to the building performance level to be met under different ground motion levels, according to TBSC 2018. Building performance objectives are defined based on the earthquake design class and building height class.

Table 3.30. Performance Objectives for Existing Cast-in-Place Reinforced Concrete, Precast Reinforced Concrete and Steel Structures (Except High-Rise Buildings $\text{BYS} \geq 2$).

Ground Motion Level	DTS = 1, 2, 3, 3a, 4, 4a		DTS = 1a, 2a	
	Ordinary Performance Objective	Evaluation/Design Approach	Advanced Performance Objective	Evaluation/Design Approach
DD-3	-	-	SH	ŞGDT
DD-2	KH	ŞGDT	-	-
DD-1	-	-	KH	ŞGDT

Based on Table 3.30, the building must meet the controlled damage performance objective under the DD-2 earthquake.

After verifying the earthquake design class and building height class obligations hold for the building, torsional irregularities are investigated.

In order to adopt the equivalent earthquake load methodology, the torsional irregularity coefficient must be less than 2 for each floor. Before the torsional irregularity check, equivalent earthquake loads were calculated by following the rules in the regulation and were applied to the diaphragm mass centers. Torsional irregularity under equivalent seismic loads was examined, and the suitability of the building is presented at the end of the section.

For performance assessment, additional eccentricity effect shall be neglected as in the regulations of TBSC 2007. In the calculation of the total equivalent earthquake load according to equation 4.19 and equation 4.8, $R_a = 1$ shall be taken.

Total equivalent seismic load acting on the building (base shear) in the earthquake direction considered shall be determined by the following equation;

$$V_{tE}^{(X)} = m_t S_{aR} (T_p^{(X)}) \geq 0.04 m_t I S_{DS} g \quad (3.3)$$

Distribution of the total equivalent seismic load amongst floors is the same as is followed in TBSC 2007. However, method differentiates from TBSC 2007 in the consideration of dominant natural vibration period of the building in the earthquake direction, $T_p^{(X)}$. TBSC 2007 limits the dominant natural vibration period of the building by the period obtained from Rayleigh Quotient. Also, TBSC 2018, permits to use Rayleigh Quotient to determine period, however, limits period to be considered in the calculation of equivalent seismic load through an empirical equation which is given below. Value of the dominant natural vibration period to be considered in the calculation of equivalent seismic load shall not be greater than 1.4 times of T_{pA} .

$$T_{pA} = C_t H_N^{3/4} \quad (3.4)$$

- (a) For buildings with the structural system comprised of solely reinforced concrete frames $C_t = 1$, with the structural system comprised of steel frames or braced frame systems $C_t = 0.08$, for the other type of buildings $C_t = 0.07$.

For the case study building, C_t is taken as 0.07, and the results are given in Table 3.31.

Table 3.31. Dominant natural vibration periods.

	2018		2007	
	$T_p^{(X)} = 2\pi \left(\frac{\sum_{j=1}^N m_i d_{fi}^{(X)2}}{\sum_{j=1}^N F_{fi}^{(X)} d_{fi}^{(X)}} \right)^{1/2}$	$1.4 T_{pA}$	$T_1 = 2\pi \left(\frac{\sum_{j=1}^N m_i d_{fi}^2}{\sum_{j=1}^N F_{fi} d_{fi}} \right)^{1/2}$	
$T_p^{(Y)}$	0.950	<u>0.628</u>	1.108	
$T_p^{(X)}$	0.710	<u>0.628</u>	0.769	

Corresponding elastic accelerations were obtained utilizing the elastic spectrum, and total equivalent seismic loads for orthogonal directions are calculated.

$$V_{tE}^{(X)} = m_t S_{aR} (1.4 T_{pA}^{(X)}) = 8986 \text{ kN}$$

$$V_{tE}^{(Y)} = m_t S_{aR} (1.4 T_{pA}^{(Y)}) = 8986 \text{ kN}$$

Equivalent seismic loads acting onto each floor is compared in Table 3.32 for the codes.

Table 3.32. Rayleigh period calculations.

Story	w_i (kN)	H_i (m)	TBSC 2018		TBSC 2007	
			$F_{i,X}$ (kN)	$F_{i,Y}$ (kN)	$F_{i,X}$ (kN)	$F_{i,Y}$ (kN)
4	2883.16	11.9	3682	3682	2555	1907
3	3004.80	8.9	2660	2660	1846	1378
2	3020.99	5.9	1773	1773	1230	918
1	3019.42	2.9	871	871	604	451
		Σ	8986	8986	6237	4655
Basement	2896.11	0	1066	1066	868	868
		Σ	10052	10052	7105	5524

Unlike TBSC 2007, there is no factor of $\lambda = 0.85$ is defined in TBSC 2018 to reduce the total base shear.

Lastly, the presence of torsional irregularity is investigated using calculated earthquake forces, and it is verified that the building is appropriate to be analyzed by the equivalent seismic load method.

Table 3.33. Torsional irregularity control for the negative X direction.

Loading	Joint	U_x	U_y	U_z	Δ	Joint	U_x	U_y	U_z	Δ	η_{bi}
EXN	TRC1	-0.188	-0.011	0.023	0.044	TLC1	-0.123	-0.012	0.019	0.034	1.13
EXN	TRC2	-0.143	-0.010	0.028	0.053	TLC2	-0.089	-0.011	0.023	0.037	1.18
EXN	TRC3	-0.090	-0.008	0.030	0.053	TLC3	-0.052	-0.008	0.024	0.032	1.24
EXN	TRC4	-0.037	-0.004	0.026	0.037	TLC4	-0.020	-0.004	0.020	0.020	1.30

Table 3.34. Torsional irregularity control for the positive X direction.

Loading	Joint	U_x	U_y	U_z	Δ	Joint	U_x	U_y	U_z	Δ	η_{bi}
EXP	TRC1	0.188	0.011	-0.023	0.044	TLC1	0.123	0.012	-0.019	0.034	1.13
EXP	TRC2	0.143	0.010	-0.028	0.053	TLC2	0.089	0.011	-0.023	0.037	1.18
EXP	TRC3	0.090	0.008	-0.030	0.053	TLC3	0.052	0.008	-0.024	0.032	1.24
EXP	TRC4	0.037	0.004	-0.026	0.037	TLC4	0.020	0.004	-0.020	0.020	1.30

Table 3.35. Torsional irregularity control for the negative Y direction.

Loading	Joint	U_x	U_y	U_z	Δ	Joint	U_x	U_y	U_z	Δ	η_{bi}
EYN	TRC1	-0.019	-0.283	-0.024	0.059	BRC1	-0.019	-0.261	-0.026	0.054	1.04
EYN	TRC2	-0.016	-0.224	-0.035	0.080	BRC2	-0.016	-0.206	-0.036	0.074	1.04
EYN	TRC3	-0.011	-0.144	-0.043	0.087	BRC3	-0.011	-0.132	-0.045	0.081	1.04
EYN	TRC4	-0.005	-0.057	-0.040	0.057	BRC4	-0.005	-0.052	-0.042	0.052	1.05

Table 3.36. Torsional irregularity control for the positive Y direction.

Loading	Joint	U_x	U_y	U_z	Δ	Joint	U_x	U_y	U_z	Δ	η_{bi}
EYP	TRC1	0.019	0.283	0.024	0.059	BRC1	0.019	0.261	0.026	0.054	1.04
EYP	TRC2	0.016	0.224	0.035	0.080	BRC2	0.016	0.206	0.036	0.074	1.04
EYP	TRC3	0.011	0.144	0.043	0.087	BRC3	0.011	0.132	0.045	0.081	1.04
EYP	TRC4	0.005	0.057	0.040	0.057	BRC4	0.005	0.052	0.042	0.052	1.05

It has been determined that the building provides the necessary conditions for the application of the Equivalent Earthquake Load Method. TBSC 2018 has significant differences in this step compared to TBSC 2007. According to TBSC 2018, the applicability of the equivalent earthquake load method or mode superposition method is not a sufficient condition alone to carry out a linear assessment procedure. TBSC 2018 introduces seven regulations to limit the applicability of linear calculation methods. According to TBSC 2018, if any of the conditions given below arises, linear methods shall not be performed.

- (a) Building height class is less than 5 ($BYS < 5$)
- (b) Discontinuity of vertical structural members
- (c) In reinforced concrete buildings, at any of the floor except the top, the average of EKO values, scaled by shear force, of vertical ductile elements is greater than the average EKO value of the beams for each earthquake direction
- (d) At any floor except the top, the average of EKO values, scaled by shear force, of vertical ductile columns, ductile walls, and strengthened partition walls is greater than 3, for each earthquake direction
- (e) At any floor except the top, the average EKO value of the ductile beams is greater than 5 for each earthquake direction

Scaled EKO values by the shear force that is defined in (c) and (d) are calculated by the following equation;

$$EKO = \frac{\sum_i V_i (EKO)_i}{\sum_i V_i} \quad (3.5)$$

In the presence of any of the conditions defined from (a) to (e), the existing building shall be evaluated by nonlinear methods.

For the case study building, while the beams meet the requirements, the elastic method could not be applied because of the columns since columns yielded higher EKO values than beams in each direction.

3.3. Nonlinear Static Analysis

Nonlinear static analysis, in other words, *pushover* analysis is fundamentally the extension of the “lateral force procedure” of linear static analysis into the nonlinear range. Pushover analysis is performed under constant gravity loads and monotonically increasing lateral loading applied to the masses of the structural model. The shape of the loading is determined so to mimic inertia forces of the dominant mode due to a horizontal component of the seismic action. Global displacement demand on the structure under seismic intensity can not be directly determined through the pushover analysis. The global displacement demand must be obtained from some other means, such as modal analysis, since what is obtained is essentially a generalized force-displacement response of the structure (Fardis, 2009). Moreover, it provides reliable results only for low-rise buildings where translational modes are dominant, and torsional irregularity is limited.

Throughout the analysis, plastic hinges, the development of the plastic mechanism and damage gradually emerges as a function of the magnitude of the monotonically increasing lateral loads, and the resulting displacements. (Fardis, 2009) Tracing the formation of plastic hinges in the sections and their occurrence sequence are of prime importance in evaluating the behavior of the structural system.

As it is stated previously, global displacement demand can not be directly obtained, and an axis change is required to represent the pushover curve and the demand curve on the same plane to determine the demand hereof. To realize this, base shear force is converted to modal acceleration, and the roof displacement is converted to modal displacement. The intersection of two curves yields the target displacement of the system under earthquake demand. For this intersection, TBSC 2007 and TBSC 2018 make use of the linear elastic displacement of the equivalent single degree of freedom system (SDOF) on the basis of equal displacement rule. Considering equal displacement rule, there are two cases. In the former case, where the dominant period is longer than the period specified in the code, elastic and elastoplastic displacements are considered to be approximately equal. In the latter case, elastoplastic displacement is obtained by increasing the elastic displacement by a coefficient.

Nonlinear models of the building to be used for nonlinear static analyses were established to determine the internal forces, displacements, and plastic deformations of the structural elements under the effect of incremental equivalent earthquake loads, on the basis of regulations in the TBSC 2007 and TBSC 2018. Models established in section 4.2 were modified so to permit the building to behave in the nonlinear range.

Nonlinear behavior of the structural elements was idealized utilizing lumped plasticity, meaning that inelasticity is concentrated on critical sections, whereas remaining parts of the structure are assumed to behave elastically. For the cases where nonlinearity of the elements is represented by the lumped plasticity approach, section capacities are introduced through pre-defined force-deformation relations of zero-length plastic hinge sections.

Force-deformation relations of the plastic hinges are obtained utilizing XTRACT software, which is a fully interactive program having the ability to calculate moment-curvatures, axial force-moment interactions for any cross-section. XTRACT software realizes analyses on discretized sections by fibers, each associated with the uniaxial stress-strain relationship of relevant materials. Since the outputs obtained from XTRACT software are the capacities of the sections, existing material strengths were multiplied by limited knowledge factor to directly generate reduced capacities compatible with limited knowledge level. Material properties used to define plastic hinges, and P-M interaction curves are given in Table 3.37.

Table 3.37. Material properties used to model hinges and interaction curves.

	TBSC 2007	TBSC 2018
$0.75 \times f_{cm}$ (MPa)	12.21	13.56
$E = 5000\sqrt{f_{cm}}$ (MPa)	20170	21260
ϵ_{cu}	0.0030	0.0035
ϵ_{su}	0.0100	0.0100

The stress-strain relationship of the materials is defined so to comply with the regulations in each code. In Turkish Building Seismic Codes, one of the several requirements to consider the core concrete inside the transverse reinforcement as confined concrete, transverse reinforcements shall be hooked 135-degree. For the case study building, reports from in-situ investigations were showing that transverse reinforcements hooked 90-degree. Therefore, there is no confined concrete material definition used to model plastic hinges. Parameters used as an input to model the unconfined concrete and steel materials in XTRACT software are presented in Figure 3.15 and Figure 3.16.

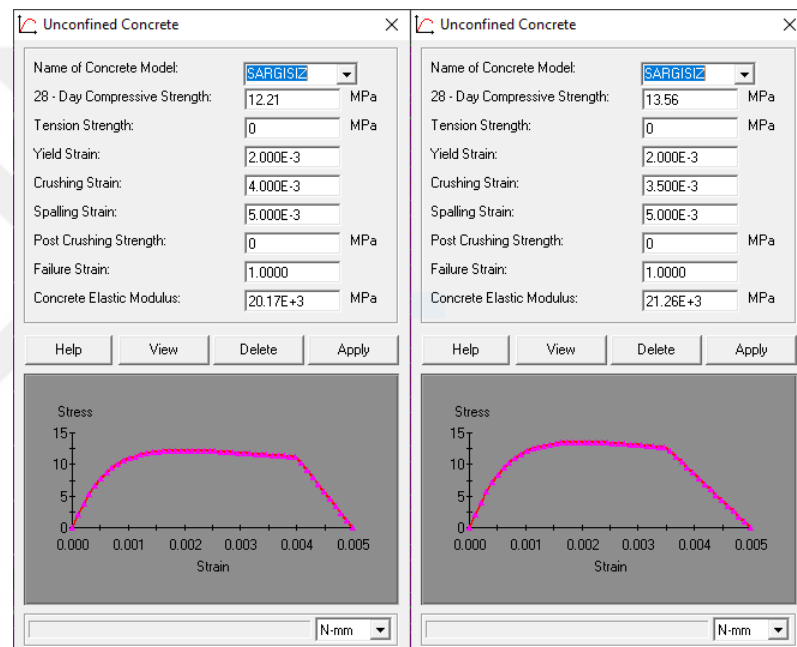


Figure 3.15. Concrete material defined in XTRACT for TBSC 2007 and TBSC 2018, respectively.

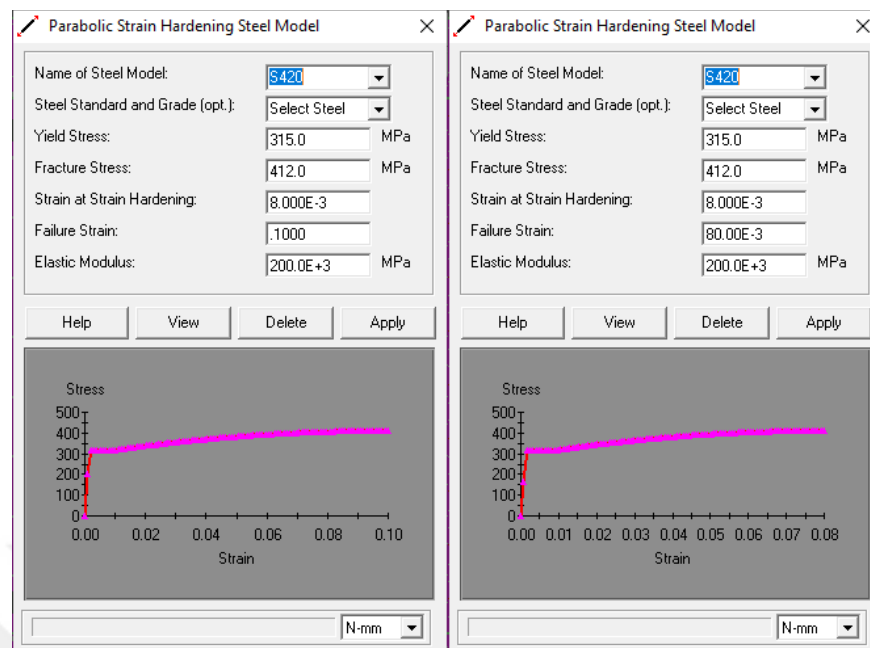


Figure 3.16. Steel material defined in XTRACT for TBSC 2007 and TBSC 2018, respectively.

Hinges only affect the nonlinear behavior of the structure meaning that their effect can be distinguished in nonlinear static and nonlinear dynamic analysis (CSI, 2019). Force- and moment-type hinges in SAP2000 are rigid-plastic, meaning that the component is initially rigid, so there is no elastic deformation, and for monotonically increasing deformation, all of the deformations are plastic. Also, plastic deformation and post-yield deformation are the same. Moment hinges in the beams are the most common examples of such components (Powell, 2010).

There is no uniaxial behavior in columns and walls, unlike beams. The force-deformation relationship has a multi-axial form due to the presence of considerable axial force acting on columns and walls, meaning that two or more forces govern the force-deformation relationship. Interaction surfaces are used to represent these forces (Powell, 2010).

For columns and walls, PMM hinges are defined in the SAP2000 software to describe the relationship between axial force and biaxial moment. The software determines the corresponding capacity moment via the interaction diagram under the effect of the current axial force.

When moment at the cross-section reaches the yield moment capacity corresponding to the current axial force, plastic deformation initiates. Plastic behavior is reflected by employing moment-rotation relationships defined in the software. Attention was given to define several moment-rotation relationships under different axial force values to obtain reliable results.

3.3.1. Nonlinear Static Analysis Based on Turkish Building Seismic Code 2007

TBSC 2007, does not introduce any different effective section stiffness values for linear and nonlinear analyses. Therefore, periods are the same as the model in 3.2.1. The only difference is the assignment of the plastic hinges at the two ends of beams and columns, and at the bottom of the walls at each floor which does not affect the behavior of the structure in the linear range.

According to TBSC 2007, *Incremental Equivalent Earthquake Load Method* can be used if the number of floors is not more than 8 excluding the basement, and the torsional irregularity factor calculated according to linear elastic behavior without additional eccentricity of any floor is less than 1.4. Furthermore, in the earthquake direction considered, the ratio of the effective mass of the dominant vibration mode calculated on the basis of linear elastic behavior to the total building mass (excluding the masses of the basements surrounded by rigid walls) shall be at least 0.70. Investigation for torsional irregularity presented in 3.2.1 holds its validity for the nonlinear model since there is no change made to effect the linear behavior of the building. In the Table 3.36, it is shown that the mass participation ratio meets the necessary condition as well.

Table 3.38. Mass participation ratios.

Mode	Period	U _X	U _Y	R _Z
1	1.184	0.007	0.032	0.758
2	1.068	0.003	0.757	0.030
3	0.741	0.740	0.001	0.008

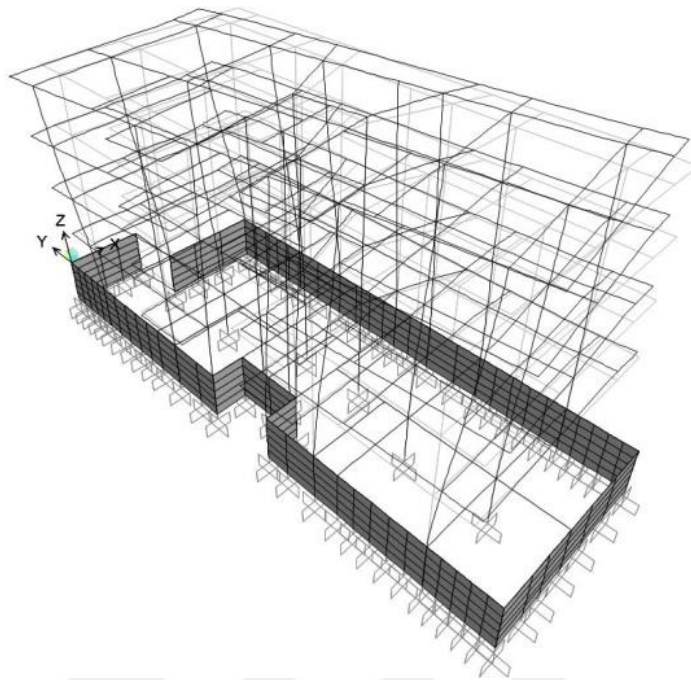


Figure 3.17. The first mode of the analytical model of TBSC 2007.

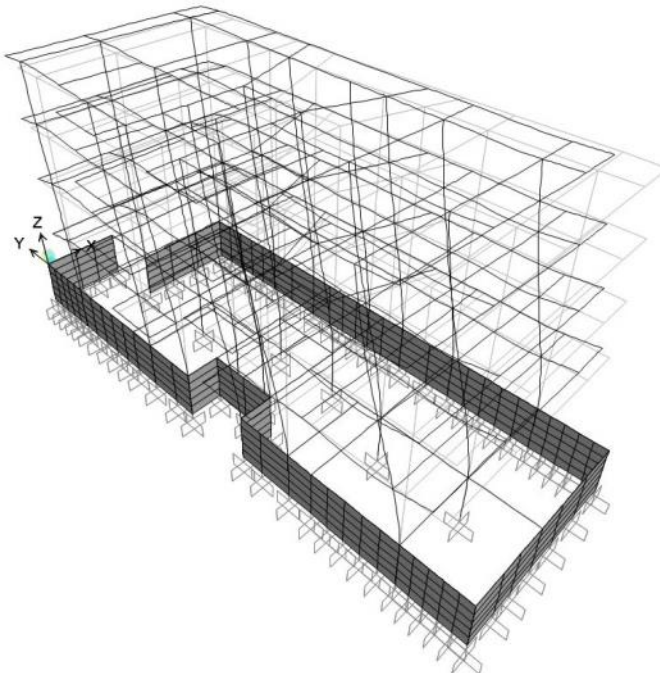


Figure 3.18. The second mode of the analytical model of TBSC 2007.

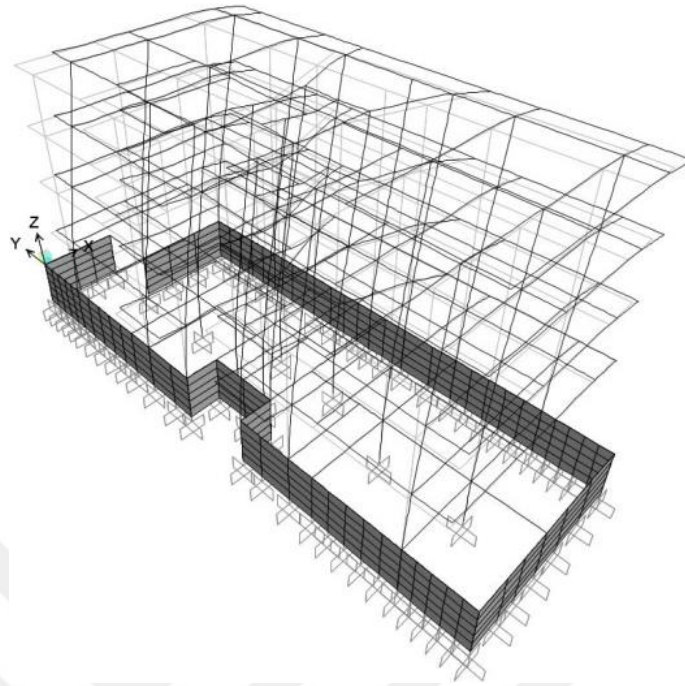


Figure 3.19. The third mode of the analytical model of TBSC 2007.

In order to define the internal force-deformation relations for lumped plastic behavior in beam sections, uniaxial bending analyses were performed, and moment-curvature relationships were obtained. The axial force was not taken into account when determining the moment-curvature relationships since the axial force demands for the beams are insignificant.

Moment-curvature relationships were obtained through the XTRACT program. Since lateral reinforcements are not met the criteria of special earthquake lateral reinforcements, core concrete was also modeled as unconfined concrete.

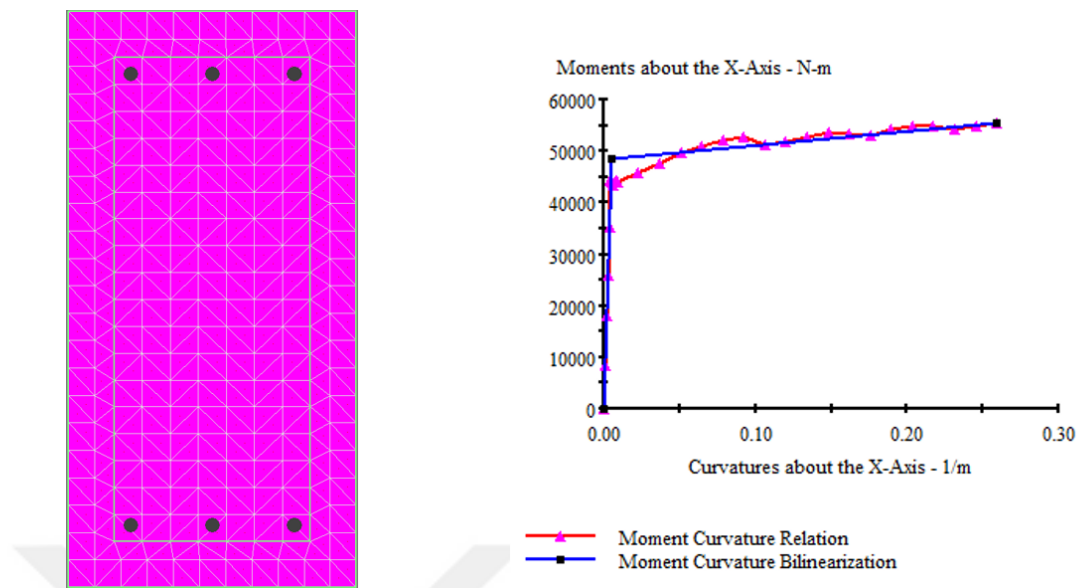


Figure 3.20. Moment-curvature analysis of a beam section in XTRACT.

A total of 74 cross-sectional analyses were carried out considering that the tensile and compression zones of the cross-section would change with the loading direction of the earthquake. The parameters obtained from the moment-curvature analyses are used to define the beam plastic hinges. The results were defined in the SAP2000 program as the moment-rotation relationship. The plastic hinge length specified in the regulation has been taken into account for the calculation of the rotations to define the linearized moment-rotation curve. Moment corresponding to yield curvature and ultimate curvature values are obtained from XTRACT software.

Table 3.39. Parameters used to model hinge S02.

Beam Section	Working Reinforcement	ϕ_y (1/m)	ϕ_u (1/m)	L_p (m)	θ_y	θ_p	M_y (kNm)
S02	Top	0.00869	0.87890	0.15	0.00130	0.13053	39.70
	Bottom	0.00842	0.52790	0.15	0.00126	0.07792	32.06

Plastic rotations, θ_p , are calculated by the following well-known equation:

$$\theta_p = (\phi_u - \phi_y)L_p \quad (3.6)$$

The interaction diagram is calculated through the XTRACT program employing the strain values defined in TBSC 2007. The interaction diagram plotted based on the given strain values are the flow surfaces, according to TBSC 2007.

$$\varepsilon_{cu} = 0.003 ; \varepsilon_{su} = 0.01$$

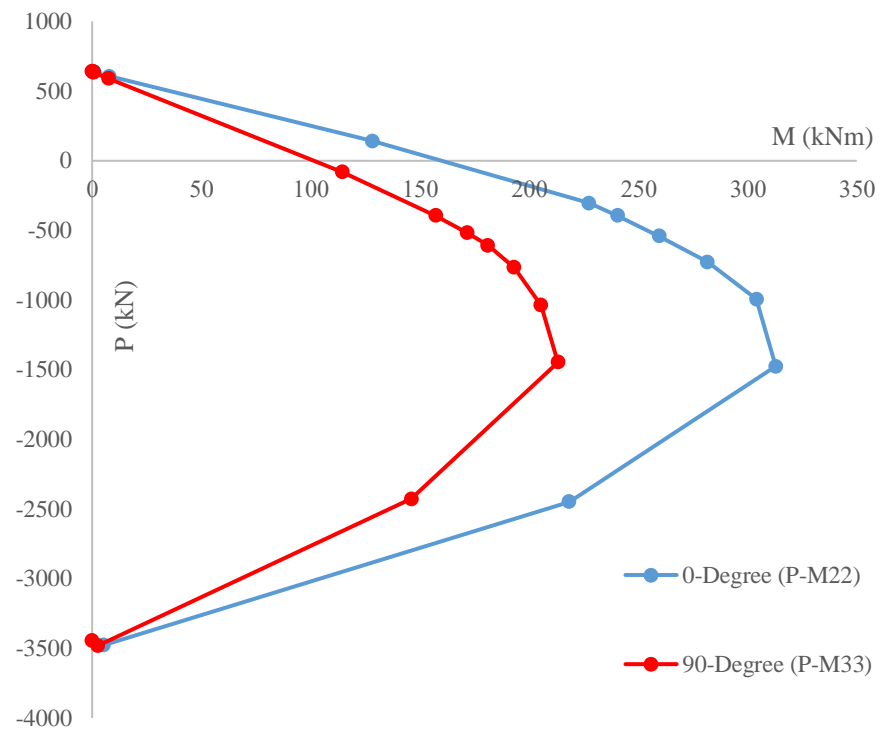


Figure 3.21. P-M interaction diagram for S101.

During pushover analysis, it was assumed that the equivalent seismic load distribution remained constant regardless of the plastic deformations in the structural system. Accordingly, pushover curves obtained from pushover analysis carried out using load shape that is proportional to the first natural vibration mode.

Conducting pushover analyses for orthogonal directions for negative and positive ways were required since the building is non-symmetrical and has unequal reinforcement distribution among beam sections. Pushover curves for positive X and positive Y directions are presented in Figure 3.24 and Figure 3.24.



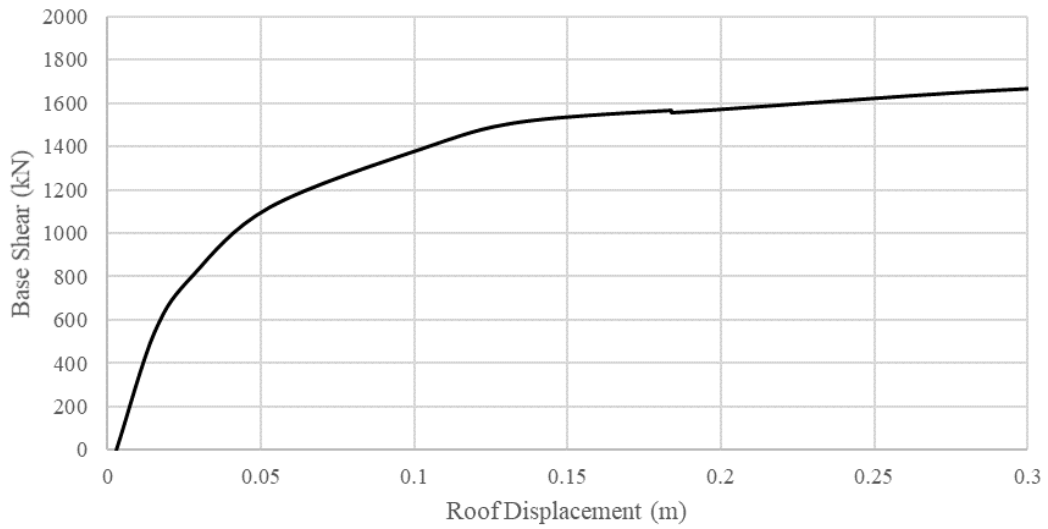


Figure 3.24. Pushover curve for positive X direction.

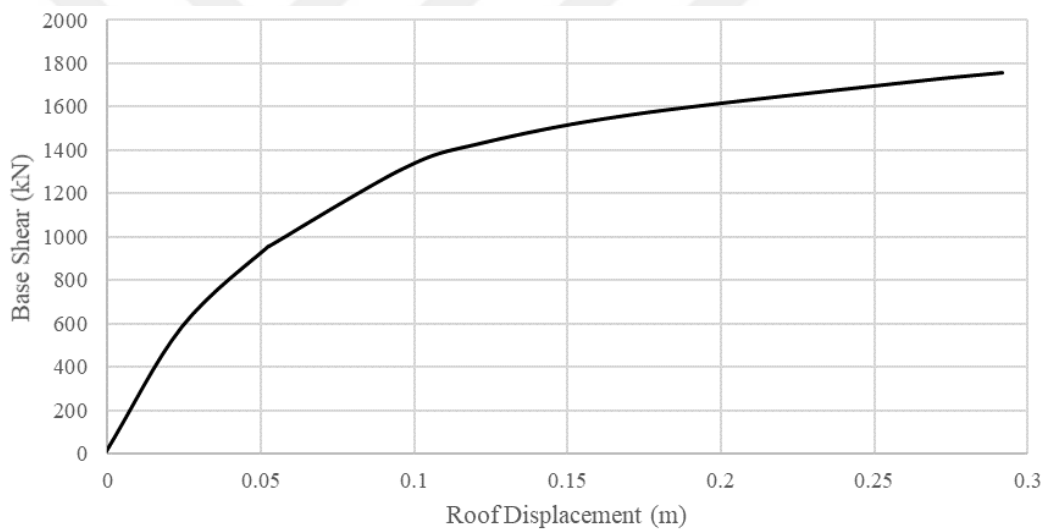


Figure 3.25. Pushover curve for positive Y direction .

Obtained pushover curves are converted to modal capacity diagrams by means of following equations.

$$a_1^{(i)} = \frac{V_{x1}^{(i)}}{M_{x1}} \quad (3.7)$$

$$d_1^{(i)} = \frac{u_{xN1}^{(i)}}{\Phi_{xN1} \Gamma_{x1}} \quad (3.8)$$

Coordinates of the modal capacity curves are given in Table 3.40 and Table 3.41.

Table 3.40. Conversion to the modal capacity diagram for positive X direction.

$u_{xN1}^{(i)}$ (m)	$V_{x1}^{(i)}$ (kN)	M_{x1}	Φ_{xN1}	Γ_{x1}	$d_1^{(i)}$ (m)	$a_1^{(i)}$ (g)
0.003	0.0	939.9	-0.043	-30.928	0.002	0.000
0.015	544.0	939.9	-0.043	-30.928	0.012	0.579
0.028	805.4	939.9	-0.043	-30.928	0.021	0.857
0.053	1118.6	939.9	-0.043	-30.928	0.040	1.190
0.103	1389.9	939.9	-0.043	-30.928	0.077	1.479
0.134	1510.3	939.9	-0.043	-30.928	0.100	1.607
0.184	1564.5	939.9	-0.043	-30.928	0.137	1.665
0.184	1553.9	939.9	-0.043	-30.928	0.137	1.653
0.271	1640.9	939.9	-0.043	-30.928	0.203	1.746
0.321	1679.2	939.9	-0.043	-30.928	0.240	1.787
0.443	1614.0	939.9	-0.043	-30.928	0.331	1.717

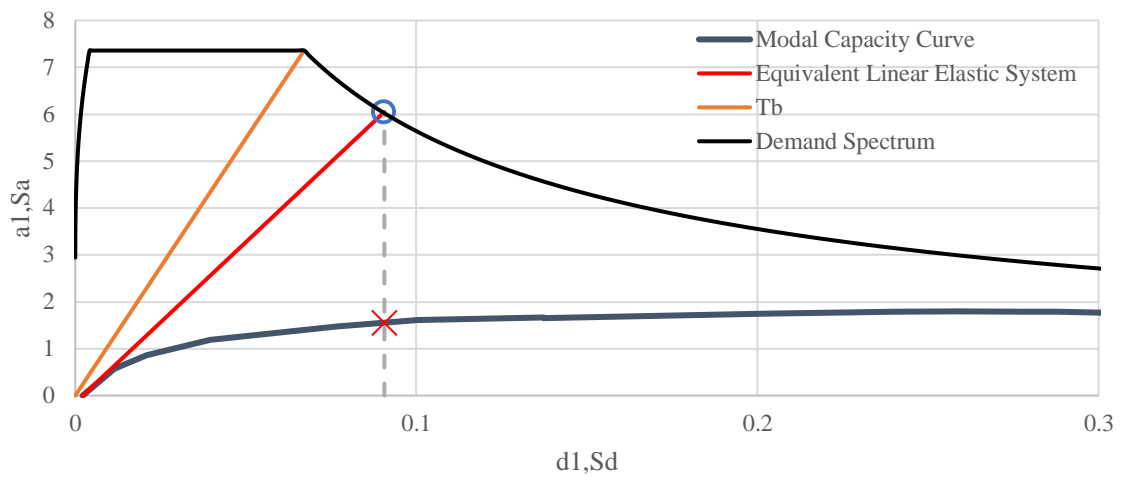


Figure 3.26. Modal capacity curve and modal displacement demand for positive X direction.

Table 3.41. Conversion to the modal capacity diagram for positive Y direction.

$u_{yN1}^{(i)}$ (m)	$V_{y1}^{(i)}$ (kN)	M_{y1}	Φ_{yN1}	Γ_{y1}	$d_1^{(i)}$ (m)	$a_1^{(i)}$ (g)
-0.001	0.0	988.6	0.040	32.182	-0.001	0.000
0.024	584.6	988.6	0.040	32.182	0.019	0.591
0.052	957.4	988.6	0.040	32.182	0.041	0.968
0.052	955.6	988.6	0.040	32.182	0.041	0.967
0.096	1314.6	988.6	0.040	32.182	0.075	1.330
0.121	1430.4	988.6	0.040	32.182	0.094	1.447
0.171	1565.1	988.6	0.040	32.182	0.133	1.583
0.265	1720.8	988.6	0.040	32.182	0.205	1.741
0.292	1757.9	988.6	0.040	32.182	0.226	1.778
0.292	1757.9	988.6	0.040	32.182	0.226	1.778

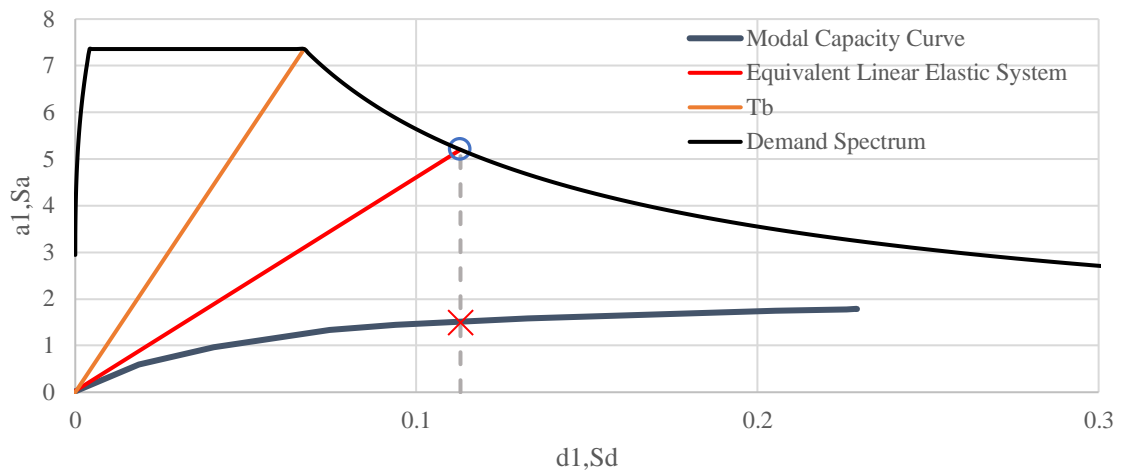


Figure 3.27. Modal capacity curve and modal displacement demand for the positive Y direction.

Displacement demands based on the TBSC 2007 are found as;

$$u_{xN1}^{(p)} = 0.121 \text{ m} \quad ; \quad u_{yN1}^{(p)} = 0.146 \text{ m}$$

In SAP2000 software, following the displacement control procedure, the nonlinear static analysis performed so that the displacement of the control joint at the top was reached to displacement demand. At that point, plastic rotations are obtained, and afterward curvatures are calculated. Deformed shapes of the building and plastic hinge states at the last step are given in Figure 3.28 and Figure 3.29.

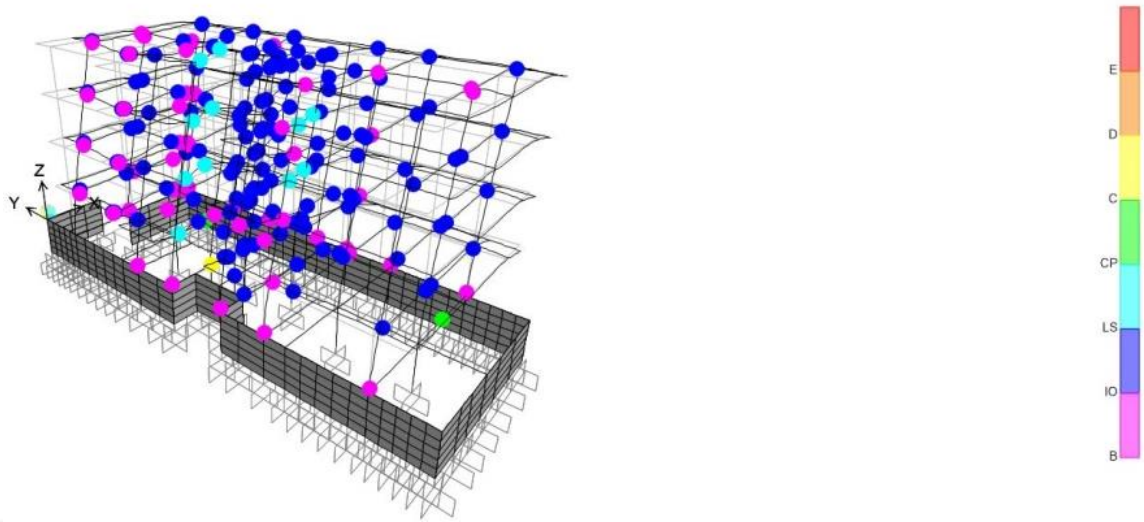


Figure 3.28. Deformed shape of the structure and plastic hinges at $u_{xN1}^{(p)} = 0.121 \text{ m}$.

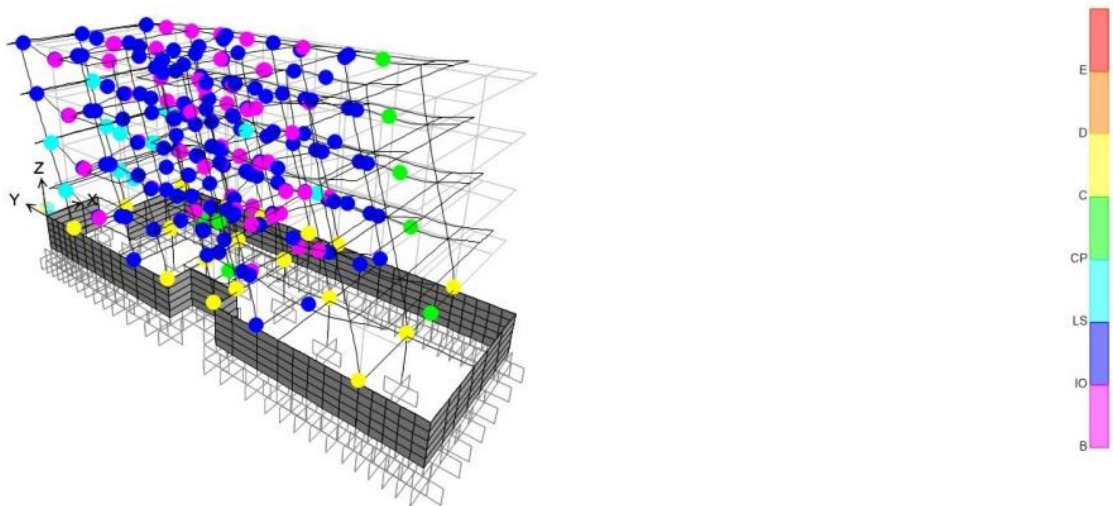


Figure 3.29. Deformed shape of the structure and plastic hinges at $u_{yN1}^{(p)} = 0.146 \text{ m}$.

Considering the strain limits and demands, members' damage regions are found. The results are given in Table 3.42. Damage states of structural members at first story under top story displacement demands Detailed steps are given for TBSC 2018 in the following chapter.

Table 3.42. Damage states of structural members at first story under top story displacement demands.

Loading	Element Type	Limited Damage	Visible Damage	Significant Damage	Collapse
+PY	Columns	23%	32%	9%	36%
	Beams	69%	29%	0%	3%
-PY	Columns	95%	0%	0%	5%
	Beams	70%	26%	3%	1%
+PX	Columns	86%	9%	0%	5%
	Beams	77%	23%	0%	0%
-PX	Columns	95%	0%	0%	5%
	Beams	77%	23%	0%	0%

3.3.2. Nonlinear Static Analysis Based on Turkish Building Seismic Code 2018

Unlike TBSC 2007, TBSC 2018 implies different effective stiffness coefficients to be used within inelastic analyses. According to TBSC 2018-5.4.5, the effective stiffness of reinforced concrete structural elements shall be calculated according to the following equations;

$$\theta_y = \frac{\phi_y L_s}{3} + 0.0015 \eta \left(1 + 1.5 \frac{h}{L_s} \right) + \frac{\phi_y d_b f_{ye}}{8 \sqrt{f_{ce}}} \quad (3.9)$$

$$(EI)_e = \frac{M_y L_s}{\theta_y} \quad (3.10)$$

A part of the table used to calculate θ_y and $(EI)_e$ is presented in Table 3.43, for one of the columns and for one of the shear walls, to illustrate an example.

Table 3.43. Calculation table to find effective stiffness about 2-2 local axis.

Frame	P	M_y	f_y	θ_y	$(EI_{22})_e$	$(EI_{22})_g$	$(EI_{22})_e / (EI_{22})_g$
W101	-366	94	0.00993	0.00345	567190	6513587	0.087
W201	-280	89	0.00980	0.00346	542650	6513587	0.083
W301	-188	78	0.00978	0.00346	484312	6513587	0.074
W401	-90	69	0.01051	0.00384	446253	6513587	0.069
C101	-467	213	0.00354	0.00550	13374	68032	0.197
C201	-350	192	0.00354	0.00626	10700	68032	0.157
C301	-232	175	0.00381	0.00644	9399	68032	0.138
C401	-114	155	0.00441	0.00686	6414	45576	0.141

Table 3.44. Calculation table to find effective stiffness about 3-3 local axis.

Frame	P	M_y	f_y	θ_y	$(EI_{33})_e$	$(EI_{33})_g$	$(EI_{33})_e/(EI_{33})_g$
W101	-366	979	0.00103	0.02235	8413	67822	0.124
W201	-280	939	0.00104	0.02207	8066	67822	0.119
W301	-188	837	0.00104	0.02203	7083	67822	0.104
W401	-90	856	0.00121	0.02361	5759	67822	0.085
C101	-467	147	0.00506	0.00478	22301	153072	0.146
C201	-350	134	0.00620	0.00477	20110	153072	0.131
C301	-232	121	0.00646	0.00496	17648	153072	0.115
C401	-114	88	0.00720	0.00536	14455	133938	0.108

Calculated effective stiffness coefficients based on the TBSC 2018 differentiate radically compared to TBSC 2007. Table 3.45 is given to illustrate a comparison between TBSC 2018 and TBSC 2007 in terms of effective stiffness coefficients.

Table 3.45. Effective stiffness comparison for columns.

Column	2018		2007	
	$(EI_{22})_e$	$(EI_{33})_e$	$(EI_{22})_e$	$(EI_{33})_e$
C101	0.146	0.197	0.430	0.430
C102	0.314	0.203	0.532	0.532
C103	0.171	0.152	0.400	0.400
C104	0.163	0.146	0.400	0.400
C105	0.331	0.215	0.519	0.519
C106	0.153	0.211	0.436	0.436
C107	0.155	0.101	0.400	0.400
C108	0.211	0.285	0.529	0.529
C109	0.153	0.400	0.574	0.574
C110	0.153	0.400	0.525	0.525
C111	0.250	0.400	0.545	0.545
C112	0.170	0.186	0.425	0.425
C113	0.109	0.152	0.400	0.400
C114	0.000	0.000	0.529	0.529
C115	0.300	0.190	0.530	0.530
C116	0.288	0.159	0.470	0.470
C117	0.245	0.145	0.435	0.435
C118	0.282	0.189	0.482	0.482
C119	0.300	0.160	0.510	0.510
C120	0.190	0.220	0.520	0.520
W101	0.124	0.087	0.400	0.400
W102	0.154	0.099	0.400	0.400

Mode shapes and periods for torsional and translational dominant vibration modes are given in Table 3.46. In Table 3.45, corresponding periods and mass participation ratios are given for TBSC 2007 as well.

Table 3.46. Comparison of periods and mass participations.

Mode	TBSC 2018				TBSC 2007			
	Period	U _X	U _Y	R _Z	Period	U _X	U _Y	R _Z
1	1.565	0.001	0.700	0.092	1.184	0.007	0.032	0.758
2	1.510	0.024	0.087	0.785	1.068	0.003	0.757	0.030
3	1.173	0.731	0.001	0.807	0.741	0.740	0.001	0.008

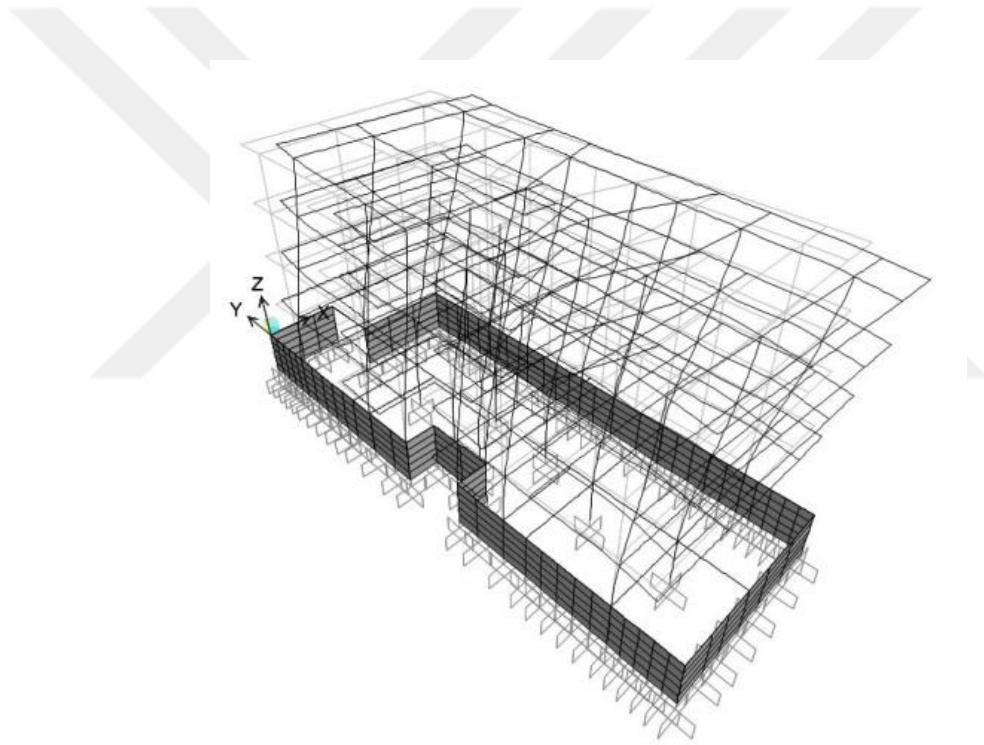


Figure 3.30 The first mode of the analytical model of TBSC 2018.

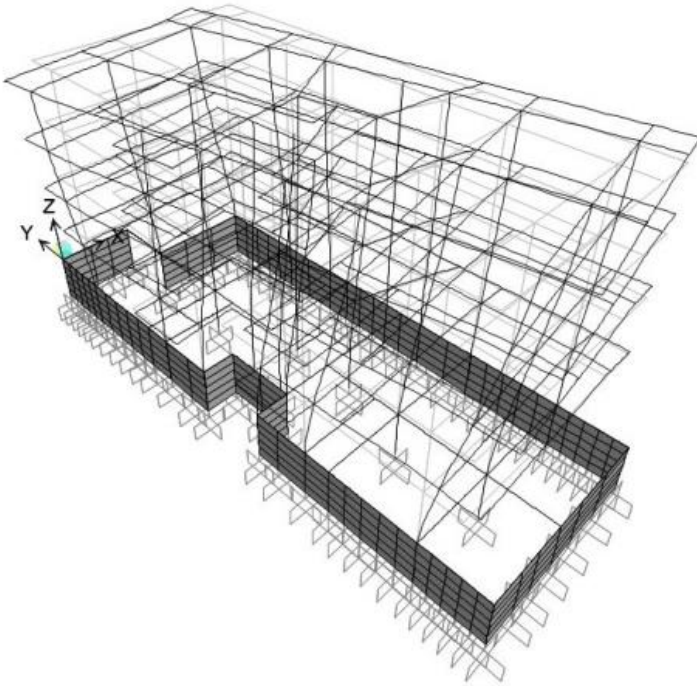


Figure 3.31. The second mode of the analytical model of TBSC 2018.

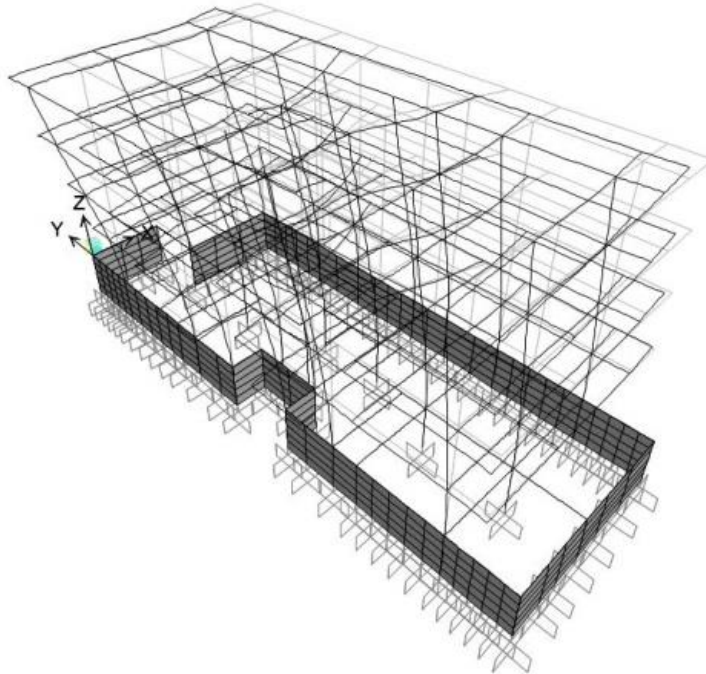


Figure 3.32. The third mode of the analytical model of TBSC 2018.

According to TBSC 2018, *Incremental Equivalent Earthquake Load Method* can be used, if the torsional irregularity factor calculated according to linear elastic behavior without additional eccentricity of any floor is less than 1.4. Furthermore, in the earthquake direction considered, the ratio of the effective mass of the dominant vibration mode calculated on the basis of linear elastic behavior to the total building mass (excluding the masses of the basements surrounded by rigid walls) shall be at least 0.70. Investigations for torsional irregularity presented in Table 3.47-Table 3.49.

Table 3.47. Torsional irregularity control for negative X direction.

Loading	Joint	U_x	U_y	U_z	Δ	Joint	U_x	U_y	U_z	Δ	η_{bi}
EXN	TRC1	-0.335	-0.022	0.026	0.071	TLC1	-0.220	-0.023	0.022	0.053	1.145
EXN	TRC2	-0.264	-0.020	0.042	0.093	TLC2	-0.167	-0.020	0.035	0.068	1.157
EXN	TRC3	-0.171	-0.016	0.051	0.099	TLC3	-0.100	-0.016	0.041	0.067	1.197
EXN	TRC4	-0.072	-0.010	0.043	0.072	TLC4	-0.033	-0.009	0.036	0.033	1.369

Table 3.48. Torsional irregularity control for positive X direction.

Loading	Joint	U_x	U_y	U_z	Δ	Joint	U_x	U_y	U_z	Δ	η_{bi}
EXP	TRC1	0.335	0.022	-0.026	0.071	TLC1	0.220	0.023	-0.022	0.053	1.145
EXP	TRC2	0.264	0.020	-0.042	0.093	TLC2	0.167	0.020	-0.035	0.068	1.157
EXP	TRC3	0.171	0.016	-0.051	0.099	TLC3	0.100	0.016	-0.041	0.067	1.197
EXP	TRC4	0.072	0.010	-0.043	0.072	TLC4	0.033	0.009	-0.036	0.033	1.369

Table 3.49. Torsional irregularity control for negative Y direction.

Loading	Joint	U_x	U_y	U_z	Δ	Joint	U_x	U_y	U_z	Δ	η_{bi}
EYN	TRC1	-0.023	-0.520	-0.029	0.106	BRC1	-0.023	-0.494	-0.034	0.097	1.042
EYN	TRC2	-0.015	-0.415	-0.055	0.145	BRC2	-0.015	-0.396	-0.059	0.140	1.018
EYN	TRC3	-0.012	-0.269	-0.073	0.159	BRC3	-0.012	-0.256	-0.076	0.156	1.012
EYN	TRC4	-0.009	-0.110	-0.061	0.110	BRC4	-0.009	-0.101	-0.074	0.101	1.043

Table 3.50. Torsional irregularity control for positive Y direction.

Loading	Joint	U_x	U_y	U_z	Δ	Joint	U_x	U_y	U_z	Δ	η_{bi}
EYP	TRC1	0.023	0.520	0.029	0.106	BRC1	0.023	0.494	0.034	0.097	1.042
EYP	TRC2	0.015	0.415	0.055	0.145	BRC2	0.015	0.396	0.059	0.140	1.018
EYP	TRC3	0.012	0.269	0.073	0.159	BRC3	0.012	0.256	0.076	0.156	1.012
EYP	TRC4	0.009	0.110	0.061	0.110	BRC4	0.009	0.101	0.074	0.101	1.043

In the Table 3.51, it is shown that the mass participation ratio meets the necessary condition as well.

Table 3.51. Mass participation ratios.

Mode	Period	U_X	U_Y	R_Z
1	1.564	0.001	<u>0.700</u>	0.092
2	1.510	0.024	0.087	0.785
3	1.173	<u>0.731</u>	0.001	0.807

Plastic hinges are modeled as it was summarized in the previous chapter based on the reduced existing material strength in accordance with limited knowledge level defined in TBSC 2018.

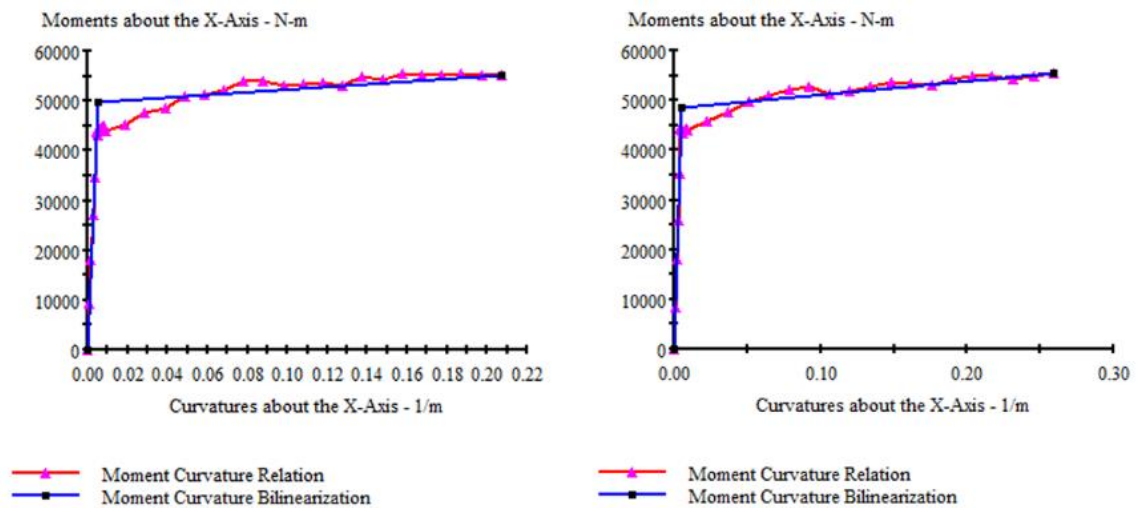


Figure 3.33. Comparison of S33 hinge properties for TBSC 2018 and TBSC 2007, respectively.

The interaction diagram is calculated through the XTRACT program employing the strain values as defined in TBSC 2018;

$$\varepsilon_{cu} = 0.0035$$

$$\varepsilon_{su} = 0.01$$

Comparative interaction curves are given in Figure 3.34. and Figure 3.35.

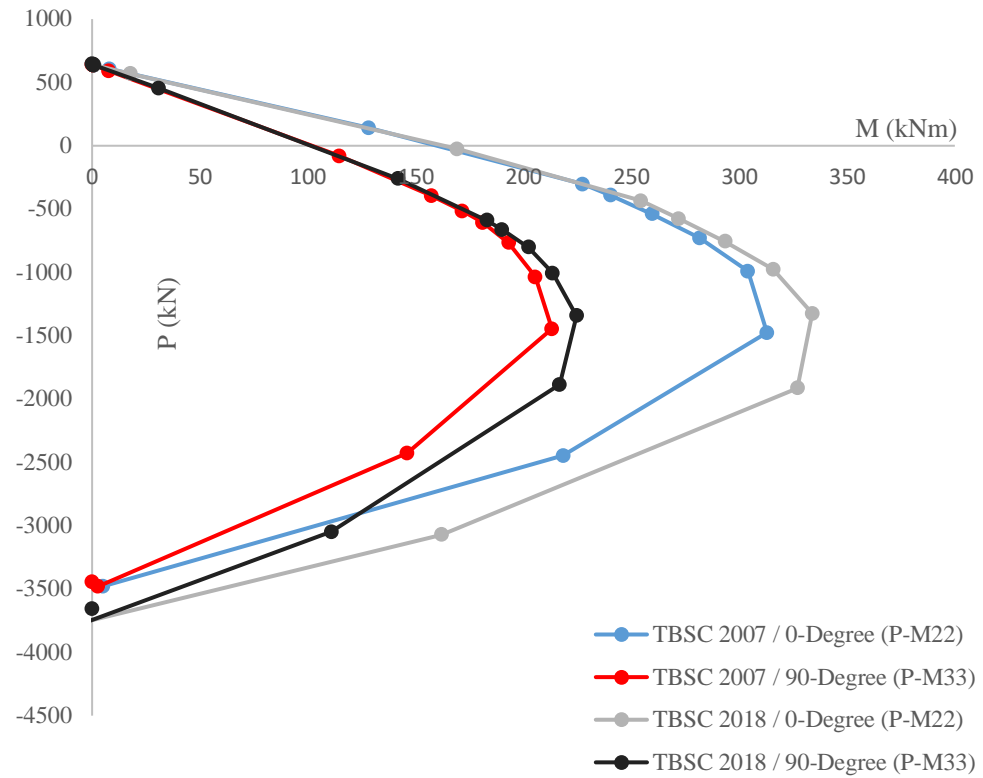


Figure 3.34. Comparison of P-M interaction curves for C101 (40x60).

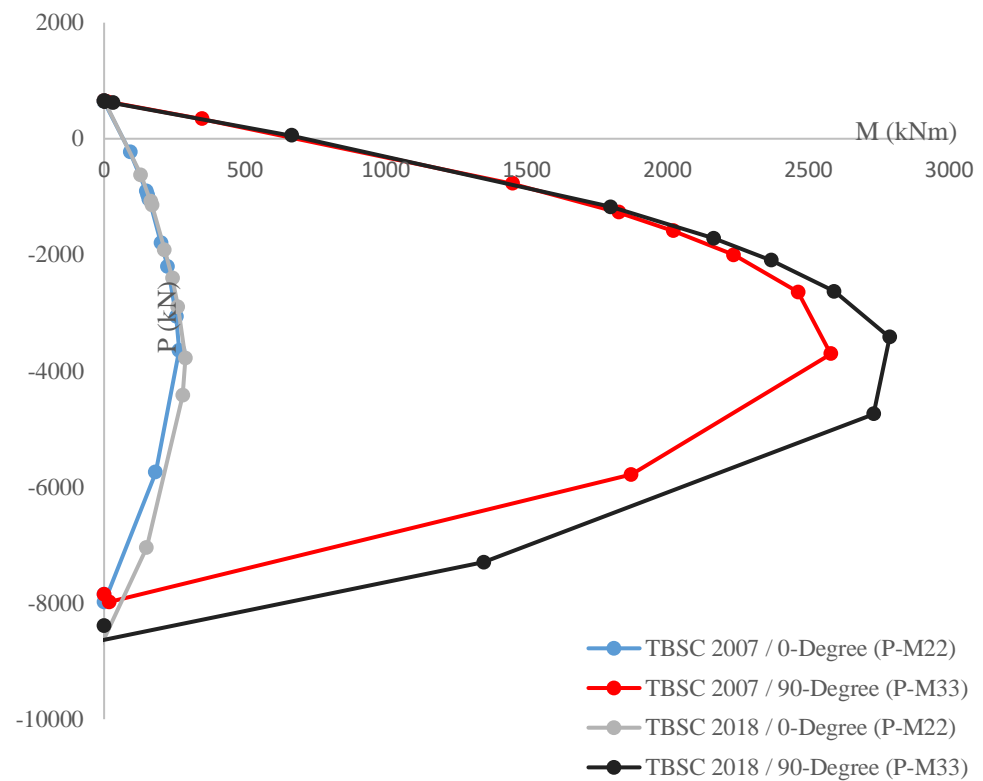


Figure 3.35. Comparison of P-M interaction curves for W101 (245x25).

Steps to be followed in TBSC 2018 are the same as the steps for the TBSC 2007 except for the loads considered in the nonlinear static analysis under vertical loads, and concurrent loading approach.

According to TBSC 2018, to evaluate the structural components, the combination of the earthquake effects with the vertical load effects is given in the following equation:

$$G + Q_e + 0.2S + E_d^{(H)} + 0.3E_d^{(Z)} \quad (3.11)$$

G stands for dead loads, S stands for snow loads, and $E_d^{(Z)}$ stands for the effect of the vertical earthquake component.

Definition of $E_d^{(H)}$ for nonlinear static analyses is another difference that is not dictated by TBSC 2007. According to TBSC 2018, in the cases where nonlinear earthquake calculations performed by *Pushover Methods*, $E_d^{(H)}$ represents the combined horizontal earthquake effect of the earthquake effects that are calculated separately on (X) and (Y) axis. The combinations shall be made according to the below equations.

$$E_d^{(H)} = \pm E_d^{(X)} \pm 0.3E_d^{(Y)} \quad (3.12)$$

$$E_d^{(H)} = \pm 0.3E_d^{(X)} \pm E_d^{(Y)} \quad (3.13)$$

As a result, a total of 8 different load cases are defined in SAP2000 software so to push the building up to the displacement demand concurrently utilizing two different load vectors on the orthogonal directions as given in Figure 3.36 showing the load case definition for pushover analysis. Load vectors are compatible with the multiplication of the mode shapes and story masses.

Load cases defined for pushover analysis are as follows;

$+P_x + 0.3P_y$	$+P_x - 0.3P_y$	$+P_y + 0.3P_x$	$+P_y - 0.3P_x$
$-P_x + 0.3P_y$	$-P_x - 0.3P_y$	$-P_y + 0.3P_x$	$-P_y - 0.3P_x$

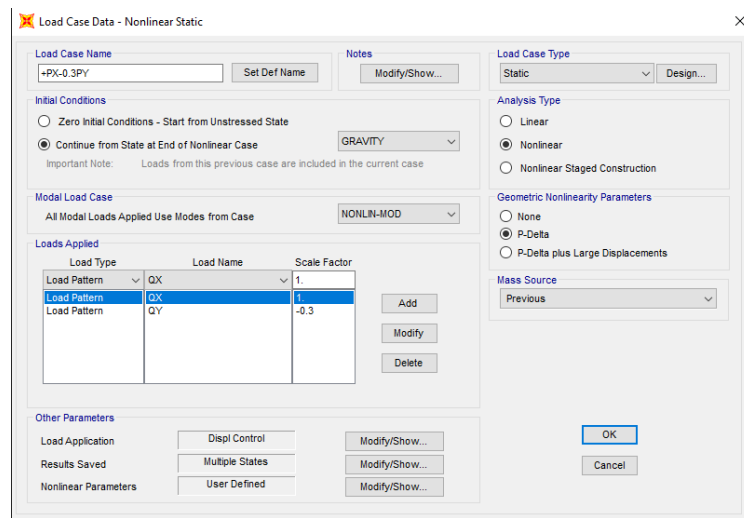


Figure 3.36. Load case definition in SAP2000 for concurrent pushover loading.

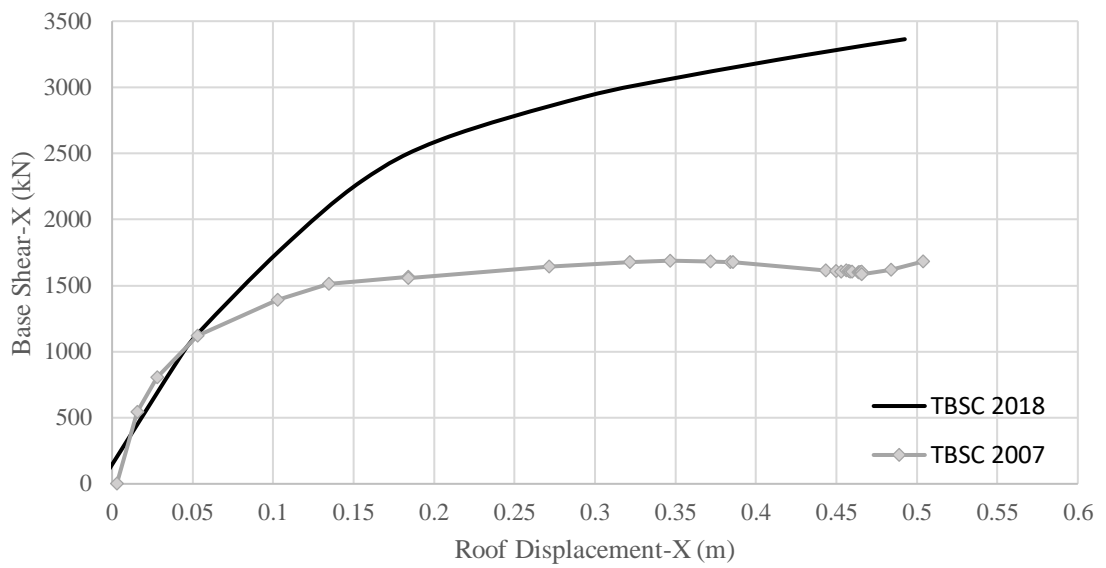


Figure 3.37. Pushover curves on the X loading direction.

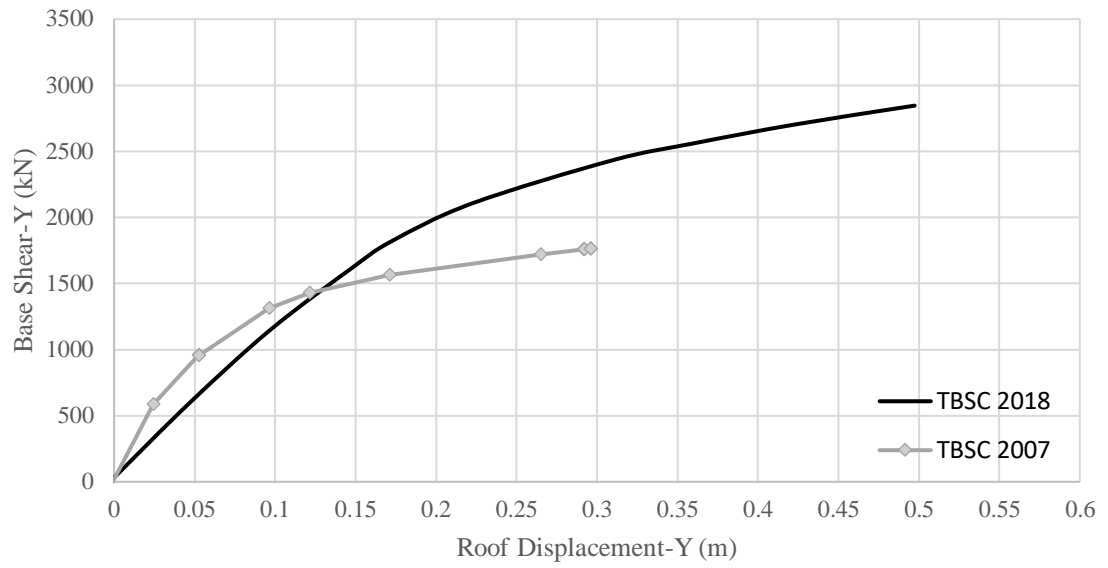


Figure 3.38. Pushover curves on the Y loading direction.

Table 3.52. Conversion to the modal capacity diagram for positive X direction.

$u_{xN1}^{(i)}$ (m)	$V_{x1}^{(i)}$ (kN)	M_{x1}	Φ_{xN1}	Γ_{x1}	$d_1^{(i)}$ (m)	$a_1^{(i)}$ (g)
-0.008	0.0	1103.0	-0.042	-31.262	-0.006	0.000
0.042	964.2	1103.0	-0.042	-31.262	0.032	0.874
0.055	1159.2	1103.0	-0.042	-31.262	0.041	1.051
0.105	1774.3	1103.0	-0.042	-31.262	0.079	1.609
0.155	2291.4	1103.0	-0.042	-31.262	0.117	2.077
0.205	2608.0	1103.0	-0.042	-31.262	0.154	2.365
0.293	2925.3	1103.0	-0.042	-31.262	0.220	2.652
0.355	3081.4	1103.0	-0.042	-31.262	0.267	2.794
0.430	3242.4	1103.0	-0.042	-31.262	0.324	2.940
0.493	3363.5	1103.0	-0.042	-31.262	0.371	3.050

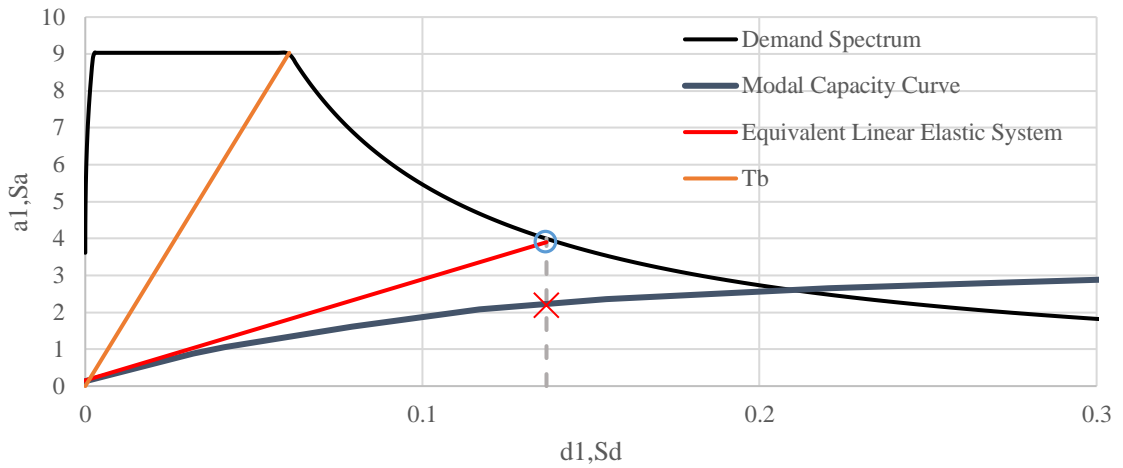


Figure 3.39. Modal capacity diagram and modal displacement demand for positive X direction.

Table 3.53. Conversion to the modal capacity diagram for positive Y direction.

$u_{yN1}^{(i)}$ (m)	$V_{y1}^{(i)}$ (kN)	M_{y1}	Φ_{yN1}	Γ_{y1}	$d_1^{(i)}$ (m)	$a_1^{(i)}$ (g)
-0.003	0.0	1144.8	0.039	33.240	-0.002	0.000
0.047	602.4	1144.8	0.039	33.240	0.036	0.526
0.097	1152.6	1144.8	0.039	33.240	0.075	1.007
0.147	1614.0	1144.8	0.039	33.240	0.113	1.410
0.172	1819.6	1144.8	0.039	33.240	0.133	1.589
0.222	2105.8	1144.8	0.039	33.240	0.171	1.840
0.310	2432.8	1144.8	0.039	33.240	0.239	2.125
0.360	2559.9	1144.8	0.039	33.240	0.277	2.236
0.422	2701.6	1144.8	0.039	33.240	0.325	2.360
0.497	2845.6	1144.8	0.039	33.240	0.383	2.486

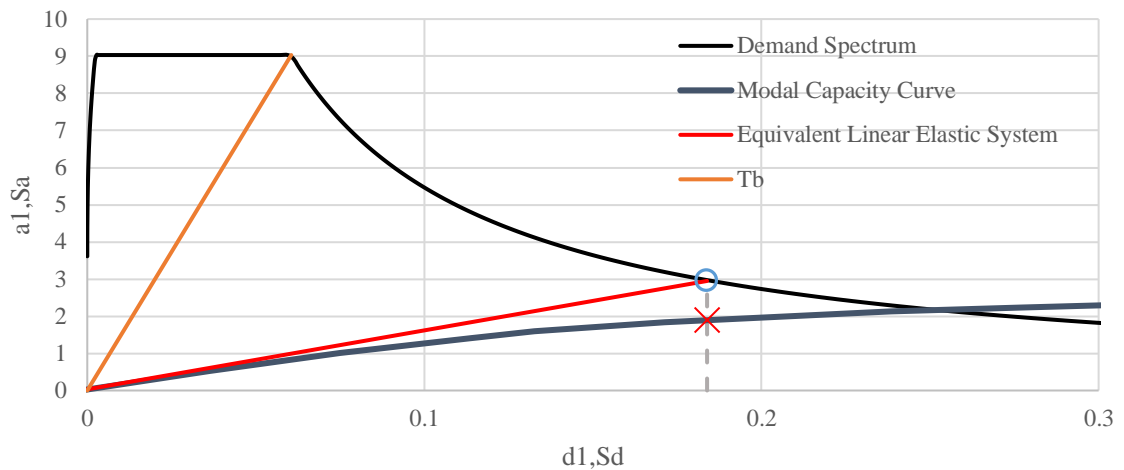


Figure 3.40. Modal capacity diagram and modal displacement demand for positive Y direction.

Displacement demands based on the TBSC 2007 are found as;

$$u_{xN1}^{(p)} = 0.182 \text{ m} \quad ; \quad u_{yN1}^{(p)} = 0.239 \text{ m}$$

Deformed shapes of the building and plastic hinge states at the last step are given in Figure 3.41 and Figure 3.42.

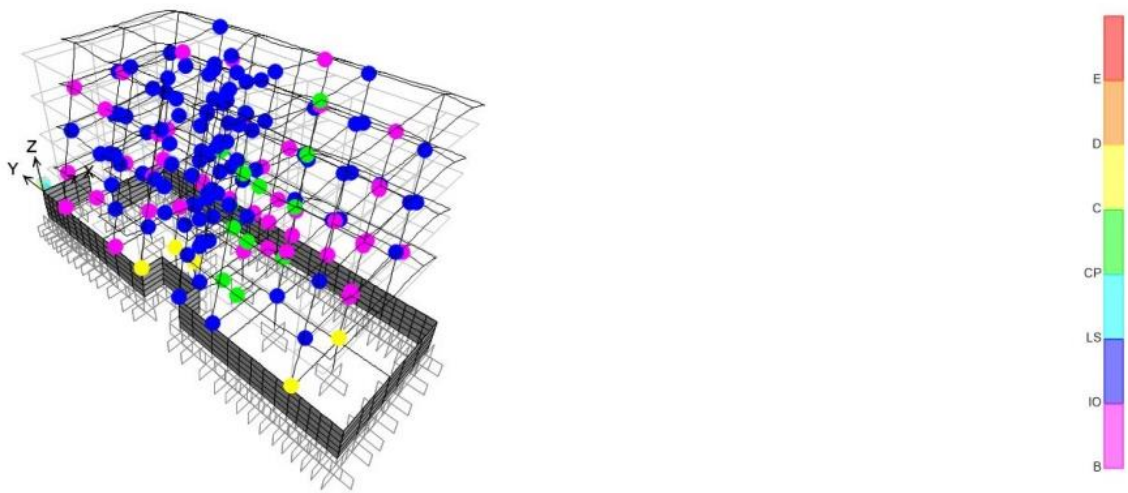


Figure 3.41. Deformed shape of the structure and plastic hinges at $u_{xN1}^{(p)} = 0.182 \text{ m}$.

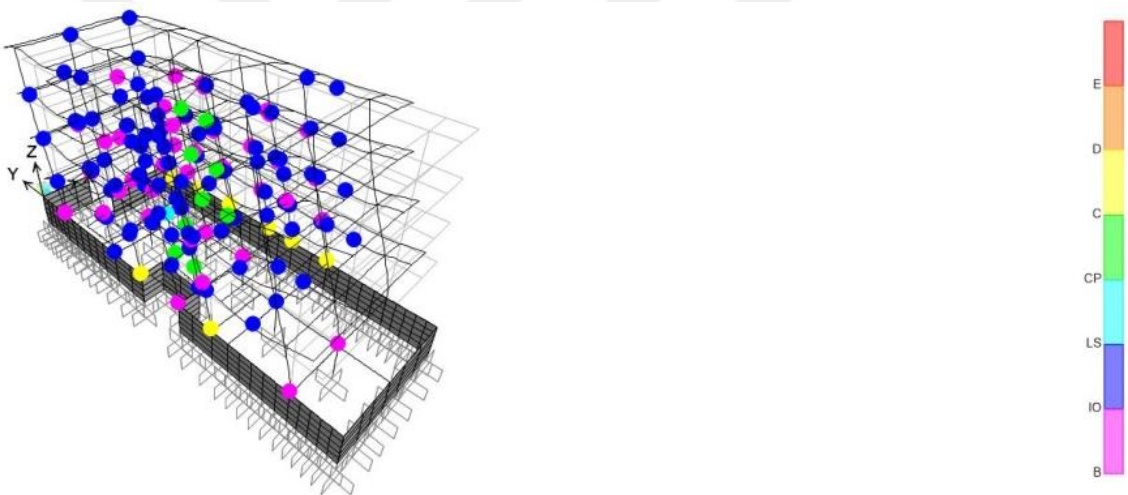


Figure 3.42. Deformed shape of the structure and plastic hinges at $u_{yN1}^{(p)} = 0.239 \text{ m}$.

In performance assessment studies, limit definitions are one of the fundamental parameters that have a critical role in the results whether these limits are based on force or based on deformation. TBSC 2018 also has significant differences in terms of these limits compared to TBSC 2007.

Table 3.54. Comparison of strain limits given for concrete.

TBSC 2018	TBSC 2007
$\varepsilon_c^{(G\ddot{O})} = 0.0035 + 0.04\sqrt{w_{we}} \leq 0.018$	$(\varepsilon_{cg})_{GC} = 0.004 + 0.014(\rho_s/\rho_{sm}) \leq 0.018$
$\varepsilon_c^{(KH)} = 0.75\varepsilon_c^{(G\ddot{O})}$	$(\varepsilon_{cg})_{GV} = 0.0035 + 0.01(\rho_s/\rho_{sm}) \leq 0.0135$
$\varepsilon_c^{(SH)} = 0.0025$	$(\varepsilon_{cu})_{MN} = 0.0035$

Table 3.55. Comparison of strain limits given for steel.

TBSC 2018	TBSC 2007
$\varepsilon_s^{(G\ddot{O})} = 0.4\varepsilon_{su}$	$(\varepsilon_s)_{GC} = 0.060$
$\varepsilon_s^{(KH)} = 0.75\varepsilon_s^{(G\ddot{O})}$	$(\varepsilon_s)_{GV} = 0.040$
$\varepsilon_s^{(SH)} = 0.0075$	$(\varepsilon_s)_{MN} = 0.010$

For concrete material, difference emerges from the confinement effect. TBSC 2007 takes into account the effect of confinement by the expression ρ_s/ρ_{sm} , and TBSC 2018 takes into account the effect of confinement by the expression $\sqrt{w_{we}}$. In consideration of confinement based on TBSC 2007, transverse reinforcements that do not satisfy the criteria of the definition of the special earthquake transverse reinforcement are completely ignored. However, on the other hand, TBSC 2018 states that 30% of the 90-degree hooked transverse reinforcements can be taken into account in the calculation of the confinement effect. This provision made a significant difference in terms of limit values in the case study building. It is evident that this provision will be important in the analysis of existing buildings considering that insufficient attention in the hooking of transverse reinforcement in the existing building stock is a commonly encountered problem. In Figure 3.43. C02 axial force-curvature diagram the difference is illustrated on P - ϕ damage curves of column C02.

Figure 3.44. Visual damage inspection for column C02 is to set an example for the damage state determination of the column and wall sections. Following the pushover analysis, the internal force and plastic rotation values are obtained from the SAP2000 program, the rotations are converted to plastic curvatures, and the total curvature values are determined by adding the yield curvatures to the plastic curvatures. The damage state is then determined by placing the obtained values on the P - ϕ curves obtained from the XTRACT program by defining the damage limits.

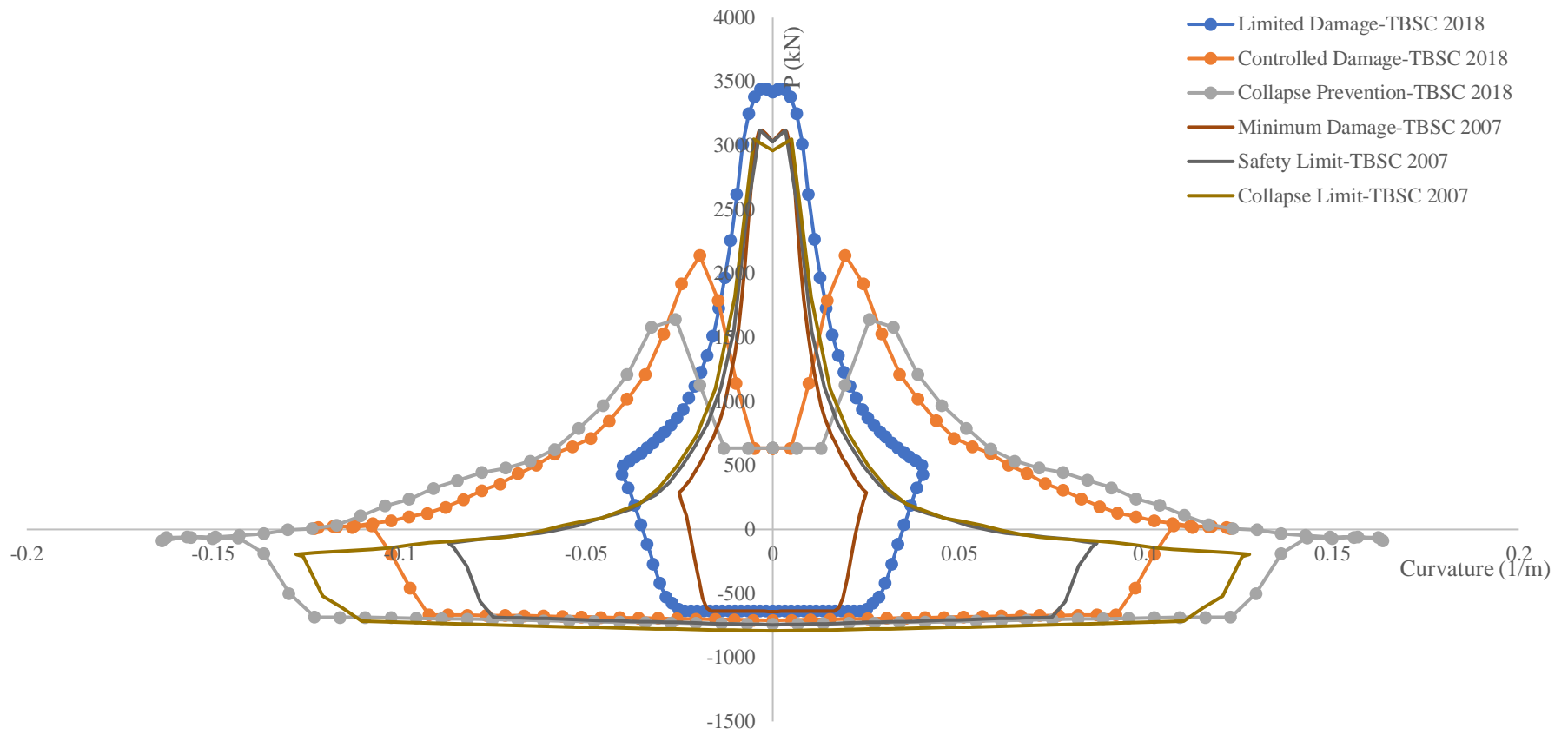


Figure 3.43. C02 axial force-curvature diagram.

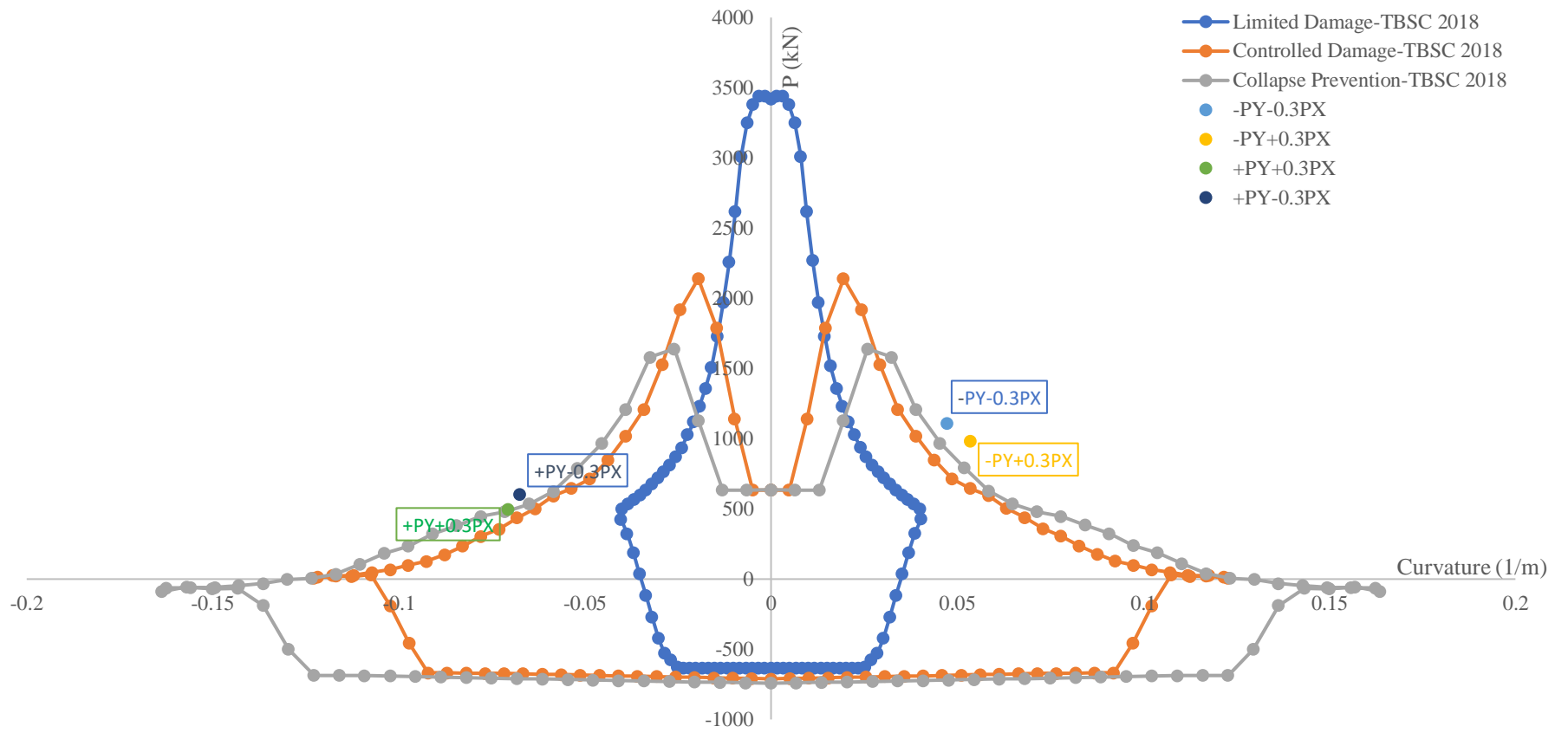


Figure 3.44. Visual damage inspection for column C02.

Damage states of the structural members in the first story are given in Table 3.56. in percentages.

Table 3.56. Damage states of structural members at first story under displacement demands.

Loading	Element Type	Limited Damage	Visible Damage	Significant Damage	Collapse
+PY+0.3PX	Columns	9%	36%	14%	41%
	Beams	66%	34%	0%	0%
+PY-0.3PX	Columns	14%	31%	0%	55%
	Beams	65%	35%	0%	0%
-PY+0.3PX	Columns	18%	27%	10%	45%
	Beams	70%	30%	0%	0%
-PY-0.3PX	Columns	9%	32%	18%	41%
	Beams	66%	34%	0%	0%
+PX+0.3PY	Columns	64%	27%	0%	9%
	Beams	66%	34%	0%	0%
+PX-0.3PY	Columns	64%	27%	0%	9%
	Beams	65%	35%	0%	0%
-PX+0.3PY	Columns	59%	32%	0%	9%
	Beams	65%	35%	0%	0%
-PX-0.3PY	Columns	64%	27%	0%	9%
	Beams	69%	31%	0%	0%

3.4. Nonlinear Dynamic Analysis

Nonlinear dynamic analysis is a computationally demanding method developed in the 1970s to be used for research purposes, to analyze specific structures, and to calibrate rules in regulations. Advances in computer and software technology that facilitate nonlinear dynamic analysis, advances in material science, structural engineering, and earthquake engineering, allowed the method to be employed extensively in engineering applications. One of the main application areas of nonlinear dynamic analysis is to evaluate the seismic performance of existing structures. Performing seismic performance analysis requires nonlinear dynamic analysis and programs capable of performing these analyses more intensely than every-day seismic design (Fardis, 2009). With the latest advances in structural engineering and earthquake engineering, nonlinear analysis has become a fundamental tool in seismic isolation and performance-based design.

Assessment through nonlinear dynamic analysis began with Chapter 7 in TBSC 2007. After TBSC 2018 came into force, the method is introduced to be used for different engineering applications, namely, Displacement-Based Design and Assessment, Design of Tall Buildings, and Design of Isolated Structures in addition to the assessment of existing buildings.

Nonlinear dynamic analysis is the most consistent analysis method in providing nonlinear deformations and rotations. It can take into account high mode and torsion effects in the structure. In this method, the equation of motion of the structural system under a seismic action is taken into consideration numerically, and all elastic and plastic deformations, displacements, and internal forces are calculated throughout time steps (Celep, 2007).

The dynamic analysis differs from the static analysis in that it does not require the calculation of a global seismic demand to provide force and deformation demands, and also, provides residual ones that are required for performance-based design and assessment (Fardis, 2009).

It is often impossible to produce an analytical solution to the equations of motion in situations such as seismic effects where the charge changes well, or where the system does not behave linearly. Such problems can be studied by stepping the time used to generate numerical solutions to differential equations (Chopra, 2007). To represent an accurate behavior and to get reliable results, the procedure should proceed with careful attention, and the effects of the algorithms and assumptions adopted throughout the process should be considered carefully. Approaches in the modeling of structural elements, accurate representation of the structure, behavior of elements and materials under cyclic loads, damping properties, and the characters of the earthquake records used in the analysis are some of the parameters that have primary effects on the results.

For nonlinear dynamic analyses, OpenSees software is utilized due to its robust solution algorithm and enablement to control the process strictly. Beams, columns, and shear walls are modeled as line elements connected to joints. Masses are lumped at the joints, which are constrained so to exhibit rigid diaphragm behavior at each story level. Nonlinearity was represented through fiber sections along with the elements due to its ability to capture hysteresis behavior more accurately than zero-length plastic hinges with the pre-defined normal stress-strain relationship. The validity of the models constructed in OpenSees compared to models in SAP2000 is presented in the subsequent chapter.

OpenSees software has a wide range of variety to model structural components and materials, ranging from behavioral definitions to solution formulations. In this thesis, *beamWithHinges* element was used to model beams, and *nonlinearBeamColumn* element is used to model columns and shear walls. *beamWithHinges* and *nonlinearBeamColumn* elements are based on the force-based formulation. The force-based formulation offers the advantage that the force-interpolation functions are exact under the assumption of linear geometry. Consequently, a single element with several integration points, in other words, control sections, suffices for the representation of the inelastic behavior of the member (Fenves & Flippou, 2004).

beamWithHinges element is based on the non-iterative flexibility formulation and considers plasticity to be concentrated over specified hinge lengths at the element ends. *beamWithHinges* divides the line element into three parts; two hinges, which are defined by assigning to each a previously-defined fiber section, at the element ends, and a linear elastic region in the middle. OpenSees provides several formulation schemes to be used for *beamWithHinges* element. In this thesis, the Modified Gauss-Radau Integration Scheme, developed by Scott & Fenves, 2006, is adopted. There are many advantages of this formulation. The integration method limits the material nonlinearity to the element ends over pre-defined hinge lengths, preserves the correct numerical solution for linear curvature distribution, and assures objective response at the section, element, and structural levels. Moreover, the *beamWithHinges* element enables the spread of plasticity through the plastic hinge region. Plastic rotations are directly associated with plastic curvature through the specified plastic hinge lengths (Scott & Fenves, 2006).

In addition to the bending moment, the presence of axial force, which can be accepted as constant along the column, extends the plastic region. With increasing axial force, the plasticity spreads along the column, and hence plastic hinge assumption becomes no longer valid (Celep, 2007). In order to consider the spread of plasticity in columns and shear walls, the *nonlinearBeamColumn* element is utilized. *nonlinearBeamColumn* element is based on the non-iterative (or iterative) force formulation and takes the spread of plasticity into account by means of several fiber sections along with the line elements. Five integration points are used in all *nonlinearBeamColumn* elements, as emphasized in Fenves & Flippou, 2004.

Fiber section models ensure directly accounting the axial force-bending moment interaction in addition to the moment-curvature relationship by integrating the material response over the control sections. Also, a fiber model has the advantage that it can account for cracking of the concrete in the elastic range, before steel yields (Powell, 2010, Terzic, 2012). Each of the fiber elements serves as an equivalent of the concrete area or a longitudinal reinforcing bar. The hysteretic response does not need to be defined since it is determined by the material properties. The hysteretic response is dominated by the behavior of the reinforcing steel in a reinforced concrete section because of the higher ductility capacity of the reinforcing steel compared to concrete material. The influence of varying axial force on strength and stiffness is directly modeled, and no prior moment-curvature analysis of members is needed. For this purpose, simple uniaxial normal stress-strain models are sufficient. Studies show that a few fibers suffice to yield an excellent representation of the hysteretic response of the section unless distinguishing between cover concrete and core concrete is desired. (Fenves & Flippou, 2004, Calvi et al., 2007).

concrete04 and *steel02* materials were used to model reinforced concrete elements. *concrete04* material follows the stress-strain relationship proposed by Popovics (1973) for loading in compression until the concrete crushing strength is achieved. The Karsan-Jirsa model (1969) is used to determine the slope of the curve for unloading and reloading in compression. In this study, the tensile strength of the concrete is neglected. The hysteretic behavior of the *concrete04* material is given in Figure 3.45. The hysteretic stress-strain relationship of the *concrete04* material

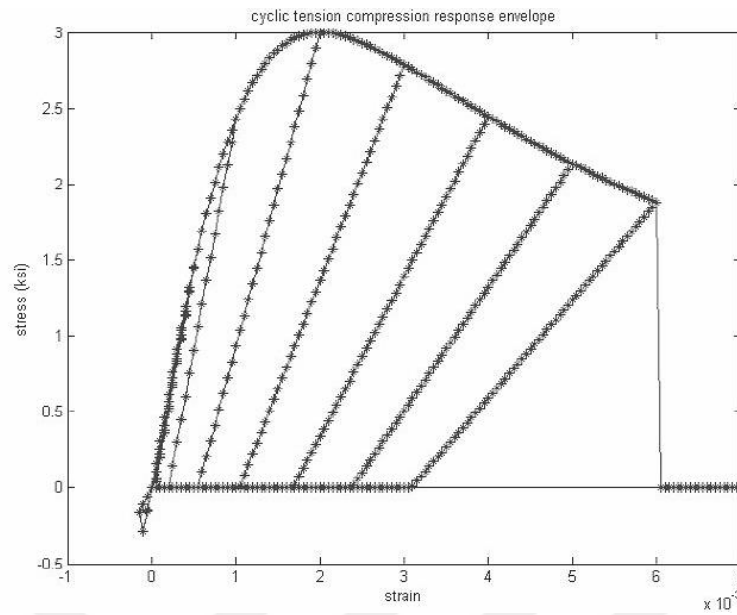


Figure 3.45. The hysteretic stress-strain relationship of the concrete04 material.

steel02 material follows the stress-strain relationship of Giuffre-Menegotto-Pinto steel material. The hysteretic behavior of *steel02* material without isotropic hardening is given in Figure 3.46.

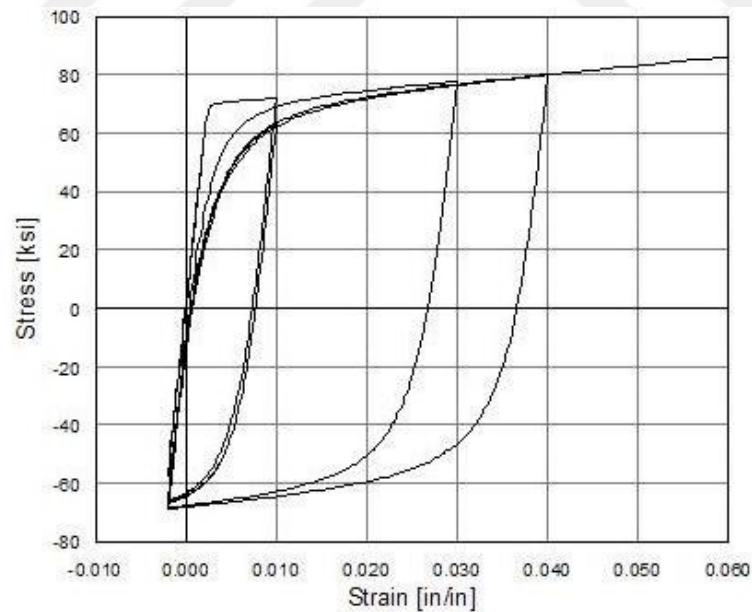


Figure 3.46. Hysteretic stress-strain relationship of the steel02 material without isotropic hardening.

Material properties to model fibers are given in Table 3.57. Material properties used in nonlinear dynamic analyses Limited knowledge level factor is applied to the material properties to achieve the decrease in the capacity of the members.

Table 3.57. Material properties used in nonlinear dynamic analyses.

	TBSC 2007	TBSC 2018
$0.75 \times f_{cm}$ (MPa)	12.21	13.56
$E = 5000\sqrt{f_{cm}}$ (MPa)	20170	21260
ϵ_{cu}	0.0030	0.0035
ϵ_{su}	0.0100	0.0100

3.4.1. Verification of Models

In order to prove the validity of the models in OpenSees, mode shapes, and dominant vibration periods of the first three modes are compared in Table 3.58, and Figure 3.47.

An important point here to emphasize is that the models in OpenSees are compared to models with gross section stiffnesses since modal analysis is based on linear-elastic analysis, which, in turn, yields no reduction in the gross section stiffnesses.

Table 3.58. Comparison of analytical models in OpenSees and SAP2000 software.

Mode	Analytical Model for TBSC 2007		Analytical Model for TBSC 2018	
	Period (s) SAP2000	Period (s) OpenSees	Period (s) SAP2000	Period (s) OpenSees
1	0.847	0.857	0.823	0.838
2	0.733	0.690	0.691	0.674
3	0.530	0.501	0.526	0.490

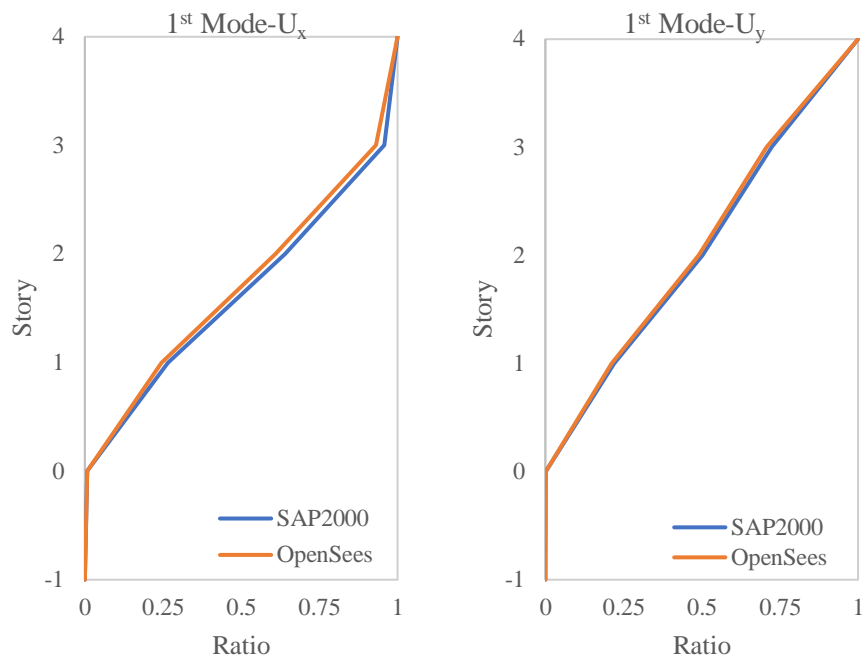


Figure 3.47. Comparison of torsional mode.

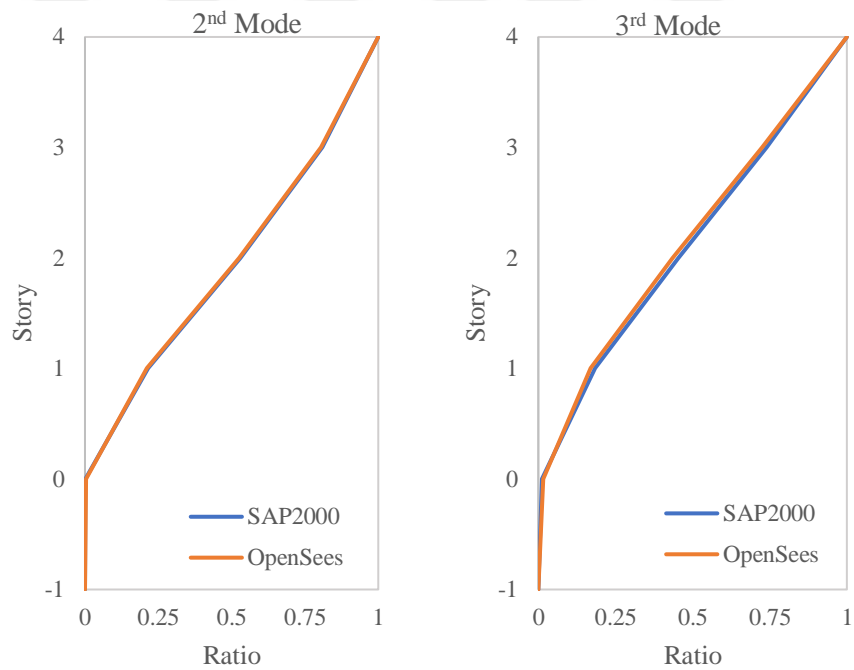


Figure 3.48. Comparison of translational modes.

It can be deduced from the proximity of the results; it is appropriate to utilize OpenSees environment for dynamic analysis in the scope of this thesis.

3.4.2. The Analysis Procedure

One of the most critical considerations in nonlinear dynamic analyses is the selection of time history records. Selected records and relevant parameters are given in Table 3.59. Selected Records for TBSC 2007 and in Table 3.60. Ground motion records were selected from earthquakes with strike-slip mechanisms and scaled in the time domain.

Table 3.59. Selected Records for TBSC 2007.

Earthquake Name	Year	Station Name	Magnitude	Rjb (km)	$V_{s,30}$ (m/sec)	5%-95% Duration (sec)	Scale Factor
Imperial V.	1979	Delta	6.53	22	242	51.4	2.0
Superstition H.	1987	El Centro	6.54	18	192	35.7	1.4
Kobe	1995	Fukushima	6.9	17	256	35.7	1.0
Kobe	1995	Tadoka	6.9	31	312	43.8	1.0
Kocaeli	1999	Bursa-Tofas	7.51	60	289	41.2	2.6
Kocaeli	1999	Iznik	7.51	30	476	19.5	2.6
Erzurum	1983	Horasan	6.9	34	-	19.0	3.0

Table 3.60. Selected Records for TBSC 2018.

Earthquake Name	Year	Station Name	Magnitude	Rjb (km)	$V_{s,30}$ (m/sec)	5%-95% Duration (sec)	Scale Factor
Imperial V.	1979	Delta	6.53	22	242	51.4	2.0
Superstition H.	1987	El Centro	6.54	18	192	35.7	1.4
Kobe	1995	Fukushima	6.9	18	256	35.7	1.0
Kobe	1995	Tadoka	6.9	32	312	43.8	1.0
Kocaeli	1999	Bursa-Tofas	7.51	60	290	41.2	2.6
Kocaeli	1999	Iznik	7.51	31	477	19.5	2.6
Erzurum	1983	Horasan	6.9	34	-	19.0	3.0
Hector Mine	1999	Amboy	7.13	42	383	26.7	2.0
Landers	1992	Fun Valley	7.28	25	389	29.6	1.6
Landers	1992	Morongo	7.28	41	368	32.9	2.4
Darfield	2010	heathcote	7	24	422	15.7	0.5

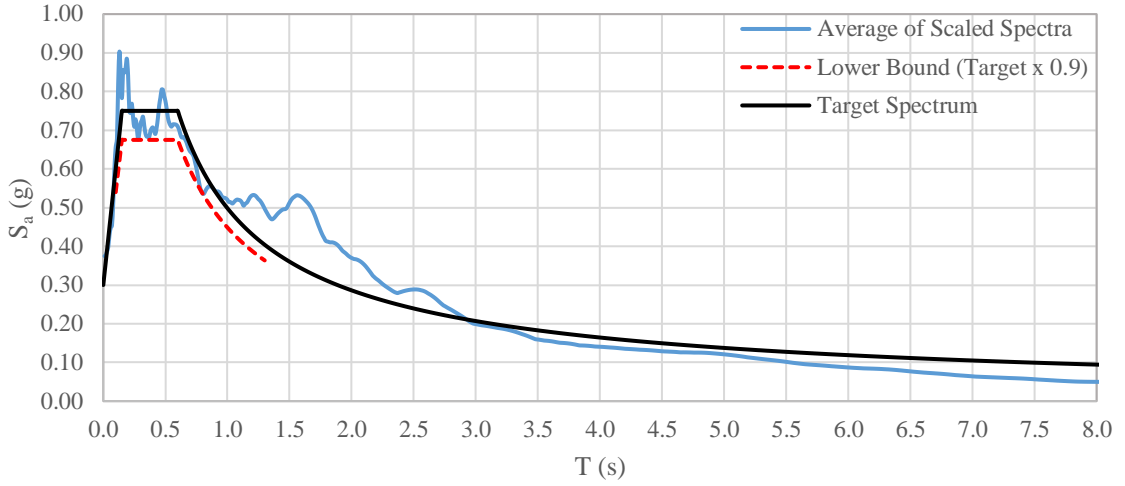


Figure 3.49. Matched spectrum for TBSC 2007 (North-South components).

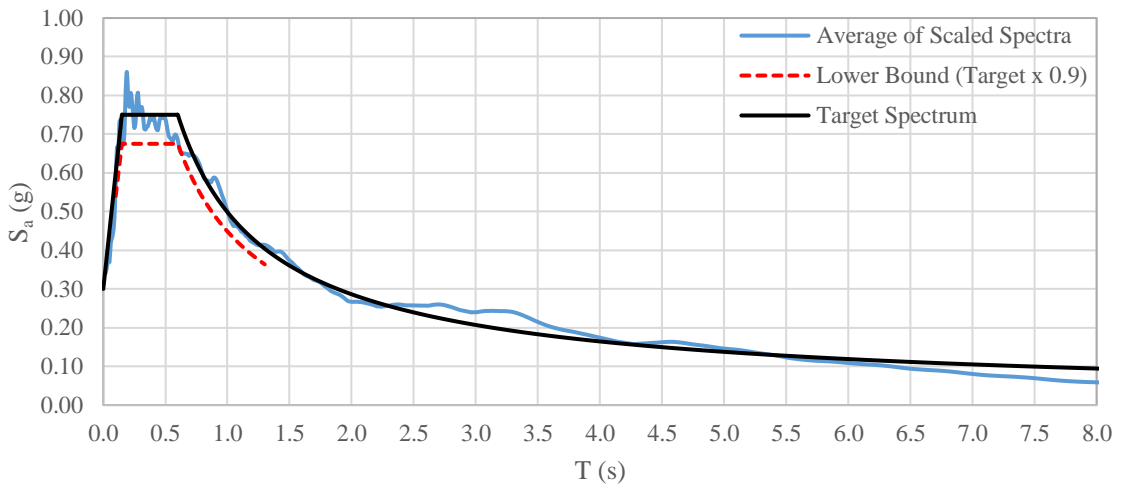


Figure 3.50. Matched spectrum for TBSC 2018 (East-West components).

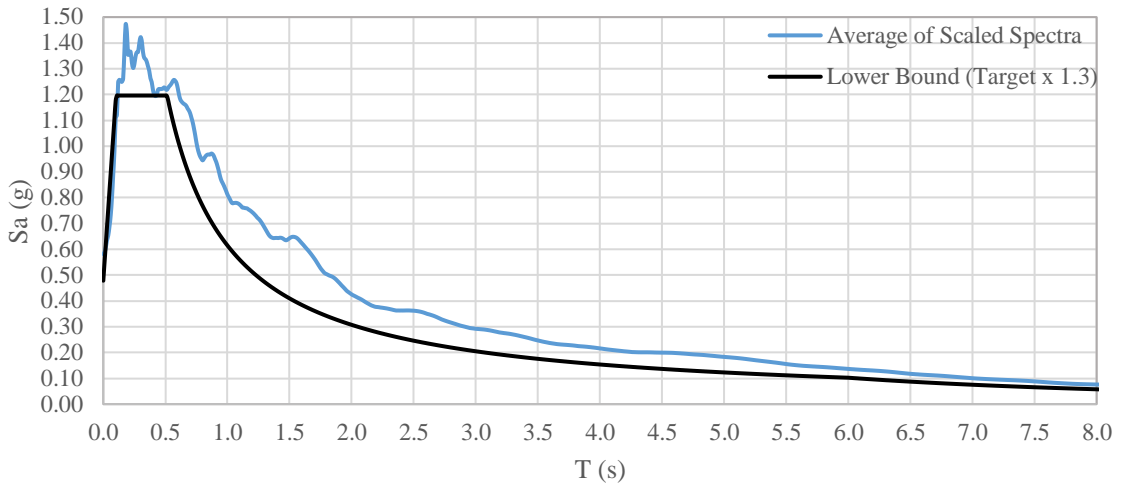


Figure 3.51. Matched spectrum for TBSC 2018.

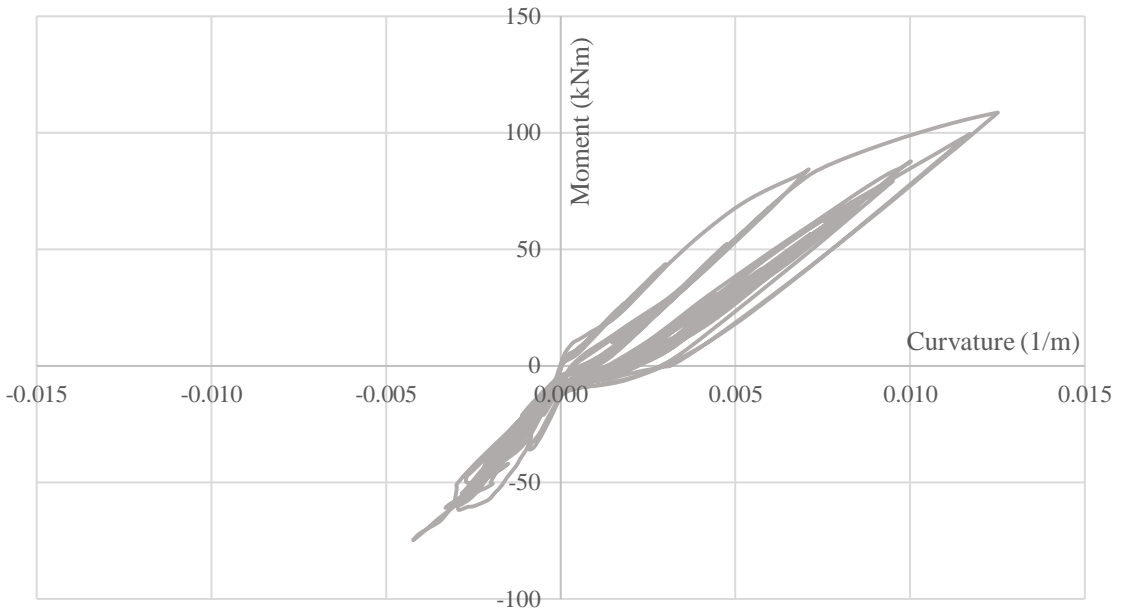


Figure 3.52. Moment-curvature history obtained from left end of B283 under Tadoka-1 time history record.

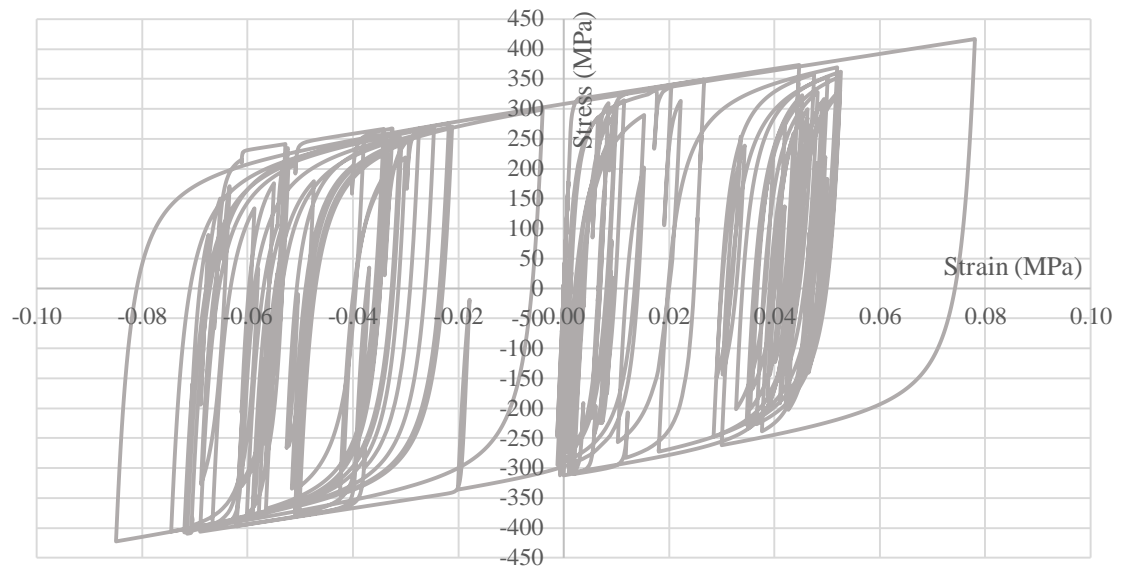


Figure 3.53. Axial stress-strain time history of the corner reinforcement at the bottom section of the wall P101 under Delta-352 time history record.

3.4.3. Analysis Results

Throughout the analysis procedure, end sections of the columns, walls, and beams were traced. One of the hardest tasks related to nonlinear dynamic analysis is to handle the results. For this reason, different kinds of macros and codes were used. In order to set an example of the assessment procedure, evaluation of beams based on the TBSC 2018 is given in Table 3.61.

Table 3.61. Beam evaluation table.

Beam	<i>i end</i>				<i>j end</i>				Member Damage State
	ϕ_{avg} of all records	ϕ_{yield}	ϕ_{GC}	Section Damage State	ϕ_{avg} of all records	ϕ_{yield}	ϕ_{GC}	Section Damage State	
232	0.061	0.009	0.428	Visible	0.056	0.009	0.428	Visible	Visible
233	0.024	0.009	0.429	Visible	0.131	0.010	0.386	Visible	Visible
235	0.003	0.006	0.195	Minimum	0.199	0.006	0.195	Collapse	Collapse
236	0.069	0.010	0.378	Visible	0.244	0.009	0.429	Visible	Visible
238	0.205	0.006	0.195	Collapse	0.008	0.006	0.187	Visible	Collapse
241	0.087	0.005	0.150	Belirgin	0.096	0.005	0.163	Visible	Visible
242	0.155	0.005	0.171	Significant	0.107	0.005	0.171	Visible	Significant
243	0.156	0.005	0.171	Significant	0.164	0.005	0.171	Significant	Significant
244	0.090	0.009	0.408	Visible	0.157	0.010	0.360	Visible	Visible
246	0.204	0.010	0.419	Visible	0.001	0.010	0.419	Minimum	Visible
248	0.119	0.005	0.153	Significant	0.122	0.005	0.153	Significant	Significant
249	0.271	0.009	0.456	Visible	0.269	0.009	0.456	Visible	Visible
250	0.110	0.010	0.361	Visible	0.166	0.010	0.361	Visible	Visible
253	0.366	0.010	0.385	Significant	0.002	0.009	0.428	Minimum	Significant
254	0.054	0.010	0.396	Visible	0.215	0.009	0.372	Visible	Visible

Most of the analyses resulted in high strain demands at the bottom of the columns reaching up to ultimate strains, and even collapse prevention damage state was not provided at the global level, as it was the case for previous analyses. For most of the records, the building became unstable at some point of the time history record and yielded very large top displacement values.

3.5. Principles for Identifying Risky Structures (RYTEIE)

3.5.1. Assessment Based on RYTEIE 2013

Based on the existing identification report, the information level was considered as comprehensive information level. Given the comprehensive information level, member capacities were not modified using any information level coefficient since the information level coefficient is unity for the comprehensive knowledge level. According to RYTEIE 2013, existing material strength is accepted as 85% of the average of the results obtained from compression tests, which are given in Table 3.62.

Table 3.62. Existing material strength for RYTEIE 2013.

Core Sample	Corrected Compressive Strength (Mpa)
C1	20.27
C2	22.13
C3	16.28
C4	22.32
C5	20.27
	$f_{cm}=17.22$

The analytical model is constructed in SAP2000 software. The analytical model is the same as the one constructed for linear analysis based on TBSC 2007 except for effective section stiffness values.

Effective section stiffness values are calculated by the following formula given in the RYTEIE 2013:

- For beams and shear walls $(EI)_e = 0.30(E_{cm}I)_o$
- For columns $(EI)_e = 0.50(E_{cm}I)_o$

The elasticity modulus of concrete is calculated based on the $E_{cm} = 5000(f_{cm})^{0.5}$ formulation.

For identifying the risk of the building, the Linear Elastic Calculation Method shall be adopted according to RYTEIE 2013.

In order to decide whether the *Equivalent Seismic Load Method* is applicable or not, several criteria shall be investigated. Since required conditions are investigated in previous sections, calculations to verify that torsional irregularity is not the case for the building are briefly summarized in the following.

Table 3.63. Calculation of the first natural vibration periods.

Story	hi	Hi	mi	wi (kN)	Ffi	dFix	dFiY
4	3.0	11.9	294	2883	392	0.02326	0.04407
3	3.0	8.9	306	3005	305	0.01721	0.03489
2	3.0	5.9	308	3021	203	0.01031	0.02239
1	2.9	2.9	308	3019	100	0.00375	0.00866
						T _{1,X} =	0.81046
						T _{1,Y} =	1.13877

Earthquake hazard defined in RYTEIE is based on the TBSC 2007. Therefore, the same parameters used in the linear assessment conducted for TBSC 2007, given in Table 3.64.

Table 3.64. Parameters to construct elastic acceleration spectrum.

Seismic Zone	2
A₀	0.3
Local Site Class	Z3
T_a (s)	0.15
T_b (s)	0.60

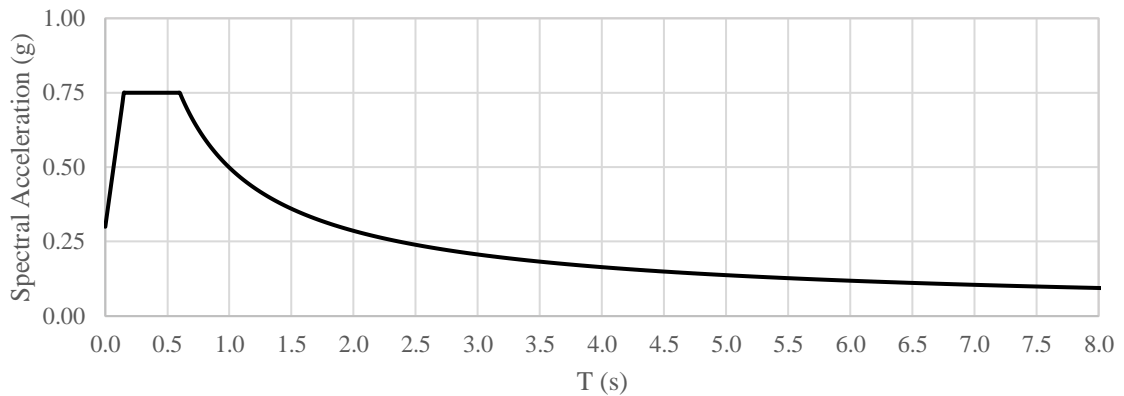


Figure 3.54. Elastic acceleration spectrum.

Table 3.65. The equivalent earthquake loads acting on the each story.

Story	w _i (kN)	H _i (m)	F _{i,x} (kN)	F _{i,y} (kN)
4	2883.16	11.9	2449.84	1866.27
3	3004.80	8.9	1769.74	1348.17
2	3020.99	5.9	1179.52	898.55
1	3019.42	2.9	579.46	441.43
		Σ	5978.56	4554.42
Basement	2896.11	0	868.83	868.83
		Σ	6847.39	5423.25

In order to verify that the building is appropriate to be assessed by the Equivalent Seismic Load method, the torsional irregularity check is a provision to be satisfied. Torsional irregularity check was conducted for corner joints and results can be seen in Table 3.66-Table 3.69.

Table 3.66. Torsional irregularity control for the negative X direction.

Loading	Joint	U _x	U _y	U _z	Δ	Joint	U _x	U _y	U _z	Δ	η _{bi}
EXN	TRC1	-0.162	-0.008	0.021	0.040	TLC1	-0.109	-0.008	0.018	0.032	2.69
EXN	TRC2	-0.122	-0.008	0.026	0.047	TLC2	-0.078	-0.008	0.021	0.033	2.62
EXN	TRC3	-0.075	-0.006	0.028	0.047	TLC3	-0.044	-0.006	0.022	0.029	2.52
EXN	TRC4	-0.028	-0.003	0.023	0.028	TLC4	-0.015	-0.003	0.017	0.015	2.45

Table 3.67. Table 54 Torsional irregularity control for the positive X direction.

Loading	Joint	U _x	U _y	U _z	Δ	Joint	U _x	U _y	U _z	Δ	η _{bi}
EXP	TRC1	0.162	0.008	-0.021	0.040	TLC1	0.109	0.008	-0.018	0.032	1.59
EXP	TRC2	0.122	0.008	-0.026	0.047	TLC2	0.078	0.008	-0.021	0.033	1.62
EXP	TRC3	0.075	0.006	-0.028	0.047	TLC3	0.044	0.006	-0.022	0.029	1.66
EXP	TRC4	0.028	0.003	-0.023	0.028	TLC4	0.015	0.003	-0.017	0.015	1.69

Table 3.68. Table 54 Torsional irregularity control for the negative Y direction.

Loading	Joint	U _x	U _y	U _z	Δ	Joint	U _x	U _y	U _z	Δ	η _{bi}
EYN	TRC1	-0.011	-0.203	-0.018	0.043	BRC1	-0.011	-0.190	-0.019	0.040	-0.48
EYN	TRC2	-0.009	-0.160	-0.027	0.057	BRC2	-0.009	-0.150	-0.026	0.054	-1.02
EYN	TRC3	-0.006	-0.103	-0.033	0.063	BRC3	-0.006	-0.096	-0.033	0.059	-2.68
EYN	TRC4	-0.003	-0.040	-0.030	0.040	BRC4	-0.003	-0.037	-0.031	0.037	-22.38

Table 3.69. Table 54 Torsional irregularity control for the positive Y direction.

Loading	Joint	U _x	U _y	U _z	Δ	Joint	U _x	U _y	U _z	Δ	η _{bi}
EYP	TRC1	0.011	0.203	0.018	0.043	BRC1	0.011	0.190	0.019	0.040	1.67
EYP	TRC2	0.009	0.160	0.027	0.057	BRC2	0.009	0.150	0.026	0.054	1.50
EYP	TRC3	0.006	0.103	0.033	0.063	BRC3	0.006	0.096	0.033	0.059	1.27
EYP	TRC4	0.003	0.040	0.030	0.040	BRC4	0.003	0.037	0.031	0.037	1.04

In order to identify the risk of the building under equivalent seismic loads, columns should be classified based on the Table 2.8 Column classification table. The calculation table used in column classification for negative X earthquake loading is given in Table 3.70 to set an example. V_e/V_f values are investigated for orthogonal earthquake directions in both ways. Results showed that columns are fallen into class B, considering the 90-degree hooks of the transverse reinforcements. Results are presented in tabular form from Table 3.71. to Table 3.74.

Table 3.70. Calculation table used to find column classes and m values (negative X earthquake loading).

<i>Column</i>	<i>Column capacity at the bottom (kNm)</i>	<i>Total bending moment transferred to column's i end (kNm)</i>	<i>Moment distribution between columns ($R_a=1$ loading)</i>	<i>Distributed beam moments to column's i end (kNm)</i>	$V_e=\Sigma M/L$ (kN)	$V_e(R_a=2)$ (kN)	$V_{e,Considered}$ (kN)	V_r (kN)	V_e/V_r	$N_k/(A_c F_c m)$	A_{sb}/sb_k	$M_{e,bottom}$ (kNm)	$M_{k,bottom}$ (kNm)	<i>m</i>
C101	240	109	0.079	8.529	86	47	47	334	0.140	0.12067	0.00150	-240	208	1.16
C102	361	89	0.155	13.815	129	62	62	400	0.154	0.20416	0.00270	-361	-341	1.06
C103	263	137	0.212	29.074	101	66	66	333	0.197	0.17521	0.00270	-263	230	1.15
C104	291	116	0.287	33.303	112	84	84	334	0.250	0.22909	0.00270	-291	244	1.19
C105	269	96	0.251	23.993	101	40	40	400	0.100	0.18849	0.00270	-269	-334	0.81
C106	124	109	0.166	18.174	49	18	18	334	0.055	0.12493	0.00150	-124	210	0.59
C107	739	137	0.100	13.724	260	157	157	497	0.316	0.04350	0.00270	-739	-378	1.96
C108	156	108	0.236	25.545	63	40	40	293	0.136	0.17988	0.00150	-156	187	0.83
C109	127	154	0.261	40.054	58	37	37	296	0.126	0.20569	0.00110	-127	178	0.72
C110	83	60	0.098	5.871	31	17	17	296	0.057	0.17914	0.00110	-83	130	0.64
C111	104	108	0.278	30.084	46	28	28	294	0.095	0.19113	0.00150	-104	190	0.55
C112	247	102	0.158	16.144	91	60	60	359	0.167	0.08726	0.00164	-247	-245	1.01
C113	159	77	0.260	20.129	62	47	47	315	0.148	0.00346	0.00127	-159	122	1.30
C114	319	107	0.206	21.951	117	56	56	383	0.145	0.17261	0.00182	-319	324	0.98
C115	328	122	0.363	44.408	129	50	50	400	0.124	0.18029	0.00270	-328	-330	1.00
C116	324	109	0.354	38.718	125	45	45	399	0.112	0.12943	0.00270	-324	-264	1.23
C117	287	108	0.516	55.735	118	33	33	399	0.083	0.11168	0.00270	-287	-255	1.13
C118	272	108	0.364	39.508	107	35	35	399	0.087	0.00403	0.00270	-272	-310	0.88
C119	221	118	0.397	46.889	92	28	28	447	0.063	0.16036	0.00324	-221	-280	0.79
C120	199	118	0.365	43.126	84	26	26	335	0.078	0.16457	0.00137	-199	303	0.66

Table 3.71. Results for negative X direction.

Column	m	$N_k/A_c f_{cm}$	$A_{sh}/s_b k$	m_{limit}	(m) State	(δ/h)	(δ/h) _{limit}	(δ/h) State	Story Shear Ratio
C101	1.155	0.12067	0.00150	2.438	Not Risky	0.0099	0.0129	Not Risky	0.01565
C102	1.058	0.20416	0.00270	2.720	Not Risky	0.0088	0.0146	Not Risky	0.02058
C103	1.146	0.17521	0.00270	2.808	Not Risky	0.0082	0.0152	Not Risky	0.02198
C104	1.192	0.22909	0.00270	2.644	Not Risky	0.0075	0.0141	Not Risky	0.02798
C105	0.806	0.18849	0.00270	2.767	Not Risky	0.0069	0.0150	Not Risky	0.01333
C106	0.590	0.12493	0.00150	2.428	Not Risky	0.0057	0.0129	Not Risky	0.00618
C107	1.956	0.04350	0.00270	3.036	Not Risky	0.0082	0.0169	Not Risky	0.05255
C108	0.834	0.17988	0.00150	2.291	Not Risky	0.0099	0.0120	Not Risky	0.01341
C109	0.716	0.20569	0.00110	2.056	Not Risky	0.0090	0.0106	Not Risky	0.01252
C110	0.637	0.17914	0.00110	2.117	Not Risky	0.0066	0.0109	Not Risky	0.00569
C111	0.550	0.19113	0.00150	2.263	Not Risky	0.0057	0.0118	Not Risky	0.00938
C112	1.007	0.08726	0.00164	2.559	Not Risky	0.0082	0.0137	Not Risky	0.02011
C113	1.300	0.00346	0.00127	2.381	Not Risky	0.0075	0.0125	Not Risky	0.01567
C114	0.982	0.17261	0.00182	2.451	Not Risky	0.0099	0.0130	Not Risky	0.01860
C115	0.995	0.18029	0.00270	2.792	Not Risky	0.0090	0.0151	Not Risky	0.01665
C116	1.225	0.12943	0.00270	2.947	Not Risky	0.0084	0.0163	Not Risky	0.01497
C117	1.125	0.11168	0.00270	3.000	Not Risky	0.0080	0.0167	Not Risky	0.01105
C118	0.878	0.00403	0.00270	3.036	Not Risky	0.0072	0.0169	Not Risky	0.01163
C119	0.791	0.16036	0.00324	3.099	Not Risky	0.0066	0.0171	Not Risky	0.00947
C120	0.658	0.16457	0.00137	2.258	Not Risky	0.0057	0.0118	Not Risky	0.00877
Wall	m	$N_k/A_c f_{cm}$	$A_{sh}/s_b k$	m_{limit}	(m) State	(δ/h)	(δ/h) _{limit}	(δ/h) State	Story Shear Ratio
P101	7.129	0.01823	0.30843	4.000	Risky	0.0078	0.0150	Not Risky	0.32391
P102	6.287	0.03038	0.38059	4.000	Risky	0.0075	0.0150	Not Risky	0.34992
								Σ	0.67383

Table 3.72. Results for positive X direction.

Column	m	$N_k/A_c f_{cm}$	$A_{sh}/s_b k$	m_{limit}	(m) State	(δ/h)	(δ/h) _{limit}	(δ/h) State	Story Shear Ratio
C101	1.149	0.16987	0.00150	2.316	Not Risky	0.0099	0.0122	Not Risky	0.01565
C102	1.075	-0.02813	0.00270	3.036	Not Risky	0.0088	0.0169	Not Risky	0.02058
C103	2.194	-0.09867	0.00270	3.036	Not Risky	0.0082	0.0169	Not Risky	0.02198
C104	3.725	0.15939	0.00270	2.856	Risky	0.0075	0.0156	Not Risky	0.02798
C105	0.815	0.10632	0.00270	3.017	Not Risky	0.0069	0.0168	Not Risky	0.01333
C106	0.560	0.07327	0.00150	2.490	Not Risky	0.0057	0.0133	Not Risky	0.00618
C107	1.824	0.18753	0.00270	2.770	Not Risky	0.0082	0.0150	Not Risky	0.05255
C108	0.774	0.22559	0.00150	2.177	Not Risky	0.0099	0.0113	Not Risky	0.01341
C109	0.672	0.19291	0.00110	2.085	Not Risky	0.0090	0.0107	Not Risky	0.01252
C110	0.423	0.19731	0.00110	2.075	Not Risky	0.0066	0.0107	Not Risky	0.00569
C111	0.624	0.14357	0.00150	2.381	Not Risky	0.0057	0.0126	Not Risky	0.00938
C112	0.974	0.12792	0.00164	2.488	Not Risky	0.0082	0.0133	Not Risky	0.02011
C113	0.815	0.18821	0.00127	2.171	Not Risky	0.0075	0.0113	Not Risky	0.01567
C114	1.055	0.19015	0.00182	2.404	Not Risky	0.0099	0.0127	Not Risky	0.01860
C115	1.096	0.14782	0.00270	2.891	Not Risky	0.0090	0.0159	Not Risky	0.01665
C116	1.202	0.11498	0.00270	2.990	Not Risky	0.0084	0.0166	Not Risky	0.01497
C117	1.168	0.14924	0.00270	2.886	Not Risky	0.0080	0.0158	Not Risky	0.01105
C118	0.864	0.17037	0.00270	2.822	Not Risky	0.0072	0.0154	Not Risky	0.01163
C119	0.911	0.17438	0.00324	3.052	Not Risky	0.0066	0.0168	Not Risky	0.00947
C120	0.661	0.16457	0.00137	2.258	Not Risky	0.0057	0.0118	Not Risky	0.00877
Wall	m	$N_k/A_c f_{cm}$	$A_{sh}/s_b k$	m_{limit}	(m) State	(δ/h)	(δ/h)_{limit}	(δ/h) State	Story Shear Ratio
P101	6.159	0.03949	0.30843	4.000	Risky	0.0078	0.0150	Not Risky	0.32391
P102	5.057	0.06568	0.38059	4.000	Risky	0.0075	0.0150	Not Risky	0.34992
								Σ	0.67383

Table 3.73. Results for negative Y direction.

Column	m	$N_k/A_c f_{cm}$	$A_{sh}/s_b k$	m_{limit}	(m) State	(δ/h)	(δ/h) _{limit}	(δ/h) State	Story Shear Ratio
C101	2.279	0.11722	0.00233	2.823	Not Risky	0.0135	0.0155	Not Risky	0.05347
C102	1.554	0.20611	0.00150	2.226	Not Risky	0.0135	0.0116	Risky	0.03613
C103	2.222	0.04604	0.00182	2.643	Not Risky	0.0135	0.0143	Not Risky	0.02830
C104	2.141	0.08231	0.00182	2.643	Not Risky	0.0135	0.0143	Not Risky	0.02895
C105	1.790	0.15274	0.00150	2.359	Not Risky	0.0135	0.0124	Risky	0.04042
C106	2.297	0.10827	0.00233	2.848	Not Risky	0.0135	0.0157	Not Risky	0.05292
C107	2.122	0.09362	0.00118	2.337	Not Risky	0.0137	0.0123	Risky	0.05234
C108	1.507	0.19731	0.00270	2.740	Not Risky	0.0140	0.0148	Not Risky	0.03500
C109	2.057	0.21671	0.00322	2.875	Not Risky	0.0140	0.0155	Not Risky	0.06860
C110	2.120	0.18417	0.00322	2.981	Not Risky	0.0140	0.0163	Not Risky	0.06650
C111	1.674	0.18310	0.00270	2.784	Not Risky	0.0140	0.0151	Not Risky	0.04206
C112	1.710	0.13252	0.00204	2.655	Not Risky	0.0142	0.0144	Not Risky	0.05074
C113	2.552	0.04616	0.00270	3.036	Not Risky	0.0142	0.0169	Not Risky	0.06090
C114	1.798	0.19405	0.00182	2.394	Not Risky	0.0146	0.0126	Risky	0.05093
C115	1.660	0.19625	0.00150	2.250	Not Risky	0.0146	0.0118	Risky	0.03874
C116	2.166	0.15433	0.00150	2.355	Not Risky	0.0146	0.0124	Risky	0.04321
C117	2.449	0.08796	0.00150	2.490	Not Risky	0.0146	0.0133	Risky	0.03832
C118	1.846	0.05386	0.00150	2.490	Not Risky	0.0146	0.0133	Risky	0.03931
C119	2.003	0.15314	0.00180	2.502	Not Risky	0.0146	0.0134	Risky	0.03834
C120	2.154	0.15782	0.00137	2.274	Not Risky	0.0146	0.0119	Risky	0.05123
Wall	m	$N_k/A_c f_{cm}$	$A_{sh}/s_b k$	m_{limit}	(m) State	(δ/h)	(δ/h)_{limit}	(δ/h) State	Story Shear Ratio
P101	2.405	0.03904	0.11624	4.000	Not Risky	0.0139	0.0150	Not Risky	0.04587
P102	2.477	0.02621	0.09586	4.000	Not Risky	0.0139	0.0150	Not Risky	0.03772
								Σ	0.42896

Table 3.74. Results for positive Y direction.

Column	m	$N_k/A_c f_{cm}$	$A_{sh}/s_b k$	m_{limit}	(m) State	(δ/h)	(δ/h) _{limit}	(δ/h) State	Story Shear Ratio
C101	2.338	0.10079	0.00233	2.823	Not Risky	0.0135	0.0155	Not Risky	0.05347
C102	1.643	0.16792	0.00150	2.226	Not Risky	0.0135	0.0116	Risky	0.03613
C103	1.952	0.10104	0.00182	2.643	Not Risky	0.0135	0.0143	Not Risky	0.02830
C104	2.297	0.04810	0.00182	2.643	Not Risky	0.0135	0.0143	Not Risky	0.02895
C105	1.639	0.19514	0.00150	2.359	Not Risky	0.0135	0.0124	Risky	0.04042
C106	2.253	0.12297	0.00233	2.848	Not Risky	0.0135	0.0157	Not Risky	0.05292
C107	3.267	0.02314	0.00118	2.337	Risky	0.0137	0.0123	Risky	0.05234
C108	1.508	0.17010	0.00270	2.740	Not Risky	0.0140	0.0148	Not Risky	0.03500
C109	2.036	0.21457	0.00322	2.875	Not Risky	0.0140	0.0155	Not Risky	0.06860
C110	2.093	0.18789	0.00322	2.981	Not Risky	0.0140	0.0163	Not Risky	0.06650
C111	1.682	0.20533	0.00270	2.784	Not Risky	0.0140	0.0151	Not Risky	0.04206
C112	1.813	0.09831	0.00204	2.655	Not Risky	0.0142	0.0144	Not Risky	0.05074
C113	2.271	0.08522	0.00270	3.036	Not Risky	0.0142	0.0169	Not Risky	0.06090
C114	1.873	0.16676	0.00182	2.394	Not Risky	0.0146	0.0126	Risky	0.05093
C115	1.735	0.17419	0.00150	2.250	Not Risky	0.0146	0.0118	Risky	0.03874
C116	2.329	0.12291	0.00150	2.355	Not Risky	0.0146	0.0124	Risky	0.04321
C117	2.088	0.13870	0.00150	2.490	Not Risky	0.0146	0.0133	Risky	0.03832
C118	1.970	0.09942	0.00150	2.490	Not Risky	0.0146	0.0133	Risky	0.03931
C119	1.839	0.17759	0.00180	2.502	Not Risky	0.0146	0.0134	Risky	0.03834
C120	2.046	0.18113	0.00137	2.274	Not Risky	0.0146	0.0119	Risky	0.05123
Wall	m	$N_k/A_c f_{cm}$	$A_{sh}/s_b k$	m_{limit}	(m) State	(δ/h)	(δ/h) _{limit}	(δ/h) State	Story Shear Ratio
P101	2.813	0.01868	0.09939	4.000	Not Risky	0.0139	0.0150	Not Risky	0.04587
P102	1.703	0.06985	0.13056	4.000	Not Risky	0.0139	0.0150	Not Risky	0.03772
								Σ	0.42896

In order to identify that the building, whether it is a risky building or not, average axial compression stresses are calculated under the $G+0.3Q$ loading combination. Based on the results, story shear ratios are compared with the limits, as can be seen from Table 3.75, the building is exceeding the limits for all cases.

Table 3.75. Comparison of risky members' total shear forces with limits.

Loading	$f_{c,avg}$ (MPa)	f_{cm} (MPa)	$f_{c,avg}/f_{cm}$	Story shear ratio limit	Story shear ratio
EXN	2.35	17.22	0.136	0.327	0.674
EXP	2.35	17.22	0.136	0.327	0.674
EYN	2.35	17.22	0.136	0.327	0.429
EYP	2.35	17.22	0.136	0.327	0.429

3.5.2. Assessment Based on RYTEIE 2019

Information level is considered as comprehensive, as it was the case for the previous chapter based on the identification report of the real building. Given the comprehensive information level, member capacities were not modified using any information level coefficient since the information level coefficient is unity for the comprehensive knowledge level. According to RYTEIE 2019, existing material strength is accepted as 85% of the average of the results obtained from compression tests which are given in Table 3.76.

Table 3.76. Existing material strength for RYTEIE 2019.

Core Sample	Corrected Compressive Strength (Mpa)
C1	20.27
C2	22.13
C3	16.28
C4	22.32
C5	20.27
$f_{cm}=17.22$	

The analytical model is constructed in SAP2000 software. According to RYTEIE, if mid-pier modeling is used to model shear walls, the torsional stiffness of rigid arm shall be neglected. Considering this restriction, necessary changes were made in the model. Furthermore, modeling

Effective section stiffness values are calculated by the following formula given in the RYTEIE 2013:

- For beams and shear walls $(EI)_e = 0.30(E_{cm}I)_o$
- For columns $(EI)_e = 0.50(E_{cm}I)_o$

The elasticity modulus of concrete is calculated based on the $E_{cm} = 5000(f_{cm})^{0.5}$ formulation.

Shear modulus of concrete is calculated based on the $G_{cm} = 0.4E_{cm}$ formulation and shear stiffnesses are taken as $G_{cm}A_{cm}$.

For identifying the risk of the building, the *Mode Superposition Method* shall be utilized according to RYTEIE 2019.

As it is shown in Table 3.77, the total mass participation ratio of the mode numbers considered in the calculations is higher than 90%.

Table 3.77. Mass participation ratios of the modes.

Mode	Period	U _X	U _Y	ΣU _X	ΣU _Y
1	1.124389	0.00084	0.37992	0.00084	0.37992
2	1.115673	0.00299	0.40659	0.00382	0.78651
3	0.736022	0.75447	0.00046	0.7583	0.78697
4	0.347759	0.00049	0.01547	0.75879	0.80244
5	0.326835	0.00038	0.10565	0.75916	0.90809
6	0.201979	0.12079	0.00013	0.87995	0.90821
7	0.19172	0.00067	0.00112	0.88062	0.90933
8	0.184064	0.00047	0.00025	0.88108	0.90959
9	0.176003	0.00194	0.01276	0.88302	0.92234
10	0.17406	0.00451	0.00902	0.88753	0.93136
11	0.173137	0.00416	0.00089	0.8917	0.93225
12	0.167647	4.25E-05	0.00294	0.89174	0.93519
13	0.165284	0.00019	0.00607	0.89193	0.94126
14	0.164034	4.45E-05	0.00052	0.89197	0.94178
15	0.162414	0.00144	0.00019	0.89342	0.94197
16	0.158925	6.95E-08	2.03E-06	0.89342	0.94197
17	0.157001	0.00049	0.00032	0.89391	0.94229
18	0.155762	0.00532	0.00174	0.89923	0.94403
19	0.155206	0.00395	0.00035	0.90318	0.94438
20	0.15302	0.00783	0.00199	0.91101	0.94637

In the previous elastic analysis, demand/capacity calculations of columns were based on the P-M interactions and, moments at perpendicular direction were omitted. Whereas, in RYTEIE 2019, demand/capacity calculations are based on M22-M33 relation since the mode superposition method is adopted.

Results for the walls under X direction loading are given in Table 3.78.

Table 3.78. Comparison of m values obtained for walls.

Wall	2019		2013	
P101	6.98	6.22	7.13	6.16
P102	6.35	5.36	6.29	5.06

4. RESULTS

Turkish Building Seismic Code 2007 was abolished after almost a decade of use, and the Turkish Building Seismic Code 2018 has been officially in force since January 1, 2019. Turkish Building Seismic Code presents important changes not only in the countrywide seismic hazard maps but also in structural modeling and analysis issues for the design of new buildings as well as in the definition of performance objectives and assessment methodologies for existing buildings. In this study, a comparative earthquake performance assessment of an existing reinforced concrete building in Istanbul, which was constructed in 2006, is presented for the requirements of the Turkish Building Seismic Code 2018 and Turkish Building Seismic Code 2007 as well. Although it is assumed that the building was designed according to the provisions of the Turkish Building Seismic Code-1998, it was identified as a risky building last year based on the simplified guidelines by the Ministry of Environment and Urbanization (Riskli Yapıların Tespit Edilmesine İlişkin Esaslar-2013). The building has four stories rising above a basement floor, and its lateral load-carrying system consists of moment-resisting frames with two shear walls around the staircase. In order to evaluate the seismic performance of the building, a three-dimensional finite element model is elaborated on the basis of the blueprints. Geometrical and material characteristics are further verified by the reports on in situ measurements and field tests. Linear and nonlinear static and dynamic analyses procedures are implemented, and a detailed assessment of the building against the performance criteria by each code is performed. Additionally, the building is assessed on the basis of the updated guidelines by the Ministry of Environment and Urbanization (Riskli Yapıların Tespit Edilmesine İlişkin Esaslar-2019).

Applicability of the methods has been investigated, and all of the methods were applicable to the case study building except the linear analysis method defined in the Turkish Building Seismic Code 2018. For the case study building, while the beams meet the requirements, the elastic method could not be applied because of the columns since columns yielded higher EKO values than beams in each direction.

Although it was found that the “columns stronger than beams” principle, which has a critical role in the global response of the structure and collapse mechanism, was present in the case study structure for all of the analysis, the collapse prevention level exceeded because of the damage occurred at the bottom sections of vertical members. The reason behind the poor performance of the building was because of the insufficient amount of reinforcement in the columns and shear walls.

The deformation limits introduced by the Turkish Building Seismic Code 2018 take into account 30% of the transverse reinforcements those which are not considered as the special earthquake stirrups. Considering the stirrup problems in the existing building stock, this provision is going to have a remarkable effect on the evaluation of existing buildings since it is introducing higher strain limits. In addition to this, the statistical approach adopted in the definition of existing material strength results in higher compressive strength values compared to TBSC 2007. This, again, is an important aspect of the evaluation of existing buildings, which yields higher strength capacities.

TBSC 2018 introduces different effective section stiffness values for linear and nonlinear analysis, unlike TBSC 2007. The formula used to calculate effective section stiffness values to be used in the nonlinear analysis results in remarkably lower values if the lumped plasticity approach is adopted, which, in turn, softens the structures. Observations of higher displacement demands in the pushover analyses were one of the outcomes of this situation. If fiber models are not used, there are going to be considerable differences between TBSC 2018 and TBSC 2007 in nonlinear analysis.

It is emphasized many times in relevant documents by the developers of the simplified guidelines by the Ministry of Environment and Urbanization (Riskli Yapıların Tespit Edilmesine İlişkin Esaslar), principles are not for evaluating the performance but deciding whether the building is risky or not. Although the aim is not to evaluate performance, expectation from a risky building is not to meet the life safety performance level, and case study building evaluated in the scope of this thesis confirmed that expectation. Considering the global performance of the building, results of all codes and regulations fitted well in this building. In addition, the demand/capacity ratios obtained for the former and latter versions of the simplified guidelines by the Ministry of Environment and Urbanization was very close. However, due to the change in analysis methods and modeling parameters, the difference between drift ratios was more prominent. Furthermore, it can be said that the complexity of the method provided within the new guideline makes one of the main aspects of this guideline questionable, which is its simplicity.

REFERENCES

Arslan, G., Borekci, M., Sahin, B., Denizer, M.I., Duman, K.S. "Performance Evaluation of In-Plan Irregular RC Frame Buildings Based on Turkish Seismic Code." International Journal of Civil Engineering, 2018. 16:323–333.

Calvi, G. M., M. J. N. Priestley, and M. J. Kowalsky. "Displacement based seismic design of structures." New Zealand Conference on Earthquake Engineering, 2007. IUSS Press, 2007.

Celep, Zekai. "Betonarme Taşıyıcı Sistemlerde Doğrusal Olmayan Davranış Ve Çözümleme: Deprem Yönetmeliği (2007) Kavramları". Beta Dağıtım., 2007.

Chadwell, C. B., and R. A. Imbsen. "XTRACT: A tool for axial force-ultimate curvature interactions." Structures 2004: Building on the past, securing the future. 2004. 1-9.

Chopra, Anil K. "Dynamics of structures. " Theory and applications to the earthquake engineers, 2007.

Computers and Structures Incorporated (CSI), "Computer Program SAP2000 (Version 20.2.0)." Berkeley, California, USA, 2019.

Çavdar, Ö., Bayraktar, A. "Pushover and nonlinear time history analysis evaluation of an RC building collapsed during the Van (Turkey) earthquake on October 23, 2011." *Natural Hazards*, 2014. 70:657–673.

Demir, F., Erkan, K.T., Dilmaç, H., Tekeli, H. "Mevcut Betonarme Binaların Doğrusal Elastik ve Doğrusal Elastik Olmayan Hesap Yöntemleri ile İncelenmesi Üzerine Bir Değerlendirme." 2. Türkiye Deprem Mühendisliği ve Sismoloji Konferansı, 2013.

Elci, H., Goker, K.A. "Comparison of Earthquake Codes (TEC 2007 and TBEC 2018) In Terms of Seismic Performance of RC Columns." *International Journal of Scientific and Technological Research*, 2018. Vol. 4, No.6.

Fahjan, Y., M. et al. "Perdeli Betonarme Yapılar İçin Doğrusal Olmayan Analiz Metotları-Nonlinear Analysis Methods For Reinforced Concrete Buildings With Shearwalls." *Seventh National Conference on Earthquake Engineering, Istanbul, Turkey, 2011.*

Fardis, Michael N. "Seismic design, assessment and retrofitting of concrete buildings: based on EN-Eurocode 8." Vol. 8. Springer Science & Business Media, 2009.

FEMA. 2000. *Prestandard and Commentary for the Seismic Rehabilitation of Buildings*. 2000. Report No. FEMA–356. Federal Emergency Management Agency.

Fenves, Gregory L., and Filip C. Filippou. "Methods of analysis for earthquake-resistant structures." *Earthquake Engineering*. CRC Press, 2004. 332-410.

McKenna, Frank, G. L. Fenves, and F. C. Filippou. "OpenSees." University of California, Berkeley: nd (2010).

Orakcal K, Massone LM, Wallace JM (2006): Analytical Modeling of Reinforced Concrete Walls for Predicting Flexural and Coupled-Shear-Flexural Responses. PEER Report 2006/07, PEER Center, U. of California, Berkeley.

PEER/ATC-72-1: Modeling and Acceptance Criteria for Seismic Design and Analysis of Tall Buildings. Applied Technology Council, Redwood City, California.

Powell, Graham Harcourt. "Modeling for structural analysis: behavior and basics." Computers and Structures, 2010.

Scott, Michael H., and Gregory L. Fenves. "Plastic hinge integration methods for force-based beam-column elements." Journal of Structural Engineering 132.2 (2006): 244-252.

Terzic, Vesna "Structural Modeling With Examples", OpenSeesDays2012, University of California, August 15-16, 2012.

The Union of Chambers of Turkish Engineers and Architects- Chamber of Civil Engineers, "Turkish Building Seismic Code (TBSC-2018) Training Manual", Ankara, Turkey, 2018

Turkish Ministry of Environment and Urbanization, “Principles for Identifying Risky Structures (RYTEIE 2013)”, Ankara, Turkey, 2013.

Turkish Ministry of Environment and Urbanization, “Principles for Identifying Risky Structures (RYTEIE 2019)”, Ankara, Turkey, 2019.

Turkish Disaster and Emergency Management Authority, “Turkish Building Seismic Code (TBSC 2018)”, Ankara, Turkey, 2018.

Turkish Disaster and Emergency Management Authority, “Revised National Seismic Hazard Map of Turkey (TDTH)”, Ankara, Turkey, 2018.

Turkish Ministry of Public Works and Settlement, “Turkish Building Seismic Code (TBSC 2007)”, Ankara, Turkey, 2007.

Yön, B., Onat, O. “Comparison Of Damage Limits For 2007 Turkish Seismic Code And 2018 Turkey Building Earthquake Code.” 5. International Conference on Earthquake Engineering and Seismology (5ICEES), 2019.